HOKKAIDO UNIVERSITY

Title	Novel syntrophy driven by methylotrophic methanogens
Author(s)	HUANG, YAN
Citation	北海道大学. 博士(農学) 甲第15147号
Issue Date	2022-09-26
DOI	10.14943/doctoral.k15147
Doc URL	http://hdl.handle.net/2115/90301
Type	theses (doctoral)
File Information	Huang_Yan.pdf

Instructions for use

Hokkaido University Collection of Scholarly and Academic Papers : HUSCAP

Novel syntrophy driven by Methylotrophic methanogens

（メチル基利用メタン生成アーキアによる新規栄養共生）

Hokkaido University Graduate School of Agriculture

Frontiers in Biosciences Doctor Course

HUANG YAN

Abstract

Methanogenic degradation of organic matter plays a vital role in the global carbon cycle. In methanogenic ecosystems, organotrophic bacteria and methanogenic archaea cooperatively drive chemical transformations via interspecies H_2/formate transfer or direct interspecies electron transfer (DIET) to combat energetic and thermodynamic limitations, an interaction termed syntrophy. It was thought the syntrophic interaction was only associated with hydrogenotrophic methanogens or acetoclastic methanogens. However, it can not explain the prevalence of methylotrophic methanogens across the Earth, especially in the methylated compounds lacking environments.

In this study, a hitherto overlooked metabolic symbiosis was discovered between a formate-utilizing anaerobe *Zhaonella formicivorans* K32 and obligate methylotrophic methanogens *Methermicoccus shengliensis* ZC-1 or AmaM, marking a fourth mode of syntrophy facilitated by methanol. Subsequently, the metabolic pathway of this novel syntrophy was studied by genomic and transcriptomic analysis. Furthermore, its survival strategy and its ecological role were discussed. The novel methanol-mediated syntrophy greatly expands the possibilities for anaerobic carbon flow by bridging two processes assumed to be independent until now - syntrophic organics degradation and methylotrophic methanogenesis.

1. Establishing formate-fed syntrophic communities driven by methylotrophic methanogens

Formate is one of the main metabolic products of anaerobic organic matter degradation, and it might be the precursor of methylated compounds. The formate utilizer *Z. formicivorans* K32 and

methylotrophic methanogen *M. shengliensis* ZC-1 or AmaM were both thermophiles derived from oil reservoirs where methyl compounds were lacking. Incubation of concentrated K32 resting cells with formate resulted in a slight accumulation of methanol, indicating its methanol metabolism ability. Further cocultivation of *Z. formicivorans* with *M. shengliensis* showed an apparent formate consumption and methane formation, consistent with the reaction $4HCOO^- + H_2O + H^+ = 3\ CH_4 + 3HCO_3^-$. Additional H_2 (*i.e.*, the inhibitory by-product of typical H_2-mediated syntrophy) did not inhibit formate utilization and methane production of K32/ZC1 coculture, indicating that H_2 was not the primary electron carrier. K32 and ZC-1 could continue formate degradation when physically separated by a dialysis membrane, suggesting the primary route was not DIET either. It was further convinced by the non-effect of conductive material amending. In tracer experiments using ^{13}C-formate and ^{12}C-bicarbonate, the proportion of ^{13}C-CH_4 was constant despite the increasing ^{13}C-CO_2, indicating the major methanogenesis route for *M. shengliensis* was not CO_2-reducing. The results indicated the only methane production pathway that could support such behavior was methylotrophic methanogenesis, namely, the novel syntrophy was mediated by methylated compounds.

2. Construction of metabolic pathway of the formate-driven syntrophy

The mechanism of formate-driven syntrophy remains unknown. *Z. formicivorans* genome encodes enzymes of the Wood-Ljungdahl pathway, the glycine/serine pathway, and the formate-methanol-reducing pathway for formate utilization. The gene expression profiles of *M. shengliensis* ZC-1 clearly showed methylotrophic methanogenesis, which agreed with the hypothesis that methanol was the primary compound mediating symbiosis. A combination of gene expression profiles and electron balance revealed that strain K32 conducted methanol generation

by aldehyde ferredoxin oxidoreductase and alcohol dehydrogenase with the oxidation of formate to CO_2 by glycine/serine-involving reversed Wood-Ljungdahl pathway. Strain K32 possesses ion gradient-driven phosphorylation performed by electron bifurcation enzyme Nfn and Hdr-flox complex for its energy conservation during the syntrophic lifestyle.

3. Prediction of the survival strategy and the ecological niche by thermodynamics

Strain K32 employs two thermodynamic/energetic options for formate catabolism, making it flexible for optimizing energy acquisition to dynamic/heterogeneous environmental conditions. The formate disproportionation pathway used by K32 encounters no thermodynamic limit of their partners and is unencumbered by thermodynamic competition, making it has thermodynamic/energetic advantages over typical H_2-mediated syntrophic formate oxidation.

Contents

Chapter 1 General Introduction

The significance of methanogenesis

Methanogenic decomposition of biomass occurs globally in anoxic environments, such as freshwater sediments, swamps, landfills, the intestinal tracts of ruminants and termites, and artificial methanogenic environments like biogas reactors and paddy fields (Thauer *et al.*, 2008, Lyu *et al.*, 2018). It was estimated that about 1 Gt (Giga ton) of methane per year was generated by methanogens, accounting for approximately 2 % of net carbon fixed by photosynthesis annually (Thauer *et al.*, 2008). As one of the most important greenhouse gas, although most of the methane is oxidized to CO_2 by aerobic and anaerobic methane-oxidizing bacteria and archaea, the global methane emission is around 500-600 Tg (teragram) per year, about 70% of which is due to methanogenesis (Lyu *et al.*, 2018). These indicate that methanogenesis plays a vital role in the global biogeochemical carbon cycle and climate change. Therefore, a better understanding of methanogenesis is essential for unarchiving the mechanism of the global carbon cycle and coping with global warming.

The methanogenesis pathways and their ecological roles

Methane is the end-product of biomass-degrading in anoxic environments when electron acceptors – sulfate (SO_4^{2-}), nitrate (NO_3^-), ferric ion (Fe^{3+}), and oxygen (O_2) are deficient. Methanogens are the primary methane producer, which works for the last step of anaerobic organic matter degradation. In general, methanogens can only use simple C1 or C2 molecules, such as H_2/CO_2, formate, acetate, and methyl-containing compounds. According to the substrate spectrum, methanogens are divided into three groups: (1) hydrogenotrophic methanogens, which use hydrogen, formate, or some simple alcohols to reduce CO_2 to CH_4; (2) aceticlastic methanogens, which split acetate to produce CO_2 and CH_4. This group has the lowest phylogenetic diversity that

only distribute in the genus of *Methanosarcina* and *Methanosaeta* (3) methylotrophic methanogens, which utilize simple methylated compounds like methanol, tri-, di- and mono-methylamine. Recently, methanogenic archaea were suggested to degrade a broader substrate range. *Methermicoccus shengliensis*, a methylotrophic methanogen isolated from oil-production water, was found to be capable of using methoxylated aromatic compounds in methanogenesis, which was proposed as methoxydotrophic methanogen (Mayumi *et al.*, 2016). Moreover, *Candidatus* Methanoliparum could degrade long-chain alkanes with methanogenesis, proposing as an alkylotrophic methanogen (Zhou *et al.*, 2022).

Generally, aceticlastic methanogenesis accounts for two-thirds of methane generation, and hydrogenotrophic methanogenesis contributes to most of the remaining one-third (Conrad, 2020). The ratio of these two pathways is affected by the stoichiometry of conversion processes, which is related to the environmental temperature, salinity, ammonia concentration, *etc* (Conrad, 2020). Despite the phylogenetically diverse, methylotrophic methanogens were regarded as a minor contributor to methanogenic organics degradation. They are usually responsible for CH_4 production in anoxic saline environments such as marine and hypersaline, sulfate-rich sediments where biota produces glycine betaine (*i.e*., one of the precursors of methylated compounds, especially trimethylamine) as an osmolyte (Liu *et al.*, 2016, Sorokin *et al.*, 2017, Conrad, 2020). However, recent findings suggested methylotrophic methanogens may play crucial roles in the microbial coal bed-derived methane (Lloyd *et al.*, 2021) and heavy oil-derived methane in the oil reservoir (Zhou *et al.*, 2022), indicating methylotrophic methanogenesis may have overlooked ecological roles. In this research, the methylotrophic methanogen *Methermicoccus shengliensis* was found participating in syntrophic formate degradation, suggesting a hitherto overlooked methanogenic process involving methylotrophic methanogens.

Anaerobic organic matter degradation processes

The overall methanogenic organic matter degradation is quite simple – the organic matter is mineralized to the most reduced form of carbon (*i.e.*, CH_4) and the most oxidized form of carbon (*i.e.*, CO_2). However, the microbial system is extremely complex, involving various microorganisms and reactions (Fig. 1.1a). Typically, apart from the last step taken by methanogens as mentioned above, (1) the organic polymers (*e.g.*, proteins, lipids, and polysaccharides) are firstly hydrolyzed to monomers by hydrolysis bacteria. (2) Sequentially, the produced monomers are fermented to reduced organic compounds (*e.g.*, butyrate, propionate, lactate, ethanol) and methanogenic precursors (*e.g.*, acetate, formate, H_2/CO_2) by fermentative bacteria. (3) The reduced organic compounds are eventually converted to methanogenic precursors by a group of syntrophic bacteria (*i.e.*, syntrophs). (4) Interconversion of acetate and H_2/CO_2 by homoacetogenic bacteria and syntrophic acetate oxidizing bacteria. The syntrophic degradation steps are the rate-limiting step of methanogenic process since they are thermodynamically restricted reactions.

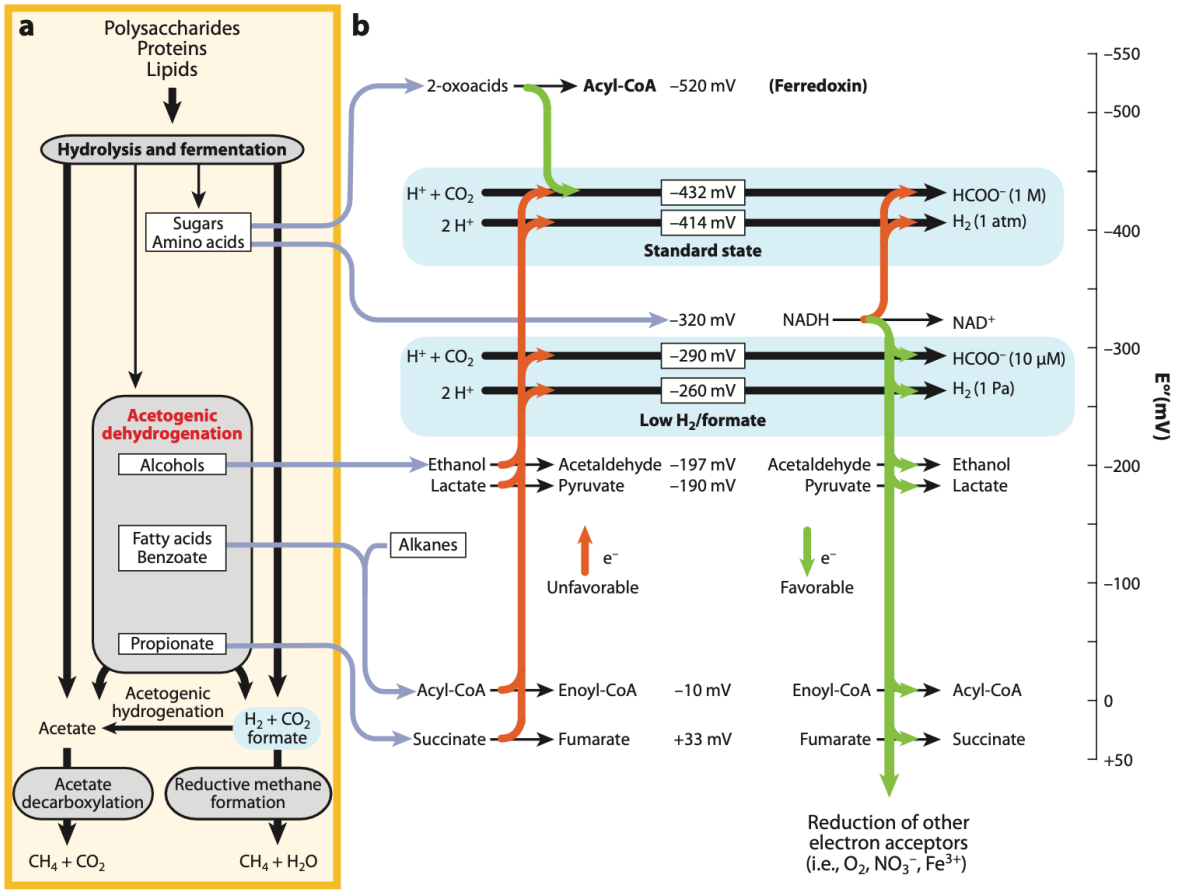

Figure 1.1. Typical schematic diagram of methanogenic organic matter degradation (a) and (b) the critical redox reactions involved in syntrophic metabolism (Sieber *et al.*, 2012)

Electron transfer for syntrophs

During syntrophic degradation, the syntrophs release reduced electron carriers (*e.g.*, $FADH_2$ and NADH with $E^{0'}$= -220 mV and -320 mV, respectively), which will be then re-oxidized by disposal of electrons to H^+ or CO_2 for the generation of H_2 or formate (*i.e.*, the electron carriers for interspecies electron transfer, $E^{0'}$= -414 and -420 mV, respectively). This process often encounters

thermodynamic limitations since the redox potential of H_2 or formate is relatively lower than the reduced electron carriers (Fig 1.1b). To carry out these reductive reactions, one strategy is to keep H_2 or CO_2 low enough by methanogens so that the redox potential of H_2 or formate will become relatively higher. However, in some cases, this strategy does not work, so syntrophs carry out reverse electron transport and electron bi(con)furcation (also called flavin-based electron bifurcation) to overcome the energy barrier (Fig 1.1b) (Sieber *et al.*, 2012, Narihiro *et al.*, 2016, Buckel & Thauer, 2018). In such routes, the exergonic reaction drives the endergonic reaction (Fig 1.1b), often taking advantage of the most reducing biological electron carrier ferredoxin ($E^{0'}$= -500 ~ -340 mV). To date, various mechanisms have been described: (a) The *Rhodobacter* nitrogen fixation complex (Rnf) carries out reverse electron transport from NADH to reduced ferredoxin (Fd_{red}) for electron-confurcating hydrogenase (ECHyd) H_2 generation; (b) The heterodisulfide reductase (Hdr)-associated ion-translocating ferredoxin: NADH oxidoreductase (Hdr-Ifo) performs reverse electron transport-driven Fd_{red} generation to facilitate energy-conserving H_2 production through either ECHyd or *Methanothermobacter*-like electron-confurcating hydrogenase; (c) The electron-transfer-flavoprotein (ETF)-oxidizing hydrogenase complex (FixABCX) uses quinol oxidation-driven H_2 production; (d) Membrane-bound hydrogenases (Mbh) performs Fd_{red}-oxidizing H_2 generation or formate (Fo) oxidizing by formate dehydrogenase H (FdhH) coupled with energy conservation by extruding protons; (e) The electron-bifurcating formate dehydrogenase (EBFdh) facilitates energy-conserving formate metabolism; (f) The NADH-dependent Fd_{red}: $NADP^+$ oxidoreductase conducts electron bi(con)furcation using NADP(H) as an electron carrier (Fig. 1.2) (Nobu *et al.*, 2015).

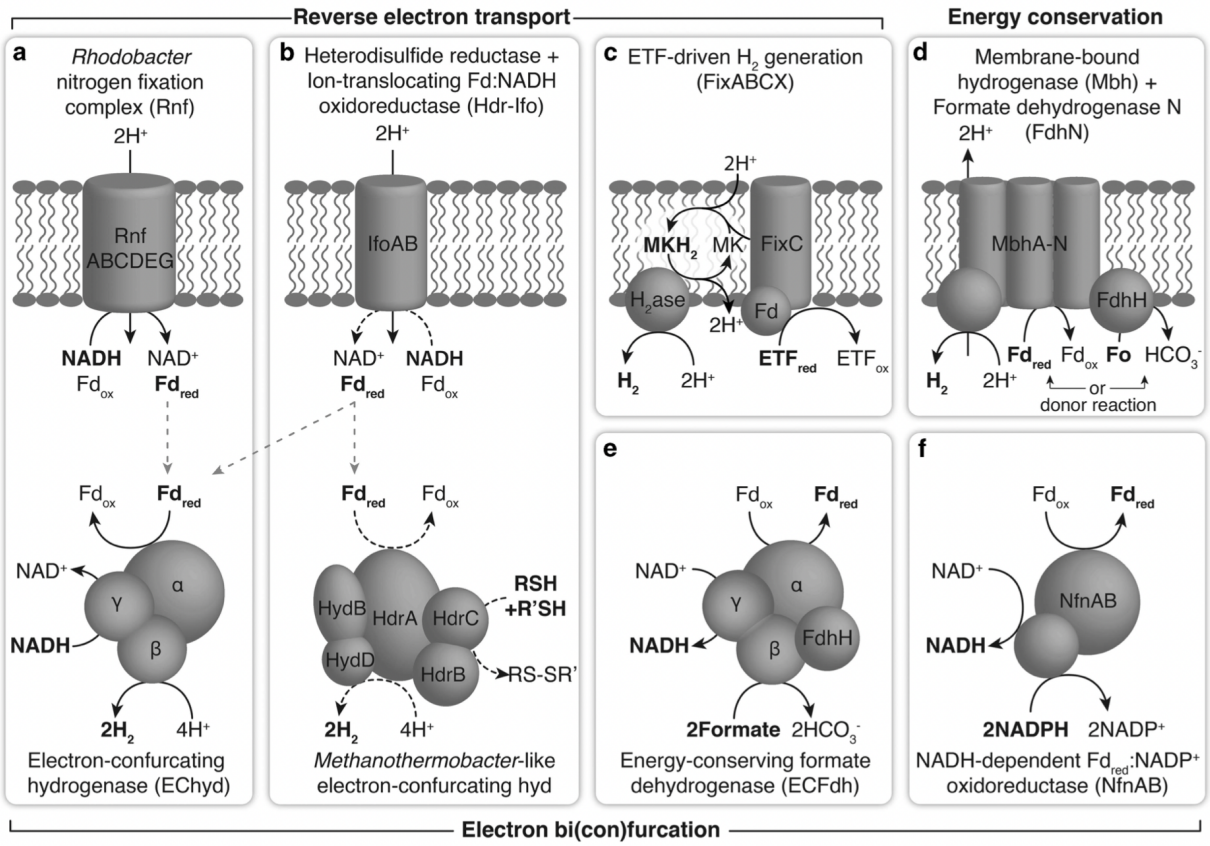

Fig 1.2 Reverse electron transport and electron confurcation mechanisms for syntrophs (Nobu *et al.*, 2015)

The mechanism of interspecies electron transfer

The oxidation of the reduced organic compounds is energetically unfavorable (Table 1.1) (Zhang *et al.*, 2019). The accumulation of products H_2, formate, to some extend, acetate will halt the reactions. Assuming a 20 mM acetate otherwise at standard condition, the highest H_2 partial pressure can be tolerated is 0.35 pa at pH 7.0. To overcome the thermodynamic limitation, the syntrophic bacteria and the methanogens must work as obligate syntrophic consortia to conduct the reaction. The methanogens remove the intermediates H_2 resulting in a low H_2 concentration to

pull the reactions. This interaction between the bacteria and methanogens is called syntrophy, which depends on interspecies H_2 transfer.

Table 1.1 Gibbs free energy values change for reactions potentially involved in methanogenic degradation of organic compounds (Zhang *et al.*, 2019).

Substrates		Reactions	$\Delta G^{0'}$(kJ/mol)
Anaerobic oxidation			
Short chain fatty acids	CH_3COOH	$CH_3COO^- + H^+ + 2H_2O \rightarrow 2CO_2 + 4H_2$	95
	CH_3CH_2COOH	$CH_3CH_2COO^- + 2H_2O \rightarrow CH_3COO^- + CO_2 + 3H_2$	72
	$C_4H_8O_2$	$C_4H_7O_2^- + 2H_2O \rightarrow 2CH_3COO^- + H^+ + 2H_2$	49
Long chain fatty acids	$C_{18}H_{32}O_2$	$C_{18}H_{31}O_2^- + 16H_2O \rightarrow 9CH_3COO^- + 14H_2 + 8H^+$	272
	$C_{18}H_{34}O_2$	$C_{18}H_{33}O_2^- + 16H_2O \rightarrow 9CH_3COO^- + 15H_2 + 8H^+$	338
	$C_{18}H_{36}O_2$	$C_{18}H_{35}O_2^- + 16H_2O \rightarrow 9CH_3COO^- + 16H_2 + 8H^+$	404
	$C_{16}H_{32}O_2$	$C_{16}H_{31}O_2^- + 14H_2O \rightarrow 8CH_3COO^- + 14H_2 + 7H^+$	353
Lactate	$CH_3CH(OH)COOH$	$CH_3CH(OH)COO^- + 2H_2O \rightarrow CH_3COO^- + 2H_2 + H^+ + HCO_3^-$	–4
Alcohol	CH_3CH_2OH	$CH_3CH_2OH + H_2O \rightarrow CH_3COO^- + 2H_2 + H^+$	9
Amino acid	$C_3H_7NO_2$	$C_3H_7NO_2 + 2H_2O \rightarrow CH_3COO^- + 2H_2 + CO_2 + NH_4^+$	10
Alkane	$C_{16}H_{34}$	$4C_{16}H_{34} + 64H_2O \rightarrow 32CH_3COO^- + 68H_2 + 32H^+$	471
Aromatics	C_6H_5COOH	$4C_6H_5COO^- + 6H_2O \rightarrow 3CH_3COO^- + CO_2 + 2H^+ + 3H_2$	50
	C_6H_6O	$C_6H_6O + 5H_2O \rightarrow 3CH_3COO^- + 3H^+ + 2H_2$	10
Methanogenesis			
H_2		$4H_2 + CO_2 \rightarrow CH_4 + 2H_2O$	–131
CH_3COOH		$CH_3COOH + 2H_2O \rightarrow CH_4 + HCO_3^-$	–31
HCOOH		$4HCOOH + H_2O \rightarrow CH_4 + 3HCO_3^-$	–130

The classical syntrophy can be illustrated by the metabolic process of *Methanobacillus omelianskii*, which was turned out to be consisting of two microorganisms – an ethanol-oxidizer (S organism) and a methanogen (*Methanobacillus bryantii*) (Wolin & Wohn, 1967). In the consortia, the S organism fermented ethanol to acetate and H_2, while M. *bryantii* reduced CO_2 to CH_4 by using the produced H_2. It is a symbiotic association since the conversion of ethanol to acetate and H_2 only becomes exergonic when methanogens (or other H_2 consumers) maintain the inhibitory metabolic

final products (*i.e.*, H_2 in this case) concentration low enough. The intermediate H_2 served as an electron carrier. Later, formate was demonstrated as an alternative electron carrier (Boone *et al.*, 1989, Dong *et al.*, 1994, Dong *et al.*, 1994, Dong & Stams, 1995, Stams *et al.*, 2006). The syntrophic butyrate degrader *Syntrophospora bryanti* worked well with formate-utilizing methanogen but not with H_2-only-utilizing methanogen (Dong *et al.*, 1994). The same phenomenon appeared in the methanogenic degradation of propionate by a coculture or triculture of acetogenic bacterium and methanogens. The absence of formate utilizing ability would block the propionate oxidation (Dong *et al.*, 1994). Decades later, a novel mechanism of interspecies electron transfer - direct interspecies electron transfer (DIET) was found in the coculture of *Geobacter metallireducens* and *Geobacter sulfurreducens* (Summers *et al.*, 2010). The two *Geobacter* species formed conductive aggregates allowing direct electron exchange via conductive proteins (*e.g.*, c-type cytochrome and e-pili) during the degradation of ethanol (Summers *et al.*, 2010). Rotaru *et al*. (2014) reported that in the ethanol-fed defined coculture of *G. metallireducens* and *Methanosaeta harundinacea*, CO_2 was reduced to CH_4 by *M. harundinacea* with the accepted electrons via DIET but not other electron carriers. The group also demonstrated that the coculture of *G. metallireducens* and *Methanosarcina barkeri* could also carry out DIET for the degradation of ethanol (Rotaru *et al.*, 2014). All DIET-capable methanogens that have now been described are strictly in the order of Methanosarcinales (*e.g.*, *M. harundinacea*, *Methanothrix soehngenii*, *Methanosarcina horonobensis*, *Methanosarcina mazei, Methanosarcina acetivorans* and *M. barkeri*) (Yee *et al.*, 2019, Yee & Rotaru, 2020, Holmes *et al.*, 2021). Very recently, *Methanobacterium* was reported as a DIET-capable methanogen outside of Methanosarcinales (Zheng *et al.*, 2020). So far, interspecies H_2/formate transfer and DIET are the primary mechanisms of syntrophy. To all the mechanisms, methanogens reduce CO_2 to CH_4 using the electrons carriers

(H_2 or formate) or electron itself generated from syntrophic bacteria. The methanogens are all hydrogenotrophic or aceticlastic ones. None of the strict methylotrophic methanogens have been reported in syntrophic organic matter degradation.

Interconversion among methanogenic precursors

The interconversion among methanogenic precursors (*i.e.*, acetate, formate, H_2, and methanol) is also critical for methanogenic organic matter degradation (Fig. 1.3). The typical process of methanogenic organic matter degradation is like a linear reaction, which is very frangible since methanogens are usually O_2- and pH-sensitive, and only use simple C1- and C2-compounds. The interconversion among methanogenic precursors, to some extent, strengthens the steadiness of methanogenic ecosystems. For instance, acetate - the main intermediate of methanogenic organic matter degradation, on the one hand, can be used as the methanogenic substrate for aceticlastic methanogens. On the other hand, it also can be converted to H_2/CO_2 by some syntrophic bacteria. Although the syntrophic oxidation of acetate has a thermodynamic disadvantage over aceticlastic methanogenesis, it does happen in some systems with high temperature, high concentration of ammonia, or high salinity, which aceticlastic methanogens are quite sensitive to (Dyksma *et al.*, 2020). In these cases, hydrogenotrophic methanogenesis replaces aceticlastic methanogens as the main methane-producing pathway. In the reversed direction, homo-acetogenic bacteria can convert H_2/CO_2 or formate into acetate (*i.e.*, homoacetogenesis process) (Diekert & Wohlfarth, 1994, Muller, 2003, Drake *et al.*, 2013), resulting in a shift of hydrogenotrophic methanogenesis to aceticlastic one. In addition, H_2/CO_2 and formate were proven to be interconvertible (Dolfing *et al.*, 2008, Kim *et al.*, 2010). The overlooked syntrophic conversion of formate to H_2/CO_2 was

found in the coculture of *Moorella* sp. strain AMP or *Desulfovibrio* sp. strain G11 with hydrogenotrophic methanogens (Dolfing *et al.*, 2008).

Besides the well-known interconversion of acetate, H_2/CO_2, and formate, the third main methanogenic precursor - methanol has also been reported as a syntrophic conversion to H_2/CO_2 (Balk *et al.*, 2002) or fermentation to acetate by acetogens (Kremp *et al.*, 2018, Kremp & Muller, 2021). Yet, the reverse reactions for the metabolism of H_2/CO_2, formate, or acetate to methanol have not been demonstrated. However, they might be the precursors of methylated compounds (*e.g.*, methanol). Further research needs to be done to shed light on these metabolisms. It will also help understand the contribution of methylotrophic methanogenesis to syntrophic degradation of organic matter by discovering the missing ecologic niches.

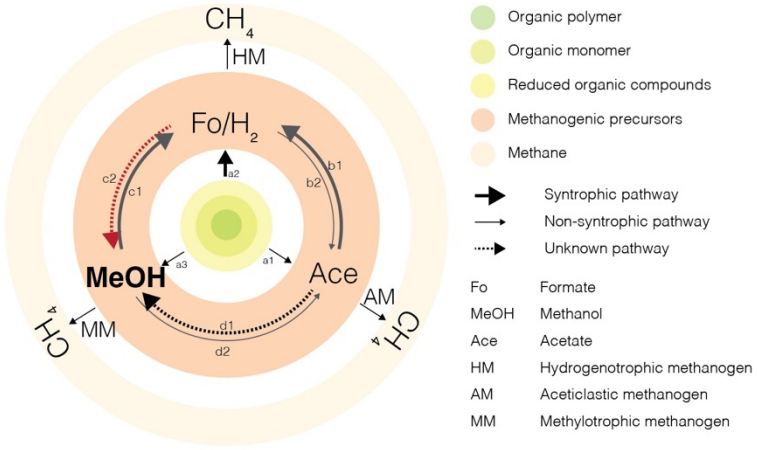

Figure 1.3 Interconversion among methanogenic precursors. The reactions include (1) the degradation of organic matters to acetate (a1), H_2/formate (a2), and methylated compounds (a3); (2) syntrophic acetate degradation (b1) and homoacetogenesis (b2); (3) syntrophic methanol degradation (c1) and unknown conversion of H_2/formate to methanol; (4) unknown conversion of

acetate to methanol and methanol fermentation to acetate (d2); (5) interconversion of H_2 and formate (Fo/H_2)

Thermodynamic advantage of methylotrophic methanogenesis

Under the standard condition, hydrogenotrophic methanogenesis has advantages over the methylotrophic and aceticlastic pathways (Table 2). The situation will change *in situ,* that the methylotrophic methanogenesis may become the most favorable reaction (Table 1.2). For the survival of microorganisms, the minimal H_2 partial pressure for hydrogenotrophic methanogenesis is about 1.5 -12 pa at 25 - 55 °C, assuming the partial pressure of CO_2 and CH_4 are the same, and the minimal energy for ATP synthesis is -20 kJ/mol (for 1/3 mol ATP). For methylotrophic methanogenesis, there is almost no thermodynamic limitation since the required methylated compounds (*e.g.*, methanol) can be lower to the level of pmol. So that, hydrogenotrophic methanogens associated syntrophy may have a less thermodynamic advantage than methylotrophic methanogens under low H_2 partial pressure ecosystems (Nobu *et al.*, 2016). Feldewert *et al.* (2020) confirmed that methyl-reducing methanogens have an energetic advantage over hydrogenotrophic methanogens at low hydrogen partial pressures based on thermodynamic calculation and culture-dependent trials. The methyl-reducing methanogens (*e.g.*, *Methanosphaera stadtmanae*, *Methanimicrococcus blatticola*, *Methanomassiliicoccus luminyensis*) could use hydrogen low to < 0.1 Pa, which was almost one order of magnitude lower than the thresholds for hydrogenotrophic methanogens (Feldewert *et al.*, 2020).

Table 1.2 Gibbs free energy values change for methanogenesis reactions

Reaction	$\Delta G°$ (kJ/mol CH_4)	$\Delta G`$ (kJ/mol CH_4)*

Hydrogenotrophic		
$4H_2 + CO_2 = CH_4 + 2H_2O$	-135	-16.7
$4HCOOH = CH_4 + 3CO_2 + 2H_2O$	-130	-41.9
Methylotrophic		
$4CH_3OH = 3CH_4 + CO_2 + 2H_2O$	-105	-60.5
$CH_3OH + H_2 = CH_4 + H_2O$	-113	-84.1[a], -55.5[b]
Aceticlastic		
$CH_3COOH = CH_4 + CO_2$	-33	-18.7

[*]ΔG` was calculated under the condition of methanogenic precursors at a concentration of 1 pa (H_2) or 10 μM (formate, methanol, and acetate) otherwise standard conditions. [a] under the condition of 10 μM methanol or 1 pa H_2. [b] under the condition of 10 μM methanol and 1 pa H_2.

The prevalence of methylotrophic methanogens

Methylotrophic methanogens are world wild distributed with little known of their ecological roles. All of the isolated and cultured methylotrophic methanogens belonged to Euryarchaeota, distributing in the order of Methanobacterials, Methanosarcinales, and Methanomassiliicoccales. Among these methanogens, only the family Methanosarcinaceae (except for *Methanomicrococcus blatticola*) uses the reducing equivalent generated by the oxidation of 1/4 methylated compounds to reduce other 3/4 methylated compounds to CH_4, namely H_2-independent methylotrophic methanogens, or methyl-fermenting methanogens. Others were all using H_2 as a reductant for the reduction of methylated compounds to CH_4, namely H_2-dependent methylotrophic methanogens, or methyl-reducing methanogens.

With the development of culture-independent technology, more and more methylotrophic methanogens were found outside of the Euryarchaeota phylum, including *Ca.* Bathyarchaeota, *Ca.* Verstraetearchaeota and *Ca.* Korarchaeota. The MAGs data suggested they are capable of H_2-dependent methylotrophic methanogenesis (Evans *et al.*, 2015, Vanwonterghem *et al.*, 2016, Borrel *et al.*, 2019, Evans *et al.*, 2019, Hua *et al.*, 2019, McKay *et al.*, 2019, Sollinger & Urich, 2019, Wang *et al.*, 2019). These uncultured methanogens were not only found in hyperosmotic and hypersaline environments but also distributed in hot springs, wetlands, freshwater sediments, coal beds, and oil reservoirs (Evans *et al.*, 2019, Lewis *et al.*, 2021), indicating their physiological and ecological roles in the global carbon cycle may also unrevealed like the cultured methylotrophic methanogens. For instance, methylotrophic methanogens were found prevalent in reservoirs (Li *et al.*, 2017), although hydrogenotrophic and aceticlastic methanogens were thought as the primary methanogens in the methanogenic petroleum hydrocarbon degradation system (Dolfing *et al.*, 2008, Jones *et al.*, 2008). In some oil reservoirs, methylotrophic methanogens were the dominant methane producer (Pham *et al.*, 2009, Li *et al.*, 2017, Liang *et al.*, 2018, Xu *et al.*, 2019), despite endogenous methyl generation from alkane and other hydrocarbon was undetected (Mesle *et al.*, 2013, Liang *et al.*, 2015). In addition, coal bed was also rich in methylotrophic methanogens, Guo *et al.* (2012) suggested methylotrophic methanogenesis was the primary biogenic methane producing pathway in Eastern Ordos Basin, China. Overall, the contribution of methylotrophic methanogens to the global carbon cycle may be underestimated in the past years. Despite the abundance and phylogenetical diversity, little was known about their physiological and ecological functions. How do methylotrophic methanogens survive in the methyl compounds lacking ecosystems? How do the methyl compounds generate in such ecosystems? The answers

will shed light on the ecological roles of methylotrophic methanogens in carbon cycling and help in understanding the mechanism of methanogenic organic matter degradation.

Importance of Methermicoccus shengliensis ZC-1 and Zhaonella formicivorans K32

Methermicoccus shengliensis ZC-1 was an oil-reservoir-derived thermophilic methylotrophic methanogen, which only used methanol, methylamine, and trimethylamine for the methanogenesis (Cheng *et al.*, 2007). It was shown as the predominant methanogen in the oil reservoir of Shengli oilfield in China although it should be no direct methylated compounds source from the degradation of crude oil (Liang *et al.*, 2018). *Zhaonella formicivorans* K32 was isolated from the same habitat. It was a formate-utilizing thermophile while performing a weak metabolic activity with hydrogenotrophic methanogen (Lv *et al.*, 2020). The physiological and ecological feathers make the two microbes an ideal model for the research on formate-driven methylotrophic methanogenesis – an unknown metabolic pathway as shown in fig 2 (reaction c2).

Purpose of this thesis

The purpose of the research presented in this thesis was to study the role of methylotrophic methanogens in syntrophic organic matter degradation and its microbial mechanism. Methylotrophic methanogen was missing in the syntrophic organic matter degradation process, while it was widespread in diverse ecological system, even in the ones without direct carbon sources. It suggests overlooked metabolic process and ecological roles related with methylotrophic methanogens. To disclose the mysteries, ***Chapter 3*** described a novel syntrophic interaction mediating by unknown compounds (*i.e.*, electron carriers other than the typical molecules H_2 and

formate, and electron). ***Chapter 4*** described the genomic character of the thermophilic formate utilizing bacterium. In ***Chapter 5***, the molecular mechanism of the novel syntrophy was studied. In ***Chapter 6***, the ecological role of methanol-mediated syntrophy was discussed. ***Chapter 7*** described and discussed the results got in this research. The results will greatly expand the possibilities for anaerobic carbon flow by bridging two processes assumed to be independent until now – syntrophic organics degradation and methylotrophic methanogenesis.

Reference

1. Balk M, Weijma J & Stams AJM (2002) *Thermotoga lettingae* sp. nov., a novel thermophilic, methanol-degrading bacterium isolated from a thermophilic anaerobic reactor. *Int J Syst Evol Microbiol* **52**: 1361-1368.
2. Boone DR, Johnson RL & Liu Y (1989) Diffusion of the Interspecies Electron Carriers H(2) and Formate in Methanogenic Ecosystems and Its Implications in the Measurement of K(m) for H(2) or Formate Uptake. *Appl Environ Microbiol* **55**: 1735-1741.
3. Borrel G, Adam PS, McKay LJ*, et al.* (2019) Wide diversity of methane and short-chain alkane metabolisms in uncultured archaea. *Nat Microbiol* **4**: 603-613.
4. Buckel W & Thauer RK (2018) Flavin-Based Electron Bifurcation, Ferredoxin, Flavodoxin, and Anaerobic Respiration With Protons (Ech) or NAD(+) (Rnf) as Electron Acceptors: A Historical Review. *Front Microbiol* **9**: 401.
5. Cheng L, Qiu TL, Yin XB, Wu XL, Hu GQ, Deng Y & Zhang H (2007) *Methermicoccus shengliensis* gen. nov., sp. nov., a thermophilic, methylotrophic methanogen isolated from oil-

production water, and proposal of Methermicoccaceae fam. nov. *Int J Syst Evol Microbiol* **57**: 2964-2969.

6. Conrad R (2020) Importance of hydrogenotrophic, aceticlastic and methylotrophic methanogenesis for methane production in terrestrial, aquatic and other anoxic environments: A mini review. *Pedosphere* **30**: 25-39.
7. Diekert G & Wohlfarth G (1994) Metabolism of homocetogens. *Antonie Van Leeuwenhoek* **66**: 209-221.
8. Dolfing J, Larter SR & Head IM (2008) Thermodynamic constraints on methanogenic crude oil biodegradation. *ISME J* **2**: 442-452.
9. Dolfing J, Jiang B, Henstra AM, Stams AJ & Plugge CM (2008) Syntrophic growth on formate: a new microbial niche in anoxic environments. *Appl Environ Microbiol* **74**: 6126-6131.
10. Dong X & Stams AJ (1995) Evidence for H_2 and formate formation during syntrophic butyrate and propionate degradation. *Anaerobe* **1**: 35-39.
11. Dong X, Cheng G & Stams AJM (1994) Butyrate oxidation by *Syntrophospora bryantii* in co-culture with different methanogens and in pure culture with pentenoate as electron acceptor. *Appl Microbiol Biotechnol* **42**: 647-652.
12. Dong X, Plugge CM & Stams AJ (1994) Anaerobic degradation of propionate by a mesophilic acetogenic bacterium in coculture and triculture with different methanogens. *Appl Environ Microbiol* **60**: 2834-2838.
13. Drake HL, Küsel K & Matthies C (2013) Acetogenic prokaryotes. *The Prokaryotes: Prokaryotic Physiology and Biochemistry* 3-60.
14. Dyksma S, Jansen L & Gallert C (2020) Syntrophic acetate oxidation replaces acetoclastic methanogenesis during thermophilic digestion of biowaste. *Microbiome* **8**: 105.

15. Evans PN, Parks DH, Chadwick GL, Robbins SJ, Orphan VJ, Golding SD & Tyson GW (2015) Methane metabolism in the archaeal phylum Bathyarchaeota revealed by genome-centric metagenomics. *Science* **350**: 434-438.
16. Evans PN, Boyd JA, Leu AO, Woodcroft BJ, Parks DH, Hugenholtz P & Tyson GW (2019) An evolving view of methane metabolism in the Archaea. *Nat Rev Microbiol* **17**: 219-232.
17. Feldewert C, Lang K & Brune A (2020) The hydrogen threshold of obligately methyl-reducing methanogens. *FEMS Microbiol Lett* **367**: 1-7.
18. Guo H, Yu Z, Liu R, Zhang H, Zhong Q & Xiong Z (2012) Methylotrophic methanogenesis governs the biogenic coal bed methane formation in Eastern Ordos Basin, China. *Appl Microbiol Biotechnol* **96**: 1587-1597.
19. Holmes DE, Zhou J, Ueki T, Woodard T & Lovley DR (2021) Mechanisms for Electron Uptake by *Methanosarcina acetivorans* during Direct Interspecies Electron Transfer. *mBio* **12**: e0234421.
20. Hua ZS, Wang YL, Evans PN*, et al.* (2019) Insights into the ecological roles and evolution of methyl-coenzyme M reductase-containing hot spring Archaea. *Nat Commun* **10**: 4574.
21. Jones DM, Head IM, Gray ND*, et al.* (2008) Crude-oil biodegradation via methanogenesis in subsurface petroleum reservoirs. *Nature* **451**: 176-180.
22. Kim YJ, Lee HS, Kim ES*, et al.* (2010) Formate-driven growth coupled with H(2) production. *Nature* **467**: 352-355.
23. Kremp F & Muller V (2021) Methanol and methyl group conversion in acetogenic bacteria: biochemistry, physiology and application. *FEMS Microbiol Rev* **45**: 1-22.
24. Kremp F, Poehlein A, Daniel R & Muller V (2018) Methanol metabolism in the acetogenic bacterium *Acetobacterium woodii*. *Environ Microbiol* **20**: 4369-4384.

25. Lewis WH, Tahon G, Geesink P, Sousa DZ & Ettema TJG (2021) Innovations to culturing the uncultured microbial majority. *Nat Rev Microbiol* **19**: 225-240.
26. Li X-X, Mbadinga SM, Liu J-F, Zhou L, Yang S-Z, Gu J-D & Mu B-Z (2017) Microbiota and their affiliation with physiochemical characteristics of different subsurface petroleum reservoirs. *International Biodeterioration & Biodegradation* **120**: 170-185.
27. Li XX, Liu JF, Zhou L, Mbadinga SM, Yang SZ, Gu JD & Mu BZ (2017) Diversity and Composition of Sulfate-Reducing Microbial Communities Based on Genomic DNA and RNA Transcription in Production Water of High Temperature and Corrosive Oil Reservoir. *Front Microbiol* **8**: 1011.
28. Liang B, Wang LY, Mbadinga SM, Liu JF, Yang SZ, Gu JD & Mu BZ (2015) Anaerolineaceae and Methanosaeta turned to be the dominant microorganisms in alkanes-dependent methanogenic culture after long-term of incubation. *AMB Express* **5**: 117.
29. Liang B, Zhang K, Wang LY, Liu JF, Yang SZ, Gu JD & Mu BZ (2018) Different Diversity and Distribution of Archaeal Community in the Aqueous and Oil Phases of Production Fluid From High-Temperature Petroleum Reservoirs. *Front Microbiol* **9**: 841.
30. Liu Y, Priscu JC, Xiong J, Conrad R, Vick-Majors T, Chu H & Hou J (2016) Salinity drives archaeal distribution patterns in high altitude lake sediments on the Tibetan Plateau. *FEMS Microbiol Ecol* **92**.
31. Lloyd MK, Trembath-Reichert E, Dawson KS, Feakins SJ, Mastalerz M, Orphan VJ, Sessions AL & Eiler JM (2021) Methoxyl stable isotopic constraints on the origins and limits of coal-bed methane. *Science* **374**: 894-897.
32. Lv XM, Yang M, Dai LR*, et al.* (2020) *Zhaonella formicivorans* gen. nov., sp. nov., an anaerobic formate-utilizing bacterium isolated from Shengli oilfield, and proposal of four

novel families and Moorellales ord. nov. in the phylum Firmicutes. *Int J Syst Evol Microbiol* **70**: 3361-3373.

33. Lyu Z, Shao N, Akinyemi T & Whitman WB (2018) Methanogenesis. *Curr Biol* **28**: R727-R732.
34. Mayumi D, Mochimaru H, Tamaki H, Yamamoto K, Yoshioka H, Suzuki Y, Kamagata Y & Sakata S (2016) Methane production from coal by a single methanogen. *Science* **354**: 222-225.
35. McKay LJ, Dlakic M, Fields MW, Delmont TO, Eren AM, Jay ZJ, Klingelsmith KB, Rusch DB & Inskeep WP (2019) Co-occurring genomic capacity for anaerobic methane and dissimilatory sulfur metabolisms discovered in the Korarchaeota. *Nat Microbiol* **4**: 614-622.
36. Mesle M, Dromart G & Oger P (2013) Microbial methanogenesis in subsurface oil and coal. *Res Microbiol* **164**: 959-972.
37. Muller V (2003) Energy conservation in acetogenic bacteria. *Appl Environ Microbiol* **69**: 6345-6353.
38. Narihiro T, Nobu MK, Tamaki H, Kamagata Y, Sekiguchi Y & Liu WT (2016) Comparative Genomics of Syntrophic Branched-Chain Fatty Acid Degrading Bacteria. *Microbes Environ* **31**: 288-292.
39. Nobu MK, Narihiro T, Kuroda K, Mei R & Liu WT (2016) Chasing the elusive Euryarchaeota class WSA2: genomes reveal a uniquely fastidious methyl-reducing methanogen. *ISME J* **10**: 2478-2487.
40. Nobu MK, Narihiro T, Rinke C, Kamagata Y, Tringe SG, Woyke T & Liu WT (2015) Microbial dark matter ecogenomics reveals complex synergistic networks in a methanogenic bioreactor. *ISME J* **9**: 1710-1722.

41. Pham VD, Hnatow LL, Zhang S, Fallon RD, Jackson SC, Tomb JF, DeLong EF & Keeler SJ (2009) Characterizing microbial diversity in production water from an Alaskan mesothermic petroleum reservoir with two independent molecular methods. *Environ Microbiol* **11**: 176-187.
42. Rotaru A-E, Shrestha PM, Liu F, Shrestha M, Shrestha D, Embree M, Zengler K, Wardman C, Nevin KP & Lovley DR (2014) A new model for electron flow during anaerobic digestion: direct interspecies electron transfer to *Methanosaeta* for the reduction of carbon dioxide to methane. *Energy Environ Sci* **7**: 408-415.
43. Rotaru AE, Shrestha PM, Liu F, Markovaite B, Chen S, Nevin KP & Lovley DR (2014) Direct interspecies electron transfer between *Geobacter metallireducens* and *Methanosarcina barkeri*. *Appl Environ Microbiol* **80**: 4599-4605.
44. Sieber JR, McInerney MJ & Gunsalus RP (2012) Genomic insights into syntrophy: the paradigm for anaerobic metabolic cooperation. *Annu Rev Microbiol* **66**: 429-452.
45. Sollinger A & Urich T (2019) Methylotrophic methanogens everywhere - physiology and ecology of novel players in global methane cycling. *Biochem Soc Trans* **47**: 1895-1907.
46. Sorokin DY, Makarova KS, Abbas B*, et al.* (2017) Discovery of extremely halophilic, methyl-reducing euryarchaea provides insights into the evolutionary origin of methanogenesis. *Nat Microbiol* **2**: 17081.
47. Stams AJ, de Bok FA, Plugge CM, van Eekert MH, Dolfing J & Schraa G (2006) Exocellular electron transfer in anaerobic microbial communities. *Environ Microbiol* **8**: 371-382.
48. Summers ZM, Fogarty HE, Leang C, Franks AE, Malvankar NS & Lovley DR (2010) Direct exchange of electrons within aggregates of an evolved syntrophic coculture of anaerobic bacteria. *Science* **330**: 1413-1415.

49. Thauer RK, Kaster AK, Seedorf H, Buckel W & Hedderich R (2008) Methanogenic archaea: ecologically relevant differences in energy conservation. *Nat Rev Microbiol* **6**: 579-591.
50. Vanwonterghem I, Evans PN, Parks DH, Jensen PD, Woodcroft BJ, Hugenholtz P & Tyson GW (2016) Methylotrophic methanogenesis discovered in the archaeal phylum Verstraetearchaeota. *Nat Microbiol* **1**: 16170.
51. Wang Y, Wegener G, Hou J, Wang F & Xiao X (2019) Expanding anaerobic alkane metabolism in the domain of Archaea. *Nat Microbiol* **4**: 595-602.
52. Wolin EA & Wohn MJ (1967) *Methanobacillus omelianskii*, a symbiotic association of two species of bacteria. *Archiv ifir Mikrobiologie* **31**: 20-31.
53. Xu D, Zhang K, Li B-G, Mbadinga SM, Zhou L, Liu J-F, Yang S-Z, Gu J-D & Mu B-Z (2019) Simulation of in situ oil reservoir conditions in a laboratory bioreactor testing for methanogenic conversion of crude oil and analysis of the microbial community. *International Biodeterioration & Biodegradation* **136**: 24-33.
54. Yee MO & Rotaru AE (2020) Extracellular electron uptake in Methanosarcinales is independent of multiheme c-type cytochromes. *Sci Rep* **10**: 372.
55. Yee MO, Snoeyenbos-West OL, Thamdrup B, Ottosen LDM & Rotaru A-E (2019) Extracellular Electron Uptake by Two *Methanosarcina* Species. *Frontiers in Energy Research* **7**: 1-10.
56. Zhang X, Zhang H & Cheng L (2019) Key players involved in methanogenic degradation of organic compounds: progress on the cultivation of syntrophic bacteria. *Acta Microbiol Sin* **59**: 211-223.
57. Zheng S, Liu F, Wang B, Zhang Y & Lovley DR (2020) *Methanobacterium* Capable of Direct Interspecies Electron Transfer. *Environ Sci Technol* **54**: 15347-15354.

58. Zhou Z, Zhang CJ, Liu PF*, et al.* (2022) Non-syntrophic methanogenic hydrocarbon degradation by an archaeal species. *Nature* **601**: 257-262.

Chapter 2 Methodology

Microorganisms

Zhaonella formicivorans K32 and *Methermicoccus shengliensis* ZC-1 were obtained from Biogas Institute CCAM (China collection of anaerobic microorganisms). *M. shengliensis* AmaM and *Methanothermobacter thermautotrophicus* TM and *Methanothermobacter thermautotrophicus* ΔH were preserved in-house from previous studies (Kato *et al.*, 2014, Mayumi *et al.*, 2016).

Medium preparation

The medium recipes are as follows. All media were prepared anaerobically with the protection of O_2-free gas N_2/CO_2 (4:1[v/v]). In detail, the prepared medium was degassed by vacuumizing under ultrasonic treatment. The degassed medium was dispensed into in serum vials and purged with N_2/CO_2 (4:1[v/v]) for 5-10 minutes then sealed with butyl rubber stoppers and aluminum seals (Tokyo Garasu Kikai, Japan). All media were autoclaved at 121 ℃ for 20 min.

(1) IET basal medium (Kato *et al.*, 2015)

Component	g/L or ml/L
KH_2PO_4	0.30 g
NH_4Cl	1.00 g
$MgCl_2 \cdot 6H_2O$	0.10 g
$CaCl_2 \cdot 2\ H_2O$	0.08 g
NaCl	0.60 g
$KHCO_3$	2.00 g
$MgSO_4 \cdot 7H_2O$	0.02 g
HEPES	9.52 g
Bacto™ Yeast Extract	0.10 g
Vitamin	10.00 ml

Trace elements solution	10.00 ml

Adjust pH to 6.5 with 6M KOH

(2) Coculture basal medium

Component	g/L or ml/L
KCl	0.35 g
NaCl	5.00 g
K_2HPO_4	0.20 g
$MgCl_2 \cdot 6H_2O$	10.20 g
$NaHCO_3$	1.00 g
HEPES	9.52 g
Bacto™ Yeast Extract	0.10 g
Vitamin solution	10.00 ml
Trace elements solution	10.00 ml

Adjust pH to 6.5 with 6M KOH

(2) Vitamin solution

Component	mg/L
Biotin	2
Folic acid	2
Pyridoxine·HCl	10
Thiamine·HCl	5
Riboflavine	5
Nicotinic acid	5
Ca-pantothenate	5
p-Aminobenzoic acid	5
Vitamin B12	0.01

Lipoic acid	5
Distilled water	1 L

Store in dark at 4 ℃

(3) Trace elements solution

Component	g/L or mg/L
Nitrilotriacetic acid (NTA)	12.80 g
$FeCl_3 \cdot 6H_2O$	1.35 g
$MnCl_2 \cdot 4H_2O$	0.10 g
$CoCl_2 \cdot 6H_2O$	0.024 g
$CaCl_2 \cdot 2H_2O$	0.10 g
$ZnCl_2$	0.10 g
$CuCl_2 \cdot 2H_2O$	0.025 g
H_3BO_3	0.01 g
$Na_2MoO_4 \cdot 2H_2O$	0.02 g
NaCl	1.00 g
$NiCl_2 \cdot 6H_2O$	0.12g
$Na_2SeO_3 \cdot 5H_2O$	4.0 mg
$Na_2WO_4 \cdot 2H_2O$	4.5 mg
Distilled water	1L

First dissolve nitrilotriacetic acid and adjust pH to 6.5 with KOH, and then add other minerals.

Store at 4 ℃

(4) Reagents stock solution

$Na_2S \cdot 9H_2O$ (6% [w/v]), cysteine-$HCl \cdot H_2O$ (6% [w/v]), methanol (4M), trimethylamine (1M) solution were prepared anaerobically and filter-sterilized (0.22 μm) with the protection of N_2

atmosphere. Yeast extract (10% [w/v]) and sodium formate (4M) were prepared anaerobically and then autoclave-sterilized (121 ℃, 20 min).

Cultivation condition

Z. *formicivorans* K32 was pre-cultured in the IET medium with yeast extract (0.5% [w/v]). *M. thermautotrophicus* TM was pre-cultured in the IET medium with H_2/CO_2 (4:1 [v/v]), 0.2 MPa). *M.* shengliensis ZC-1 and AmaM were pre-cultured in medium described by Cheng *et al.* (2007) using methanol (40 mM) as the sole energy and carbon source. K32/ZC-1 and K32/AmaM co-cultures were cultivated using coculture basal medium with 20 mM formate at 55 °C. K32/TM co-cultures were cultivated in IET medium with glycine and methylated compounds including methanol and trimethylamine.

For all cultures, the reducing agents (*i.e.*, 0.3 g/L each of $Na_2S·9H_2O$ and cysteine-$HCl·H_2O$) and energy and carbon sources, including yeast extract (5.0 g/L), methanol (40 mM), sodium formate (20 mM) were supplemented to the sterilized medium from filter- or autoclave-sterilized stock solutions. For autotrophic cultivation, gas phase was replaced with H_2/CO_2 (4:1 [v/v], 0.2 MPa). All strains were routinely cultivated under anaerobic condition in serum vials under an atmosphere of N_2/CO_2 (4:1 [vol/vol]) (unless stated otherwise) sealed with butyl rubber stoppers and aluminum seals (Tokyo Garasu Kikai, Japan) without shaking at 55 °C.

For the establishment of K32/ZC-1 and K32/AmaM co-cultures, 5% (v/v) of pre-cultured *Z. formicivorans* K32 and *M. shengliensis* (ZC-1 or AmaM) were inoculated into coculture basic medium with 20 mM formate. Subcultures of K32/ZC-1 co-cultures were used for transcriptome analysis. Cultures without additional formate were used as negative controls.

Scanning electron microscopy

Scanning electron microscopy was performed for the observation of cell-to-cell interaction as described previously (Igarashi *et al.*, 2019). Sample preparation steps are as follows,

(1) Prepare fixation buffer (2% glutaraldehyde (w/v) in 0.1 M sodium cacodylate buffer), wash buffer (0.1 M sodium cacodylate buffer), ethanol dilution, and t-butanol.
(2) Submerge samples into fixation buffer and incubate at room temperature for 60 min.
(3) Replace fixation buffer by wash the samples with 0.1 M sodium cacodylate buffer for twice, 10 min each.
(4) Dehydrate the samples with an ascending ethanol series as follows at room temperature: 25% for 1-3 min, 50% for 1-3 min, 70% for 15 min, 90% for 15 min, 95% for 15 min, 100% for 10 min for three times.
(5) Substitute ethanol with the mixture of 100% ethanol/ t-butanol (1:1) and the by t-butanol for three times, 10 min for each.
(6) Freezer (-20 °C) samples to solidify t- butanol for more than 30 min.
(7) Dry the samples by t- butanol freeze dryer (VFD-21S, Japan).
(8) Attach the dried sample to glass plate or aluminum stub for observation.

Chemical analysis

CH_4 and H_2 in the gas phases were measured using a gas chromatograph (GC- 2014, Shimadzu, Japan) equipped with Rt-QPLOT column (30m, 0.32 mm, Restek, Bellefone, RA, United States) and molecular sieve 13X column (Shimadzu), a thermal conductivity detector and a flame ionization detector described by Kato *et al*. (2014).

Organic acids (including formate and acetate) and methanol were analyzed by a high-performance liquid chromatography system (D-2000 LaChrom Elite HPLC, HITACHI, Japan) equipped with Aminex HPX-87H column (BioRad Laboratories), a L2400 UV detector and a RI detector, using 10 mM H_2SO_4 as the mobile phase at a flow rate of 0.7 ml/min (Igarashi *et al.*, 2019).

DNA and RNA extraction, sequencing, and data processing

DNA and RNA for sequencing were extracted from cultures in exponential phase. Cells were collected by centrifugation (17000 × *g*) at 4 °C for 5-15 min.

DNA was extracted using bacteria DNA extraction kit (DP302, TIANGEN, China) after pretreated by bead-beating (6.0 m/s for 45 s twice, 0.5 g of 0.1-mm glass beads [G4649, Sigma]) as previous report (Cheng *et al.*, 2014).

Whole genome sequencing of strain K32 was performed on a Nanopore PromethION platform (GrandOmics Biosciences, Wuhan, China). Genome was assembled using in house pipeline including unicycler v0.4.8 (off) (Wick *et al.*, 2017) and flye v2.8 (--plasmids --nano-raw) (Kolmogorov *et al.*, 2019) and then adjusted by pilon v1.23 (default) (Walker *et al.*, 2014), nextpolish v1.2.4 (default) (Hu *et al.*, 2020) and circulator v1.5.1 (fixstart) (Hunt *et al.*, 2015).

For total RNA extraction, the cell pellet was suspended in 100 µl lysozyme working solution (2 mg/ml in TE buffer, pH 8.0) and incubated at room temperature for 10 mins. The hydrolysate was then transferred into 2-mL polypropylene tubes containing silica beads (Lysing Matrix E, MP Biomedicals) with 1.0 ml ISOGEN II (Nippon Gene, Japan) and 0.2 ml chloroform. The resulting slurry was homogenized in a Fastprep 24 instrument (version 4, MP Biomedicals) for 40 s at a speed of 6.0 m/s. The aqueous layer was recovered after centrifugation (15,000 × *g*, 4 °C, 5 min)

for the purification of total RNA using a RNeasy Mini kit (Qiagen) with DNase treatment (RNase-free DNase set, Qiagen) as described in the manufacturer's instructions. The purified total RNA was spectroscopically quantified using a NanoDrop ND-1000 spectrophotometer (NanoDrop Technologies) (Kato *et al.*, 2014).

For RNA sequencing, the quality of total RNA was analyzed by 5200 fragment Analyzer System using Agilent HS RNA Kit (Agilent Technologies). Fragment libraries were generated by using MGIEasy RNA Directional Library Prep Set (MGI Tech) after removing rRNA using riboPool (siTOOLs Biotech), according to manufacturer's instructions. The library quantity and quality were measured by a Qubit 3.0 Fluorometer using dsDNA HS Assay Kit (Thermo Fisher Scientific) and a Fragment Analyzer using dsDNA 915 Reagent Kit. Circular DNA libraries were prepared using MGIEasy Circularization Kit (MGI Tech). DNA Nanoball (DNB) was made by using DNBSEQ-G400RS High-throughput Sequencing Kit (MGI Tech). Sequencing was performed using DNBSEQ-G400 sequencer under DNBSEQ-G400RS High-throughput Sequencing Set at 2x200 bp model by Bioengineering Lab (Kanagawa, Japan). The raw reads were trimmed by Trimmomatic v0.39 (phred33, ILLUMINACLIP: 2:30:10, LEADING:3, TRAILING:3, SLIDINGWINDOW:6:30 MINLEN:33) (Bolger *et al.*, 2014) and mapped to genomes of K32 and ZC-1 (GCA_000711905.1) using BBMap v38.88 (minid=0.99) (sourceforge.net/projects/bbmap/). The gene expression level was calculated as reads per kilobase transcript per million reads (RPKM) and then normalized to the average of ribosomal protein of each sample.

Concentrated cell experiment

Yeast extract-fed K32 cells from exponential phase culture were harvested by centrifugation at 10,000 × *g* for 5 min and washed three times with 10 mL yeast extract-free IET medium under

anoxic condition. The pellets were resuspended and transferred into anaerobic serum vials and purged with N_2 gas for 10 min. The resuspended cells were then inoculated in a medium containing 60 mM sodium formate with 20 times cell density as the preculture. Organic acids and alcohols were analyzed after incubation at 55 ˚C.

Isotopic tracer experiments

K32/ZC-1 co-culture was cultivated in 20 ml medium. Bicarbonate-free basal medium with N_2 as the gas atmosphere was prepared firstly. 0.5 mM [^{12}C] bicarbonate and 20 mM [^{13}C]- or [^{12}C]-formate were supplemented to the medium from sterilized stock solutions after autoclaving. Sampling and the determination of [^{13}C] content of methane and CO_2 were performed as described previously (Igarashi *et al.*, 2019).

Thermodynamic calculations

Gibbs free energy change (ΔG) was calculated based on ΔG_f^0 and ΔH_f^0 values at 298 K and adjusted to *in situ* temperature (55 ˚C) using Gibbs-Helmholtz equation and van't Hoff equation (Hanselmann, 1991).

Data availability

The genome sequence of *Zhaonella formicivorans* K32 has been deposited in eLMSG (an eLibrary of Microbial Systematics and Genomics, https://www.biosino.org/elmsg/index) under accession number LMSG_G000003453.1 and is also available under NCBI Bioproject PRJNA523471.

The draft genome and the raw sequence data of *Natroniella acetigena* Z-7937^T have been deposited at NCBI GenBank and Sequence Read Archive (SRA) under the accession numbers JALKBX000000000 and SRR19259016.

The draft genome and the raw sequence data of *Fuchsiella alkaliacetigena* Z-7100^T have been deposited at NCBI GenBank and Sequence Read Archive (SRA) under the accession number JALKBZ000000000, and SRR19261504.

The transcriptomics data have been deposited in NODE (http://www.biosino.org/node) with accession number OEP002841.

Reference

1. Bolger AM, Lohse M & Usadel B (2014) Trimmomatic: a flexible trimmer for Illumina sequence data. *Bioinformatics* **30**: 2114-2120.
2. Cheng L, Shi S, Li Q, Chen J, Zhang H & Lu Y (2014) Progressive degradation of crude oil n-alkanes coupled to methane production under mesophilic and thermophilic conditions. *PLoS One* **9**: e113253.
3. Cheng L, Qiu TL, Yin XB, Wu XL, Hu GQ, Deng Y & Zhang H (2007) *Methermicoccus shengliensis* gen. nov., sp. nov., a thermophilic, methylotrophic methanogen isolated from oil-production water, and proposal of Methermicoccaceae fam. nov. *Int J Syst Evol Microbiol* **57**: 2964-2969.
4. Hanselmann KW (1991) Microbial energetics applied to waste repositories. *Experientia* **47**: 645-687.

5. Hu J, Fan J, Sun Z & Liu S (2020) NextPolish: a fast and efficient genome polishing tool for long-read assembly. *Bioinformatics* **36**: 2253-2255.
6. Hunt M, Silva ND, Otto TD, Parkhill J, Keane JA & Harris SR (2015) Circlator: automated circularization of genome assemblies using long sequencing reads. *Genome Biol* **16**: 294.
7. Igarashi K, Miyako E & Kato S (2019) Direct Interspecies Electron Transfer Mediated by Graphene Oxide-Based Materials. *Front Microbiol* **10**: 3068.
8. Kato S, Yumoto I & Kamagata Y (2015) Isolation of acetogenic bacteria that induce biocorrosion by utilizing metallic iron as the sole electron donor. *Appl Environ Microbiol* **81**: 67-73.
9. Kato S, Sasaki K, Watanabe K, Yumoto I & Kamagata Y (2014) Physiological and transcriptomic analyses of the thermophilic, aceticlastic methanogen *Methanosaeta thermophila* responding to ammonia stress. *Microbes Environ* **29**: 162-167.
10. Kolmogorov M, Yuan J, Lin Y & Pevzner PA (2019) Assembly of long, error-prone reads using repeat graphs. *Nat Biotechnol* **37**: 540-546.
11. Mayumi D, Mochimaru H, Tamaki H, Yamamoto K, Yoshioka H, Suzuki Y, Kamagata Y & Sakata S (2016) Methane production from coal by a single methanogen. *Science* **354**: 222-225.
12. Walker BJ, Abeel T, Shea T*, et al.* (2014) Pilon: an integrated tool for comprehensive microbial variant detection and genome assembly improvement. *PLoS One* **9**: e112963.
13. Wick RR, Judd LM, Gorrie CL & Holt KE (2017) Unicycler: Resolving bacterial genome assemblies from short and long sequencing reads. *PLoS Comput Biol* **13**: e1005595.

Chapter 3 A novel syntrophy mediated by unusual electron carriers

Introduction

In Earth's anaerobic ecosystems, microbial organic compound degradation often cannot access respirable electron acceptors and encounter thermodynamic restrictions (Schink, 1997). To overcome this, anaerobes rely on a cross-domain symbiosis, in which a bacterium oxidizes the organic compound and hands off the byproduct electrons to a partner archaeon that disposes them through reductive methane generation (*i.e.*, syntrophy) (Stams & Plugge, 2009). Thus far, three major forms of syntrophy have been reported: H_2 and formate exchange or direct interspecies electron transfer (Wolin & Wohn, 1967, Thiele & Zeikus, 1988, Boone *et al.*, 1989, Dong *et al.*, 1994, Dong *et al.*, 1994, Rotaru *et al.*, 2014, Rotaru *et al.*, 2014). However, none take the methylotrophic methanogens involved in. The all methanogens participated in syntrophic organic compound degradation were hydrogenotrophic methanogens (mainly for H_2 and formate exchange) and aceticlastic methanogens (generally for direct interspecies electron transfer) (Fig. 3.1).

Natural sources of methylated compounds are diverse (*e.g.*, lignin-derived compounds, algae-derived dimethyl sulfide, animal-derived choline, and natural osmolytes like methylglycines) but not ubiquitous, especially in anaerobic ecosystems often lacking the above sources (Mesle *et al.*, 2013, Sousa *et al.*, 2018), yet methanogens specialized in methylotrophy are pervasive (Gao *et al.*, 2016, Li *et al.*, 2017, Liang *et al.*, 2018, Xu *et al.*, 2019). This suggests the presence of endogenous metabolic processes that generate methylated compounds and we hypothesized that one potential source are other one-carbon (C1) compounds (*i.e.*, no direct link with multi-carbon catabolic processes) with the most likely being formate, a C1 compound widely produced by anaerobic organic matter degradation (Dong & Stams, 1995, McInerney *et al.*, 2008, Yang *et al.*, 2016, Nobu *et al.*, 2017) (Fig. 3.1).

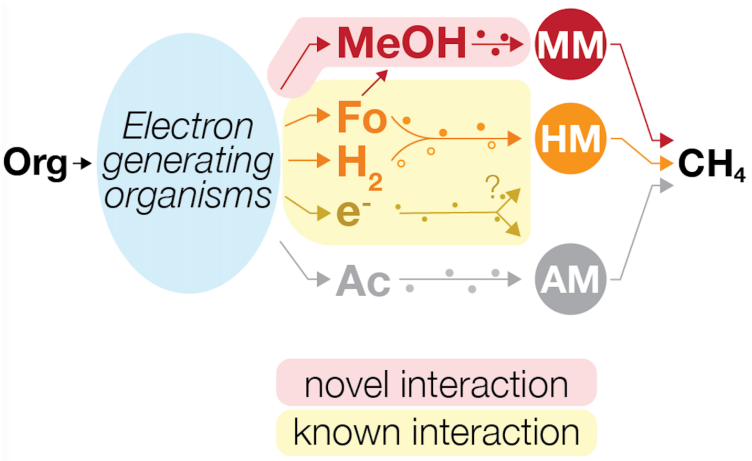

Figure 3.1 Schematic diagram of methylated compounds involving methanogenic organics degradation. The proposed formate-based methylotrophic pathway is showed in red. MM, methylotrophic methanogens; HM, hydrogenotrophic methanogens; AM, aceticlastic methanogens; Org, organic matter; MeOH, methanol; Fo, formate; Ac, acetate

Here, we discover a novel symbiotic interaction through establishing a co-culture between an anaerobic formate-utilizing bacterium (*Zhaonella formicivorans* K32 (Lv *et al.*, 2020) and obligate methylotrophic archaea (*Methermicoccus shengliensis* ZC-1 and AmaM (Cheng et al., 2007, Mayumi et al., 2016)). Experimental evidence indicated a novel mechanism excluding H_2 and formate exchange or direct interspecies electron transfer involved in this interaction.

Result and discussion

Methanol generation for formate-fed culture

Formate is one of the main metabolic products of anaerobic organic matter degradation. It is not only the methanogenic substrate for formate-utilizing hydrogenotrophic methanogens, but also provides energy and carbon sources for anaerobes like acetogens. Although the energetic limitation

of the conversion of formate to bicarbonate and H_2 ($\Delta G° = +5.2$ kJ/mol, pH 7.0), growth on formate-oxidizing and H_2-producing has been found in syntrophic communities of *Moorella* sp. strain AMP / *Methanothermobacter* sp. strain NJ1 and *Desulfovibrio* sp. strain G11 / *Methanobrevibacter arboriphilus* AZ1 (Dolfing *et al.*, 2008) and a single thermophilic bacterium *Thermococcus onnurineus* NA1 with a growth temperature of 80 °C ($\Delta G` = -8 \sim -20$ kJ/mol). *Z. formicivorans* K32 was a recently isolated formate utilizer while showing weak formate degradation activity with a conventional H_2-utilizing partner - *Methanothermobacter thermautotrophicus* ΔH (Lv *et al.*, 2020), indicating the H_2-mediated syntrophic degradation might not be the central metabolism. It had been suggested a metabolic relationship between formate and methanol in anaerobic sulfur-reducing bacterium *Desulfotomaculum kuznetsovii* performing by alcohol dehydrogenase and aldehyde ferredoxin oxidoreductase (Sousa *et al.*, 2018). Considering the phylogenetic closest relatives (*i.e.*, *Moorella*) of *Z. formicivorans* K32 were capable of methylated compounds metabolism (Drake & Daniel, 2004), here we look to the metabolic ability of formate and methanol for *Z. formicivorans* K32. The strain extremely poorly used formate alone (Lv *et al.*, 2020). Incubation of concentrated resting cells with formate revealed a weak degradation of formate and a slight accumulation of methanol (Fig. 3.2), in agree with the hypothesis that formate could be the precursor of methylated compounds (*i.e.*, methanol). It had been reported that *Moorella* sp. strain AMP carried out a syntrophic lifestyle with H_2-consuming methanogen in methanol-fed culture lacking cobalt, which was unlike the acetogenic growth with cobalt (Jiang *et al.*, 2009). The former one may employ a methanol dehydrogenase conducing methanol oxidation to formaldehyde as *D. kuznetsovii*, while the later one applied a typical corrinoid-containing methyltransferase for methanol degradation. Considering the metabolic results and phylogenetic relationship, it showed a possibility that *Z. formicivorans* K32 also possessed a pathway for the

conversion of formate to methanol with most likely alcohol dehydrogenase and aldehyde ferredoxin oxidoreductase.

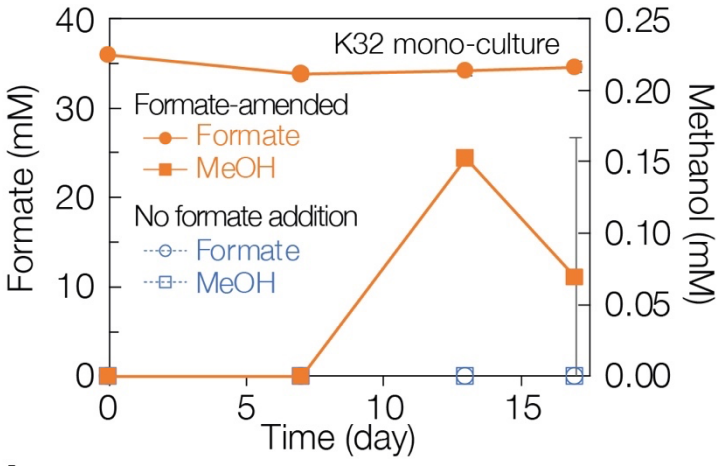

Figure 3.2 Formate degradation for *Z. formicivorans* monoculture (a) and Methanol production of formate-fed *Z. formicivorans* concentrated resting cells (b)

Methanogenesis of formate-fed cocultures

Co-cultivation of *Z. formicivorans* K32 with an obligate methylotrophic methanogen isolated from the same habitat (*i.e.*, oil reservoir) - *M. shengliensis* ZC-1, showed a drastically higher rate and extent of formate degradation compared to when incubated with the H_2-utilizing partner (Lv *et al.*, 2020) (Fig. 3.3a), indicating that methylated compounds are likely the primary interspecies electron carrier for *Z. formicivorans* K32. Consumption of 8.05 mM formate resulted in the formation of 1.83 mM CH_4, which is consistent with the reaction $4HCOO^- + H_2O + H^+ = CH_4 + 3HCO_3^-$. This rapid formate degradation was replicable using a co-culture with another strain of *M. shengliensis* (*i.e.*, AmaM) having 10.25 mM formate consumption with 2.29 mM CH_4 generation (Fig. 3.3b).

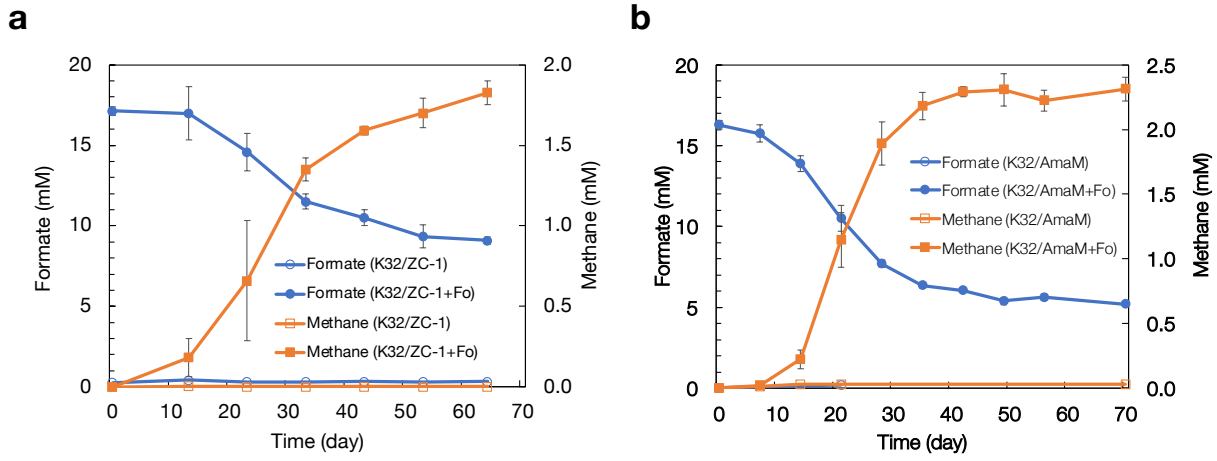

$4HCOO^- + H_2O + H^+ = CH_4 + 3HCO_3^-$ $4HCOO^- + H_2O + H^+ = CH_4 + 3HCO_3^-$

(8.05 mM) (1.83 mM) (10.25 mM) (2.29 mM)

Figure 3.3 Formate-driven methanogenesis of *Z. formicivorans* K32 / *M. shengliensis* ZC-1 coculture (a) and *Z. formicivorans* K32 / *M. shengliensis* AmaM coculture (b).

Z. formicivorans K32 / *M. shengliensis* cocultures formed aggregates during growth (Fig 3.4 d and e). In agreement with previous studies that the formation of aggregates promoted the syntrophic relationship and the metabolic rate (Shen *et al.*, 2016). The cell shape of *Z. formicivorans* K32 in the cocultures become longer than the yeast extract-fed monoculture. It was not clear for the change of cell shape. Under syntrophic condition, the cells were suffering energy constraint. The changes might improve the molecule transport and exchange rate between cells, which would be beneficial to syntrophic lifestyle.

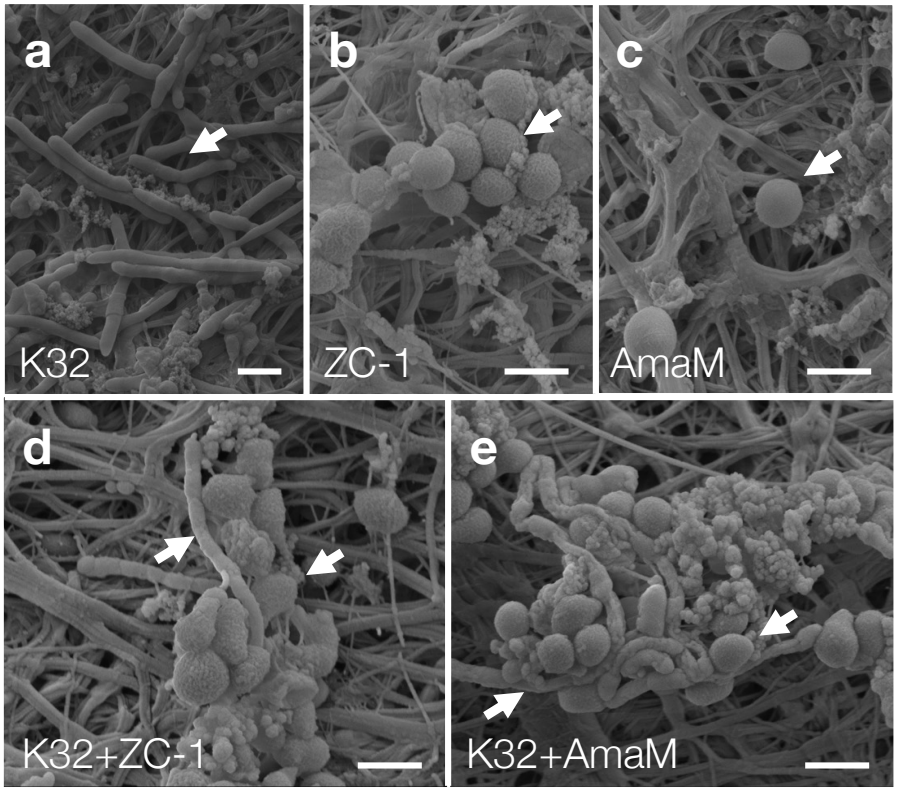

Figure 3.4 Scanning electron micrograph of yeast extract-fed *Z. formicivorans* K32 monoculture (a), methanol-fed *M. shengliensis* ZC-1monoculture (b), and AmaM monoculture (c), formate-fed co-culture of *Z. formicivorans* K32 and *M. shengliensis* ZC-1 (d) or AmaM (e). Arrows indicate cells of *Z. formicivorans* (rods) and *M. shengliensis* (cocci). Bar, 1 μm.

H_2-independent methanogenesis of formate-fed cocultures

The triculture of *Z. formicivorans, M. shengliensis,* and *M. thermautotrophicus* had a higher CH_4 production and formate degradation over the coculture of *Z. formicivorans* and *M. shengliensis* (Fig. 3.5a, b). However, the formate degradation and methane production patterns were similar in these two conditions. It's possible that the amended hydrogenotrophic methanogen strain ΔH drove

other H_2 producing reactions since the hydrogen in the triculture showed a lower hydrogen partial pressure (about 20 pa) than in the coculture (about 60-70 pa, Fig. 3.5c). Considering the weak syntrophic interaction of strain ΔH with strain K32, the syntrophic formate degradation pattern seems did not changed in the triculture. Gene expression profiles will help understand the syntrophic formate degradation pattern (will be discussed latter).

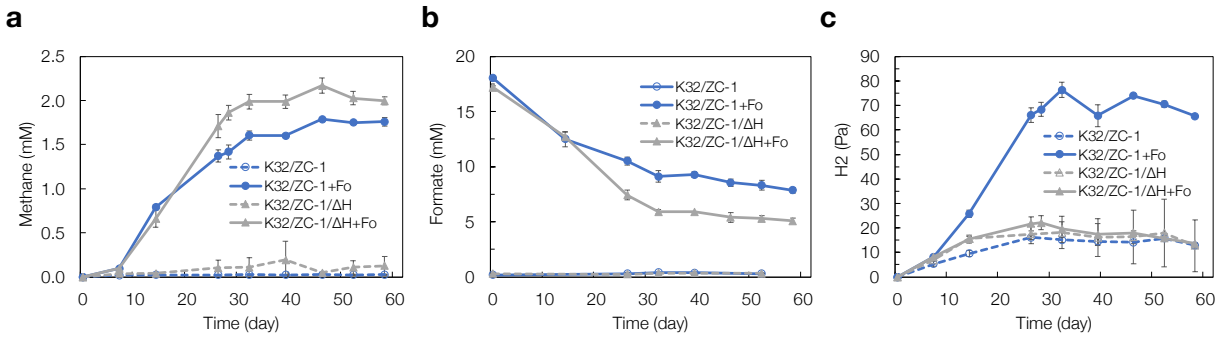

Figure 3.5 Formate and methane changes of formate-fed K32/ZC-1/ΔH triculture. Fo, formate. Error bars represent the standard deviation of the triplicates.

Despite the promotion of catabolism by hydrogenotrophic methanogen, formate utilization and methane generation by *Z. formicivorans* K32 with *M. shengliensis* ZC-1 were not inhibited by the addition of H_2 (Fig. 3.6), which would strongly inhibit typical H_2-mediated symbiosis (Ahring & Westermann, 1988, Worm *et al.*, 2010), indicating that H_2 is not the primary electron carrier. In agreement with the triculture, H_2-consumer did not change the primary formate degradation pathway.

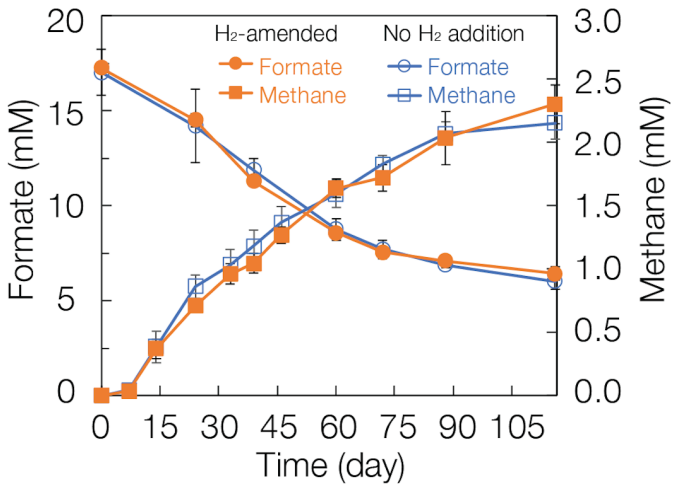

Figure 3.6 Formate and methane changes of formate-fed K32/ZC-1 co-culture amending with (orange line) or without hydrogen (3.0 kPa, blue line). Error bars represent the standard deviation of the triplicates

DIET free methanogenesis of formate-fed cocultures

The formate degradation and methane generation of *Z. formicivorans* / *M. shengliensis* cocultures were not promoted by the amending of conductive material - magnetite (Fe_3O_4) nanoparticles which was reported as a good promotor or substitute for the DIET-mediated syntrophy (Fig. 3.7 a and b) (Cruz Viggi *et al.*, 2014, Lovley, 2017, Wang *et al.*, 2018, Zhuang *et al.*, 2018). The subcultures of both K32/ZC-1 co-culture and K32/AmaM coculture also showed no enhancement in methane production (Fig 3.7 c and d), suggested that DIET was not the main electron transfer route.

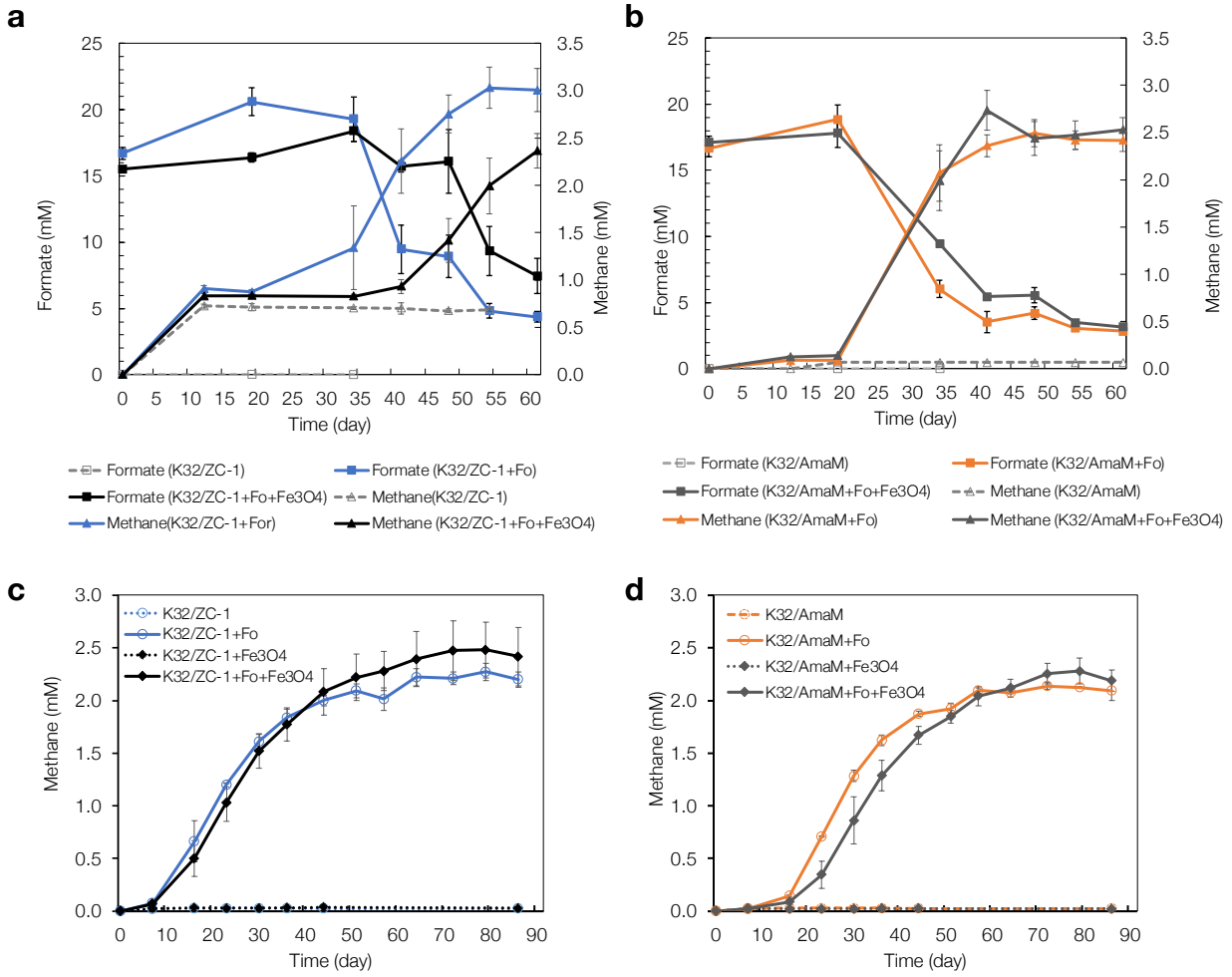

Figure 3.7 Formate and methane changes of formate-fed *Z. formicivorans* / *M. shengliensis* co-cultures amending with or without nanoparticles magnetite (nono-Fe_3O_4). The initial K32/ZC-1 and K32/AmaM cocultures are shown in a and b, respectively. The sub-cocultures of K32/ZC-1 and K32/AmaM are shown in c and d, respectively. Fo, formate. Error bars represent the standard deviation of the triplicates.

Z. formicivorans K32 and *M. shengliensis* ZC-1 could continue formate degradation when physically separated by a dialysis membrane (Spectra/Por 5, 12-14 kD, Repligen), further confirming the primary route is not direct interspecies electron transfer either (Fig 3.8).

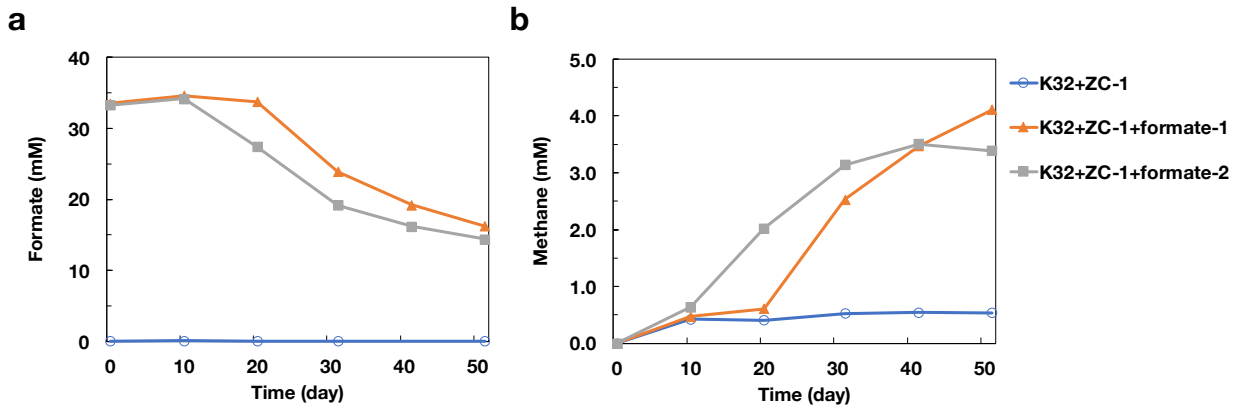

Figure 3.8 Formate and methane changes of the formate-fed K32/ZC-1 co-culture separated with (duplicates marked with square and triangle) or without (empty circle) dialysis membrane.

Formate-derived non-CO_2 reducing methanogenesis

In tracer experiments using ^{13}C-formate and ^{12}C-bicarbonate, despite the increasing ^{13}C-CO_2 (derived from ^{13}C-formate oxidation), the proportion of ^{13}C-labeled methane was constant throughout the experiment (Fig. 3.9), indicating that the major methanogenesis route for *M. shengliensis* is not CO_2-reducing (*i.e.*, neither H_2- nor electron-utilizing). Considering the results above, the only methane production pathway that can support such behavior is methylotrophic methanogenesis, which *M. shengliensis* is known to specialize in (Cheng *et al.*, 2007, Mayumi *et al.*, 2016).

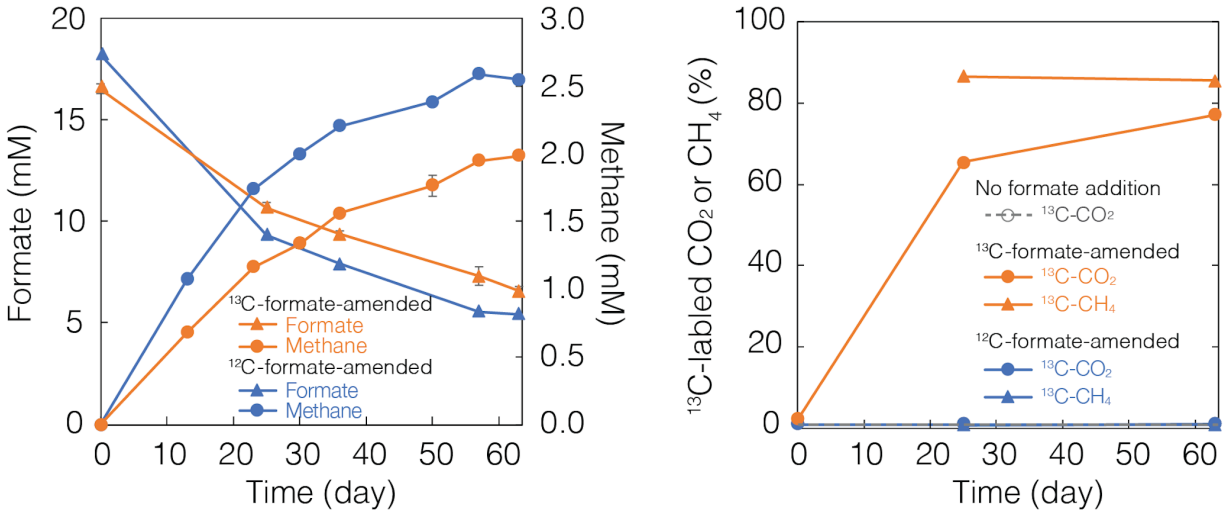

Figure 3.9 Formate and methane changes (left), and the proportion of ^{13}C-labeled methane and CO2 (right) of K32/ZC-1 co-culture growth on ^{13}C-formate (orange) or ^{12}C-formate (blue) and [^{12}C]-bicarbonate. Error bars represent the standard deviation of the triplicates.

Methylated compounds metabolism of *Z. formicivorans* K32

In the methanol-fed K32/ZC-1 coculture, formate was generated across the growth (Fig 3.10a), suggesting a metabolic relationship between formate and methanol. In the methanol-fed K32 with a H_2-utilizing methanogen *M. thermautotrophicus* TM, CH_4 was generated, indicating K32 was capable of utilizing methylated compounds (Fig 3.10b). The results were in accordance with the methanol production in formate-fed K32 resting cells, indicating *Z. formicivorans* K32 certainly possesses a pathway for interconversion of C1 compounds of formate and methanol, which make it possible to support the growth of ZC-1 by providing methanol as the intermediates.

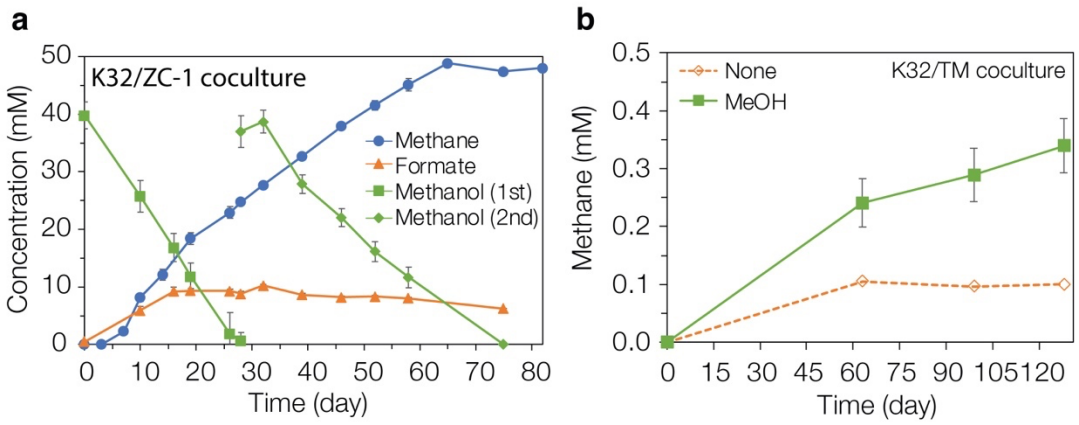

Figure 3.10 Formate and methanol interconversion. **a.** Growth of *Z. formicivorans* K32 and *M. shengliensis* ZC-1 co-culture on methanol. Methanol was added twice at day 0 and day 28. Formate was produced during the degradation of methanol, and kept at a concentration around 9-10 mM, and then slowly degraded. Error bars represent the standard deviation of the quadruplicates. **b.** Growth of co-culture of *Z. formicivorans* K32 and *M. thermautotrophicus* TM on methanol. MeOH, methanol; Error bars represent the standard deviation of the triplicates.

Thermodynamic-driven symbiosis between formate degradation and methylotrophic methanogenesis

In theory, catabolic conversion of formate to methanol would be thermodynamically favorable under standard condition (*i.e.*, Gibbs free energy change [$\Delta G^\circ = -28.5$ kJ/mol]). However, it would be a thermodynamically challenging process requiring metabolic symbiosis with methylotrophic methanogenesis *in situ* (*i.e.*, Gibbs free energy change [$\Delta G` = -4.57$ kJ/mol] of reaction 1 does not meet minimum energy margin for life [–20 kJ/mol] when coupled with formate oxidation to CO_2 under 1 mM formate, pH 7.0, 0.2 atm CO_2, and 0.1 mM methanol at 328 K). The cocultures of *Z.*

formicivorans and *M. shengliensis* clearly showed a thermodynamic driven symbiosis with the Gibbs free energy changes of -34 to -28 kJ/rection assuming methanol was kept at 0.01 mM by *M. shengliensis* comparing methanol was accumulated (Fig 3.11).

$$3\ HCOO^- + 3\ H^+ = CH_3OH + 2\ CO_2 + H_2O \quad \text{(reaction 1)}$$

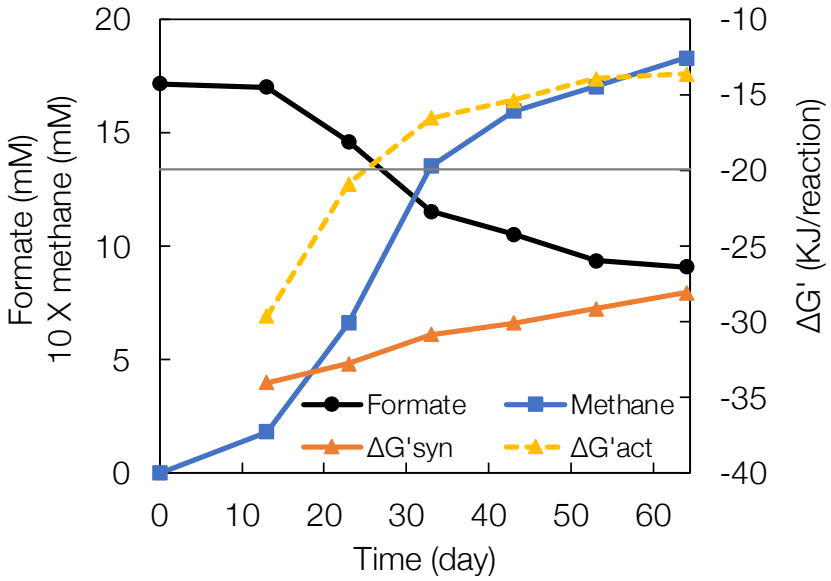

Figure 3.11 The Gibbs free energy changes (ΔG) for formate conversion to methanol and CO_2 in the formate-fed coculture assuming CO_2 = 0.2 atm and pH 7.0 at 55 °C. ΔG'syn was calculated under the syntrophic condition when methanol was kept at 0.01 mM by methanogens. ΔG'syn was calculated when methanol was accumulated during formate degradation. The minimal energy required for the growth of microorganism was assumed as -20 kJ (gray line).

Conclusion

Through establishing thermophilic co-cultures of formate-utilizing bacterium *Z. formicivorans* K32 with methylotrophic methanogens *M. shengliensis* ZC-1 or AmaM, a novel methanogenic syntrophy other than the typical ones that were mediated by H_2 or formate exchange, and direct interspecies electron transfer was discovered. Methanol production of formate-fed K32 cells, combining the methanol metabolism of K32/ZC-1 coculture or K32/TM coculture suggested the electron carrier in the novel syntrophy could be highly possible of methanol. The results indicated an unprecedented symbiotic interaction across the domain of bacteria and archaea, which take strict methylotrophic methanogens involved in.

Reference

1. Ahring BK & Westermann P (1988) Product inhibition of butyrate metabolism by acetate and hydrogen in a thermophilic coculture. *Appl Environ Microbiol* **54**: 2393-2397.
2. Boone DR, Johnson RL & Liu Y (1989) Diffusion of the Interspecies Electron Carriers H(2) and Formate in Methanogenic Ecosystems and Its Implications in the Measurement of K(m) for H(2) or Formate Uptake. *Appl Environ Microbiol* **55**: 1735-1741.
3. Cheng L, Qiu TL, Yin XB, Wu XL, Hu GQ, Deng Y & Zhang H (2007) *Methermicoccus shengliensis* gen. nov., sp. nov., a thermophilic, methylotrophic methanogen isolated from oil-production water, and proposal of Methermicoccaceae fam. nov. *Int J Syst Evol Microbiol* **57**: 2964-2969.

4. Cruz Viggi C, Rossetti S, Fazi S, Paiano P, Majone M & Aulenta F (2014) Magnetite particles triggering a faster and more robust syntrophic pathway of methanogenic propionate degradation. *Environ Sci Technol* **48**: 7536-7543.
5. Dolfing J, Jiang B, Henstra AM, Stams AJ & Plugge CM (2008) Syntrophic growth on formate: a new microbial niche in anoxic environments. *Appl Environ Microbiol* **74**: 6126-6131.
6. Dong X & Stams AJ (1995) Evidence for H_2 and formate formation during syntrophic butyrate and propionate degradation. *Anaerobe* **1**: 35-39.
7. Dong X, Plugge CM & Stams AJ (1994) Anaerobic degradation of propionate by a mesophilic acetogenic bacterium in coculture and triculture with different methanogens. *Appl Environ Microbiol* **60**: 2834-2838.
8. Dong X, Cheng G & Stams AJM (1994) Butyrate oxidation by *Syntrophospora bryantii* in co-culture with different methanogens and in pure culture with pentenoate as electron acceptor. *Appl Microbiol Biotechnol* **42**: 647-652.
9. Drake HL & Daniel SL (2004) Physiology of the thermophilic acetogen *Moorella thermoacetica*. *Res Microbiol* **155**: 422-436.
10. Gao P, Tian H, Wang Y, Li Y, Li Y, Xie J, Zeng B, Zhou J, Li G & Ma T (2016) Spatial isolation and environmental factors drive distinct bacterial and archaeal communities in different types of petroleum reservoirs in China. *Sci Rep* **6**: 20174.
11. Jiang B, Henstra AM, Paulo PL, Balk M, van Doesburg W & Stams AJ (2009) Atypical one-carbon metabolism of an acetogenic and hydrogenogenic *Moorella thermoacetica* strain. *Arch Microbiol* **191**: 123-131.
12. Li XX, Liu JF, Zhou L, Mbadinga SM, Yang SZ, Gu JD & Mu BZ (2017) Diversity and Composition of Sulfate-Reducing Microbial Communities Based on Genomic DNA and RNA

Transcription in Production Water of High Temperature and Corrosive Oil Reservoir. *Front Microbiol* **8**: 1011.

13. Liang B, Zhang K, Wang LY, Liu JF, Yang SZ, Gu JD & Mu BZ (2018) Different Diversity and Distribution of Archaeal Community in the Aqueous and Oil Phases of Production Fluid From High-Temperature Petroleum Reservoirs. *Front Microbiol* **9**: 841.
14. Lovley DR (2017) Syntrophy Goes Electric: Direct Interspecies Electron Transfer. *Annu Rev Microbiol* **71**: 643-664.
15. Lv XM, Yang M, Dai LR*, et al.* (2020) *Zhaonella formicivorans* gen. nov., sp. nov., an anaerobic formate-utilizing bacterium isolated from Shengli oilfield, and proposal of four novel families and Moorellales ord. nov. in the phylum Firmicutes. *Int J Syst Evol Microbiol* **70**: 3361-3373.
16. Mayumi D, Mochimaru H, Tamaki H, Yamamoto K, Yoshioka H, Suzuki Y, Kamagata Y & Sakata S (2016) Methane production from coal by a single methanogen. *Science* **354**: 222-225.
17. McInerney MJ, Struchtemeyer CG, Sieber J, Mouttaki H, Stams AJ, Schink B, Rohlin L & Gunsalus RP (2008) Physiology, ecology, phylogeny, and genomics of microorganisms capable of syntrophic metabolism. *Ann N Y Acad Sci* **1125**: 58-72.
18. Mesle M, Dromart G & Oger P (2013) Microbial methanogenesis in subsurface oil and coal. *Res Microbiol* **164**: 959-972.
19. Nobu MK, Narihiro T, Liu M, Kuroda K, Mei R & Liu WT (2017) Thermodynamically diverse syntrophic aromatic compound catabolism. *Environ Microbiol* **19**: 4576-4586.
20. Rotaru A-E, Shrestha PM, Liu F, Shrestha M, Shrestha D, Embree M, Zengler K, Wardman C, Nevin KP & Lovley DR (2014) A new model for electron flow during anaerobic digestion:

direct interspecies electron transfer to *Methanosaeta* for the reduction of carbon dioxide to methane. *Energy Environ Sci* **7**: 408-415.

21. Rotaru AE, Shrestha PM, Liu F, Markovaite B, Chen S, Nevin KP & Lovley DR (2014) Direct interspecies electron transfer between *Geobacter metallireducens* and *Methanosarcina barkeri*. *Appl Environ Microbiol* **80**: 4599-4605.
22. Schink B (1997) Energetics of syntrophic cooperation in methanogenic degradation. *Microbiol Mol Biol Rev* **61**: 262-280.
23. Shen L, Zhao Q, Wu X, Li X, Li Q & Wang Y (2016) Interspecies electron transfer in syntrophic methanogenic consortia: From cultures to bioreactors. *Renewable and Sustainable Energy Reviews* **54**: 1358-1367.
24. Sousa DZ, Visser M, van Gelder AH*, et al.* (2018) The deep-subsurface sulfate reducer *Desulfotomaculum kuznetsovii* employs two methanol-degrading pathways. *Nat Commun* **9**: 239.
25. Stams AJ & Plugge CM (2009) Electron transfer in syntrophic communities of anaerobic bacteria and archaea. *Nat Rev Microbiol* **7**: 568-577.
26. Thiele JH & Zeikus JG (1988) Control of Interspecies Electron Flow during Anaerobic Digestion: Significance of Formate Transfer versus Hydrogen Transfer during Syntrophic Methanogenesis in Flocs. *Appl Environ Microbiol* **54**: 20-29.
27. Wang T, Zhang D, Dai L, Dong B & Dai X (2018) Magnetite Triggering Enhanced Direct Interspecies Electron Transfer: A Scavenger for the Blockage of Electron Transfer in Anaerobic Digestion of High-Solids Sewage Sludge. *Environ Sci Technol* **52**: 7160-7169.
28. Wolin EA & Wohn MJ (1967) *Methanobacillus omelianskii*, a symbiotic association of two species of bacteria. *Archiv ifir Mikrobiologie* **31**: 20-31.

29. Worm P, Müller N, Plugge CM, Stams AJM & Schink B (2010) Syntrophy in Methanogenic Degradation. *(Endo)symbiotic Methanogenic Archaea,* Vol. 19 (Hackstein JHP, ed.) p.^pp. 143-173. Springer Berlin Heidelberg, Berlin, Heidelberg.
30. Xu D, Zhang K, Li B-G, Mbadinga SM, Zhou L, Liu J-F, Yang S-Z, Gu J-D & Mu B-Z (2019) Simulation of in situ oil reservoir conditions in a laboratory bioreactor testing for methanogenic conversion of crude oil and analysis of the microbial community. *International Biodeterioration & Biodegradation* **136**: 24-33.
31. Yang GC, Zhou L, Mbadinga SM, Liu JF, Yang SZ, Gu JD & Mu BZ (2016) Formate-Dependent Microbial Conversion of CO2 and the Dominant Pathways of Methanogenesis in Production Water of High-temperature Oil Reservoirs Amended with Bicarbonate. *Front Microbiol* **7**: 365.
32. Zhuang L, Ma J, Yu Z, Wang Y & Tang J (2018) Magnetite accelerates syntrophic acetate oxidation in methanogenic systems with high ammonia concentrations. *Microb Biotechnol* **11**: 710-720.

Chapter 4 Genome evaluation of formate utilizing bacterium *Zhaonella formicivorans* K32

Introduction

Formate is a ubiquitous fermentation product of organic matter in nature. It is essential in the anaerobic carbon cycle as i) a methanogenic precursor for hydrogenotrophic methanogens (Thauer *et al.*, 2008, Lyu *et al.*, 2018); ii) one of the key electron carriers for syntrophic communities (Stams & Plugge, 2009, Morris *et al.*, 2013, Schink *et al.*, 2017); iii) the energy and carbon source for formate-utilizing bacteria, either producing CO_2 and H_2 (Dolfing *et al.*, 2008, Kim *et al.*, 2010) or condensing to acetate (Kremp *et al.*, 2018, Kremp & Muller, 2021), to some extent, converting to methanol and CO_2 as we proposed in *Chapter* 3. Although the biochemical pathways and genes involved in the typical formate metabolism have been described, little is known of the syntrophic formate degradation, and none have been elucidated for methanol-mediated formate degradation.

Zhaonella formicivorans was the third syntroph reported capable of syntrophic formate degradation. Unlike *Moorella thermoacetica* AMP (= DSM 21394) and *Desulfovibrio* sp. G11, *Z. formicivorans* K32 was much inefficient in the formate degradation with hydrogenotrophic methanogens (Dolfing *et al.*, 2008, Lv *et al.*, 2020). However, it was an excellent formate utilizer with methylotrophic methanogens, as shown in *Chapter* 3, which may stand for a significant but overlooked niche in methanogenic ecosystems. This study used the type strain *Z. formicivorans* strain K32 as a model strain for the methanol-generating formate degradation associates. The central metabolisms, formate-related pathways, and energy conservation strategies are present and discussed based on the genomic analysis to further our understanding of methylotrophic methanogen involving syntrophic formate degradation.

Results and discussion

Genome statistics

The *Z. formicivorans* K32 genomic DNA was sequenced by the Nanopore sequencing platform (PromethION), resulting in 1.48 Gb raw reads. Quality trimming (mean_qscore_template >= 7, reads length >= 1,000 bp) yielded 1.37 Gb clean data. *De novo* assembly generated a 3.3 Mb complete genome with a G+C content of 45.57 % using flye version 2.8 (--plasmids --nano-raw). Function prediction and annotation of the complete genome with prodigal version 2.6.3 (-p None -g 11) resulted in 3,224 protein-coding genes, 60 tRNA, 15 rRNA, and 5 CRISPR (Table 4.1, Fig. 4.1).

Table 4.1 Summary of *Z. formicivorans* K32 genome sequencing statistics

Processes	Contents	Statistics
Sequencing	Total Raw Reads	156,049
	Total Raw Bases (bp)	1,476,564,465
	Average Read Length (bp)	9,462.18
	Reads N50 (bp)	16,058
Pre-assembly	Number of Reads used in Assembly	145,226
	Number of Bases used in Assembly (bp)	1,374,543,142
	Average Read Length (bp)	9,464.86
	Reads N50 (bp)	16,021
Assembly	Number of Contigs	1
	Contig Size (nt)	3,314,304
	Genome size (bp)	3,314,304
	Genome GC content (%)	45.57
Annotation	Number of CDS	3,224

Number of tRNA	60
Number of rRNA	15
Number of CRISPR	5

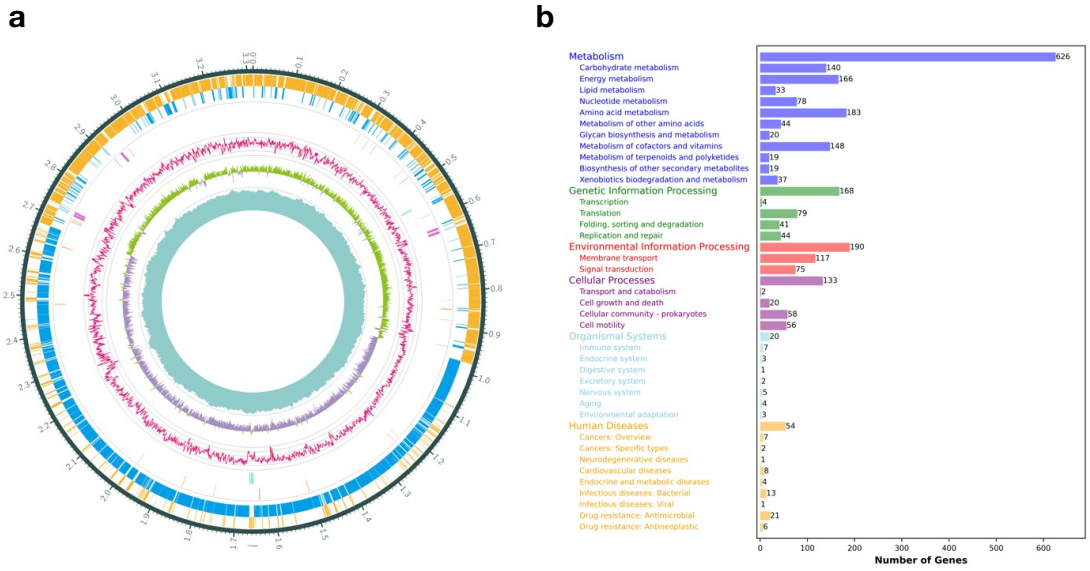

Figure 4.1 General information of strain K32 genome. **a.** A circular map of the strain K32 genome (from outer to inner circle) with forward strand genes and reverse strand genes, RNA genes (orange: transfer RNA and purple: ribosomal RNA), CRISPR (blue) and gene island (green), G+C content, G+C skew and sequence depth. **b.** KEGG catalogs for protein-coding genes of strain K32

Central metabolism and general physiology

The genome of strain K32 encodes the glycolysis (Embden-Meyerhof pathway), pentose phosphate pathway, UDP-N-acetyl-D-glucosamine biosynthesis for central carbohydrate

metabolism (Appendices Supplementary Table 1). The genome also contains genes for amino acid biosynthesis, including threonine, cysteine, methionine, valine/isoleucine, leucine, lysine, ornithine, arginine, proline, polyamine, and histidine (Appendices Supplementary Table 1). Genes encoding cofactor (*i.e.*, Coenzyme A, C1-unit, and heme) and vitamin (*i.e.*, thiamine, pyridoxal-P) biosynthesis are also present (Appendices Supplementary Table 1).

Metabolism of formate

The formate assimilation can be conducted by three main pathways - the reductive acetyl-CoA pathway (*i.e.*, Wood-Ljungdahl pathway), the serine pathway, and the reductive pentose phosphate cycle (*i.e.*, Calvin-Benson-Bassham cycle) (Yishai *et al.*, 2016). The *Z. formicivorans* genome possesses the first two pathways (Fig.4.2 and Table 4.2). Formate oxidation is typically conducted by formate dehydrogenase (Kim *et al.*, 2010). *Z. formicivorans* K32 harbors two formate dehydrogenase clusters (K32-1_02853-02857, and K32-1_03286-03289) and several other formate dehydrogenases scattering in the genome (Table 4.2 and 4.3), which make strain K32 capable of oxidizing formate to CO_2 with the generation of two reducing equivalences per formate. The reduction of formate can be performed by the reductive Wood-Ljungdahl pathway (Fig.4.2a and Table 4.2), which possesses formate-tetrahydrofolate ligase (K32-1_02922), bifunctional 5,10-methylene-tetrahydrofolate dehydrogenase / methenyl tetrahydrofolate cyclohydrolase (K32-1_00737) and methylenetetrahydrofolate reductases (K32-1_00875 and K32-1_02858) for the formyl branch, and acetyl-CoA synthase / CO dehydrogenase gene cluster, and carbon-monoxide dehydrogenases (K32-1_01219, K32-1_01489, K32-1_01971 and K32-1_02449) for the methyl branch (K32-1_00865, K32-1_00868-00873). Theoretically, the strain K32 can assimilate formate

to acetyl-CoA using the Wood-Ljungdahl pathway like other acetogenic bacteria, resulting in the consumption of six reducing equivalent in total (Pierce *et al.*, 2008, Muller, 2019, Moon *et al.*, 2021) (Fig. 4.2a).

In addition, the *Z. formicivorans* K32 genome also encodes enzymes for the reductive glycine pathway, including glycine cleavage system (K32-1_01311, 02827-02831), glycine reductase clusters (K32-1_01886-01889, 01894-01900, 01905-01916), acetate kinase (K32-1_01142), acetate-CoA ligase (K32-1_00364), pyruvate ferredoxin oxidoreductase (K32-1_02733), serine hydroxymethyltransferase (K32-1_00082), and serine dehydratase (K32-1_00076-00077, 02021) (Fig. 4.2b and Table 4.2) (Sanchez-Andrea *et al.*, 2020). Through the reductive glycine pathway, formate can be converted to acetyl-CoA with the consumption of four reducing equivalent. It is possible to generate reducing equivalents by pyruvate ferredoxin oxidoreductase (K32-1_02733) if taking advantage of the glycine/serine sub-branch. It may become one strategy for *Z. formicivorans* K32 to balance the electron consumption and generation in the formate catabolism.

To evaluate methanol metabolism, one methanol- cobalamin methyltransferase (K32-1_02410), six aldehyde ferredoxin oxidoreductases (K32-1_00034, K32-1_00094, K32-1_01525, K32-1_01861, K32-1_02760, and K32-1_03130), and three alcohol dehydrogenases (K32-1_00095, K32-1_00231, and K32-1_03232) were detected. Although methylotrophic acetogens are able to utilize methyl compounds via cobalamin-dependent methyltransferase systems combining the Wood-Ljungdahl pathway (Kremp *et al.*, 2018, Kremp & Muller, 2021), *Z. formicivorans* K32 genome is hard to support it for the lacking of cobalamin corrinoid proteins that serves as an intermediate methyl group acceptor and another methyltransferase which transfers the methyl group to the final acceptor THF. However, the latter two enzymes may enable strain K32 to reduce

formate to formaldehyde by aldehyde ferredoxin oxidoreductase and sequentially reduce to methanol by alcohol dehydrogenase as a reverse reaction shown in the previous study (Fig. 4.2c and Table 4.2) (Sousa *et al.*, 2018). This pathway has a high possibility of providing the methanol source for the formate-fed coculture.

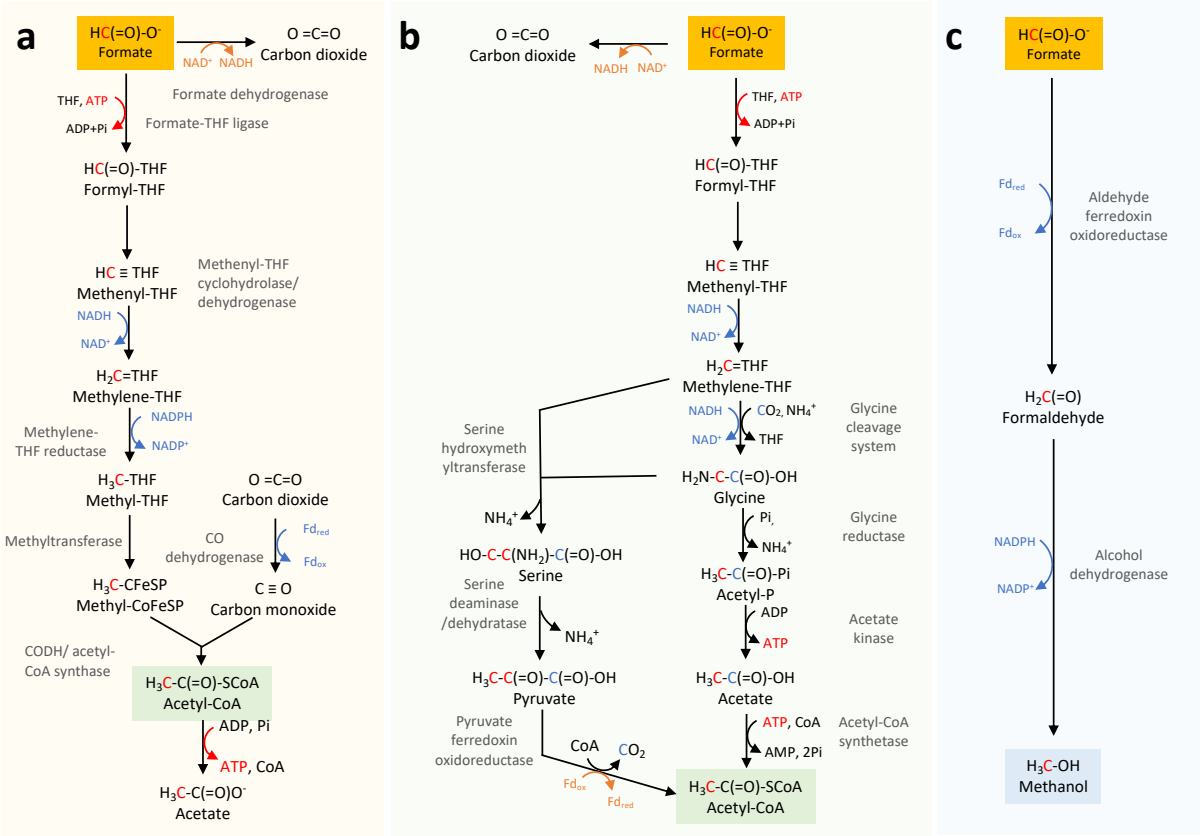

Figure 4.2 Proposed formate utilizing pathways for *Z. formicivorans* K32. **a**. Wood-Ljungdahl pathway. **b**. reductive glycine pathway. **c**. formate-methanol pathway.

Table 4.2 Formate metabolism pathways of *Z. formicivorans* K32

Locus Tag	Gene name	Description
Wood-Ljungdahl pathway (WLP)		
K32-1_00963	fdnI	Cytochrome b subunit of formate dehydrogenase
K32-1_00968	fdnI	Cytochrome b subunit of formate dehydrogenase
K32-1_00971	fdnI	Cytochrome b subunit of formate dehydrogenase

K32-1_01383	fdhD	Formate dehydrogenase accessory sulfurtransferase FdhD
K32-1_02762	fdhD	Formate dehydrogenase accessory sulfurtransferase FdhD
K32-1_02853	focA,fdhC1	Formate/nitrite transporter family protein,formate dehydrogenase subunit gamma/cytochrome b subunit
K32-1_02854	fdhB	Formate dehydrogenase iron-sulfur subunit
K32-1_02855	fdhB	Formate dehydrogenase iron-sulfur subunit
K32-1_02856	yjgC	Formate dehydrogenase subunit alpha
K32-1_02857	yjgC	Formate dehydrogenase subunit alpha
K32-1_03286	fdhB	Formate dehydrogenase iron-sulfur subunit
K32-1_03287	fdhA2	Formate dehydrogenase alpha subunit, Molybdopterin oxidoreductase 4Fe-4S domain
K32-1_03288	yjgC	Formate dehydrogenase subunit alpha
K32-1_03289	yjgC, fdhF	Formate dehydrogenase subunit alpha
K32-1_02922	fhs	Formate--tetrahydrofolate ligase
K32-1_00737	folD	5,10-methylene-tetrahydrofolate dehydrogenase/Methenyl tetrahydrofolate cyclohydrolase
K32-1_00875	metF, MTHFR	Methylenetetrahydrofolate reductase
K32-1_02858	metF	Methylenetetrahydrofolate reductase
K32-1_00865	cooC	Carbon monoxide dehydrogenase accessory protein
K32-1_00866	-	Transposase
K32-1_00867	-	Transposase IS116/IS110/IS902 family
K32-1_00868	cooS, acsA	Carbon-monoxide dehydrogenase, catalytic subunit
K32-1_00869	cdhC,cdhA,acsB	CO dehydrogenase/CO-methylating acetyl-CoA synthase complex, beta subunit
K32-1_00870	cdhE, acsC	CO dehydrogenase/acetyl-CoA synthase delta subunit|Corrinoid/iron-sulfur protein large subunit
K32-1_00871	-	2Fe-2S iron-sulfur cluster binding domain | ferredoxin
K32-1_00872	cooC	CO dehydrogenase maturation factor
K32-1_00873	cdhD, acsD	CO dehydrogenase/acetyl-CoA synthase, delta subunit
K32-1_00874	metH2, acsE	5-methyltetrahydrofolate:corrinoid/iron-sulfur protein co-methyltransferase
K32-1_01216	dsrA	4Fe-4S binding domain
K32-1_01217	nirB	Pyridine nucleotide-disulphide oxidoreductase,NAD(P)/FAD-dependent oxidoreductase
K32-1_01218	hycB, cooF	4Fe-4S binding domain
K32-1_01219	cooS, acsA	Carbon-monoxide dehydrogenase, catalytic subunit
K32-1_01489	cooS, acsA	Carbon-monoxide dehydrogenase, catalytic subunit
K32-1_01971	cooS, acsA	Carbon-monoxide dehydrogenase, catalytic subunit
K32-1_02448	nirB	Pyridine nucleotide-disulphide oxidoreductase,NAD(P)/FAD-dependent oxidoreductase
K32-1_02449	cooS, acsA	Carbon-monoxide dehydrogenase, catalytic subunit
K32-1_02450	hycB, cooF	HycB 4Fe-4S binding domain
Reductive glycine pathway (non-WLP part)		
K32-1_01311	gcvH, GCSH	Glycine cleavage system protein GcvH
K32-1_02827	gltB2	FMN-binding glutamate synthase family protein
K32-1_02828	gcvT, AMT	Glycine cleavage system aminomethyltransferase GcvT
K32-1_02829	gcvH, GCSH	Glycine cleavage system protein GcvH
K32-1_02830	gcvP1, gcvPA	Aminomethyl-transferring glycine dehydrogenase subunit GcvPA
K32-1_02831	gcvP2, gcvPB	Aminomethyl-transferring glycine dehydrogenase subunit GcvPB
K32-1_01886	plsX, grdD	Glycine reductase

K32-1_01887	fabH, grdC	Glycine reductase
K32-1_01888	grdA	Glycine/sarcosine/betaine reductase complex selenoprotein A
K32-1_01889	grdA	Glycine/sarcosine/betaine reductase complex selenoprotein A
K32-1_01894	grdH	Glycine/betaine/sarcosine/D-proline family reductase selenoprotein B
K32-1_01895	grdI	Glycine/sarcosine/betaine reductase component B subunit
K32-1_01897	plsX, grdD	Glycine reductase
K32-1_01898	fabH, grdC	Glycine reductase
K32-1_01899	grdA	Glycine/sarcosine/betaine reductase complex selenoprotein A
K32-1_01900	grdA	Glycine/sarcosine/betaine reductase complex selenoprotein A
K32-1_01905	grdB	Glycine reductase complex selenoprotein B
K32-1_01906	grdB	Glycine reductase complex selenoprotein B
K32-1_01907	grdE	Glycine/sarcosine/betaine reductase component B subunit
K32-1_01910	plsX, grdD	Glycine reductase
K32-1_01911	fabH, grdC	Glycine reductase
K32-1_01912	grdB	Glycine reductase complex selenoprotein B
K32-1_01913	grdB	Glycine reductase complex selenoprotein B
K32-1_01914	grdA	Glycine/sarcosine/betaine reductase complex selenoprotein A
K32-1_01915	grdA	Glycine/sarcosine/betaine reductase complex selenoprotein A
K32-1_01916	grdE	Glycine/sarcosine/betaine reductase component B subunit
K32-1_01142	ackA	Acetate kinase
K32-1_00364	acs, acsS	Acetate-CoA ligase
K32-1_02733	porA, korA, oorA, oforA	Pyruvate ferredoxin oxidoreductase
K32-1_00082	glyA, SHMT	Serine hydroxymethyltransferase
K32-1_00076	sdaB, tdcG	L-serine ammonia-lyase, iron-sulfur-dependent, subunit beta
K32-1_00077	sdaA, tdcG	L-serine ammonia-lyase, iron-sulfur-dependent, subunit alpha
K32-1_02021	cdsB	Serine dehydratase subunit alpha family protein
Formate-methanol Pathway		
K32-1_00034	ydhV	Aldehyde ferredoxin oxidoreductase
K32-1_00094	ydhV, aor	Aldehyde ferredoxin oxidoreductase
K32-1_00095	adhE	Iron-containing alcohol dehydrogenase
K32-1_01525	ydhV, aor	Aldehyde ferredoxin oxidoreductase
K32-1_01861	adhV, aor	Aldehyde ferredoxin oxidoreductase
K32-1_01862	hycB	HycB 4Fe-4S binding domain
K32-1_01863	wrbA	NADPH-dependent FMN reductase
K32-1_02759	hycB	4Fe-4S dicluster domain-containing protein
K32-1_02760	ydhV	Aldehyde ferredoxin oxidoreductase
K32-1_02761	-	YdhW family putative oxidoreductase system protein
K32-1_03129	-	4Fe-4S binding domain
K32-1_03130	ydhV, aor	YdhV Aldehyde ferredoxin oxidoreductase
K32-1_00095	adhE	Iron-containing alcohol dehydrogenase
K32-1_00231	yqdH	Iron-containing alcohol dehydrogenase
K32-1_03232	gldA	Iron-containing alcohol dehydrogenase/Glycerol dehydrogenase

Whether anaerobes can use alcohol dehydrogenase plus aldehyde: ferredoxin oxidoreductase for alcohol metabolism is unclear. The sulfate-reducing bacterium *Desulfotomaculum kuznetsovii* that is capable of growth with methanol as a sole carbon and energy source employs two methanol-degrading pathways - a cobalt-dependent methanol methyltransferase and a cobalt-independent methanol dehydrogenase (Sousa *et al.*, 2018). Looking into genomes of other acetogens (*i.e.*, *Moorella thermoacetica* AMP and *Desulfovibrio* sp. G11) that the former is capable of using methanol, but the latter only use ethanol (McInerney *et al.*, 1981, Paulo *et al.*, 2004, Sheik *et al.*, 2017), shows the strain AMP possesses methanol methyltransferase system and alcohol dehydrogenase/aldehyde: ferredoxin oxidoreductase but the strain G11 only has alcohol dehydrogenase/aldehyde: ferredoxin oxidoreductase (Table 4.3). Given that strain AMP was only sustained in coculture with a hydrogen-consuming methanogen in cobalt-lacking methanol-fed culture instead of growing acetogenically with cobalt amendment (Jiang *et al.*, 2009), it highly indicated that strain AMP also harbors two methanol-utilizing system like *D. kuznetsovii*. The absence of cobalt forced strain AMP catabolize methanol by alcohol dehydrogenase. The alcohol dehydrogenase enables both strain AMP and G11 to metabolize alcohol (*i.e.*, methanol and ethanol). We further examined genomes of another two alcohol-consuming acetogens (*i.e.*, *Fuchsiella alkaliacetigena* Z-7100 and *Natroniella acetigena* Z-7937 of the order Halanaerobiales) which are capable of using ethanol but not methanol with acetate as the primary product. Both strains have no methanol methyltransferase system but possess alcohol dehydrogenases. However, instead of employing aldehyde: ferredoxin oxidoreductase, *N. acetigena* applies acetaldehyde dehydrogenase for acetyl-CoA/acetate production. Considering their ethanol metabolism, it strongly suggested anaerobes can employ alcohol dehydrogenase for alcohol metabolism. However, more genome investigate should be done for a deeper understanding.

Table 4.3 Genes related to alcohol metabolism of strains *Z. formicivorans* K32 (1), *D. kuznetsovii* 17 (2), *M. thermoacetica* AMP (3) and *Desulfovibrio* sp. G11 (4), *F. alkaliacetigena* Z-7100 (5) and *N. acetigena* Z-7937 (6).

	1	2	3	4	5	6
Methyltransferase MtaA		Desku_0050 Desku_0060	GCA_001875325.1_00398	-	-	-
Methanol: cobalamin methyltransferase MtaB	K32-1_02410	Desku_0051	GCA_001875325.1_02059	-	-	-
Methyltransferase cognate corrinoid protein	-	Desku_0052	-	-	-	-
Alcohol dehydrogenase	K32-1_00095 K32-1_00231 K32-1_03232	Desku_2952	GCA_001875325.1_01669	GCA_900119095.1_00791 GCA_900119095.1_00200	Falka_01391	Nacet_02252
Aldehyde ferredoxin oxidoreductase	K32-1_00034 K32-1_00094 K32-1_01525 K32-1_01861 K32-1_02760 K32-1_03130	Desku_2951	GCA_001875325.1_02116 GCA_001875325.1_00962	GCA_900119095.1_01235	-	-
Acetaldehyde dehydrogenase	K32-1_02578		GCA_001875325.1_00249	GCA_900119095.1_01887 GCA_900119095.1_01891 GCA_900119095.1_01900 GCA_900119095.1_01425		Nacet_01305 Nacet_01587

Energy conservation and electron flow

Anaerobes usually take advantage of reverse electron transport and electron bifurcation energy conservation to overcome the thermodynamic restriction (Sieber *et al.*, 2012, Nobu *et al.*, 2015, Narihiro *et al.*, 2016). The potential electron carriers for *Z. formicivorans* K32 could be NADH, NADPH, and ferredoxin based on the formate metabolic pathways. *Z. formicivorans* possesses an electron bifurcating enzyme NfnAB (NADH-dependent Fd_{red}: $NADP^+$ oxidoreductase, K32-1_00736-00736, Table 4.3), making it possible to catalyze electron transfer among NADP(H), NAD(H) and ferredoxin (2 NADPH + Fd_{ox} + NAD^+ = 2 $NADP^+$ + Fd_{red}^{2-} + NADH + H^+) (Wang *et al.*, 2010, Demmer *et al.*, 2015). Since the K32 genome does not harbor Rnf complex (the *Rhodobacter* nitrogen fixation complex), the strain K32 may not conduct electron transfer between NAD(H) and ferredoxin. Instead, the genome possesses a Hdr: Flox system (flavin oxidoreductase-heterodisulfide reductase, K32-1_01374-01383, Table 4.3), which may work as a substitute for Rnf for syntrophs (Nobu *et al.*, 2015). In addition, the genome of strain K32 also contains a FixABCX complex (the electron-transfer-flavoprotein-oxidizing hydrogenase complex, K32-1_02813-02816), which may also support the electron delivery between NADH and ferredoxin (Buckel & Thauer, 2018, Buckel & Thauer, 2018). Other proteins capable of electron transfer are electron-bifurcating Fd- and NAD-dependent [FeFe]-hydrogenase (K32-1_00597-00600), Fd-and NADP-dependent [FeFe]-hydrogenase (K32-1_00603-00610), Fd-and NAD-dependent formate dehydrogenases (K32-1_02853-02857, 03286-03289) (Table 4.3). Moreover, *Z. formicivorans* encodes one ATP synthase gene cluster (K32-1_02309-02318), one NADH-quinone oxidoreductase gene cluster (K32-1_01102-01112), multiple thioredoxins, cytochromes, and Na^+/H^+ antiporters/transporters (Table 4.4). The results suggest that *Z. formicivorans* K32 is flexible to maintain a syntrophic lifestyle by employing multiple energy conservation systems.

Table 4.4 *Z. formicivorans* K32 genes relevant to energy conservation

Locus Tag	Gene	Description
Hdr:Flox complex		
K32-1_01374	floxA	Sulfite reductase, contains an FAD and NADPH binding module
K32-1_01375	floxB	Sulfite reductase, 4Fe-4S dicluster domain-containing protein
K32-1_01376	floxC	Sulfite reductase, 4Fe-4S dicluster domain-containing protein
K32-1_01377	frhD	Methyl-viologen-reducing hydrogenase, delta subunit
K32-1_01378	hdrA	Heterodisulfide reductase, subunit A (polyferredoxin)
K32-1_01379	hdrA	Heterodisulfide reductase iron-sulfur subunit A
K32-1_01380	hdrB	Heterodisulfide reductase iron-sulfur subunit B
K32-1_01381	hdrC	Heterodisulfide reductase iron-sulfur subunit C
K32-1_01382	-	Membrane protein
K32-1_01383	fdhD	Formate dehydrogenase accessory sulfurtransferase FdhD
FixABCX		
K32-1_01879	fixC	Electron transfer flavoprotein-quinone oxidoreductase/FAD/NAD(P)-binding domain
K32-1_01880	fixX	Electron transfer flavoprotein-ubiquinone oxidoreductase, 4Fe-4S
K32-1_02813	fixA	Electron transfer flavoprotein subunit beta
K32-1_02814	fixB	Electron transfer flavoprotein subunit alpha
K32-1_02815	fixC	Electron transfer flavoprotein-quinone oxidoreductase/FAD/NAD(P)-binding domain
K32-1_02816	fixX	Ferredoxin like protein / 4Fe-4S dicluster domain-containing protein
Nfn		
K32-1_00735	nfnB	Nitroreductase/dihydropteridine reductase nfnB; dihydropteridine reductase, NAD(P)H-dependent
K32-1_00736	nfnA, gltA	NADPH-dependent glutamate synthase/NADH-dependent ferredoxin:NADP+ oxidoreductase, alpha subunit
Formate dehydrogenase		
K32-1_00606	fdhB1	Formate dehydrogenase iron-sulfur subunit
K32-1_00963	fdnI	Cytochrome b subunit of formate dehydrogenase
K32-1_00968	mhcC	Cytochrome c3
K32-1_00971	fdnI	Cytochrome b subunit of formate dehydrogenase
K32-1_01204	fdnH	Formate dehydrogenase-N, Fe-S (beta) subunit, nitrate-inducible
K32-1_01383	fdhD	Formate dehydrogenase accessory protein
K32-1_01726	fdnB	4Fe-4S dicluster domain-containing protein
K32-1_01729	fdnB	4Fe-4S dicluster domain-containing protein
K32-1_02853	focA,fdhC1	Formate/nitrite transporter family protein,formate dehydrogenase subunit gamma/cytochrome b subunit
K32-1_02854	fdhB	Formate dehydrogenase iron-sulfur subunit
K32-1_02855	fdhB	Formate dehydrogenase iron-sulfur subunit
K32-1_02856	fdhA2, hoxU	Formate dehydrogenase subunit alpha,bidirectional hydrogenase complex protein HoxU
K32-1_02857	fdhA1, fdhF	Formate dehydrogenase, alpha subunit/formate dehydrogenase-H, selenopolypeptide subunit
K32-1_03286	fdhB	Formate dehydrogenase iron-sulfur subunit

K32-1_03287	fdhA2	Formate dehydrogenase alpha subunit, Molybdopterin oxidoreductase 4Fe-4S domain
K32-1_03288	yjgC	Formate dehydrogenase subunit alpha,Molybdopterin oxidoreductase
K32-1_03289	yjgC, fdhF	Formate dehydrogenase subunit alpha,formate dehydrogenase-H, selenopolypeptide subunit
Hydrogenase		
K32-1_00597	hydE	[FeFe] hydrogenase H-cluster radical SAM maturase HydE
K32-1_00599	hydF	[FeFe] hydrogenase H-cluster maturation GTPase HydF
K32-1_00600	hydG	[FeFe] hydrogenase H-cluster radical SAM maturase HydG
K32-1_00603	Nar1	Iron only hydrogenase large subunit,4Fe-4S binding protein
K32-1_00606	hndA	NADP-reducing hydrogenase subunit HndA,ferredoxin-like subunit
K32-1_00607	-	ATP-binding protein
K32-1_00608	hndB, hydD	(2Fe-2S) ferredoxin domain-containing protein ,quinone-reactive Ni/Fe hydrogenase (hydD),maturation protease
K32-1_00609	hndC2	NADP-reducing hydrogenase subunit HndC,major subunit
K32-1_00610	yjgC, hndD	NADP-reducing hydrogenase subunit HndD,4Fe-4S binding domain protein
K32-1_01107	echF	ech hydrogenase subunit F
K32-1_01111	echC	ech hydrogenase subunit C
K32-1_01203	HybB	Ni/Fe-hydrogenase cytochrome b subunit
K32-1_01204	HybB	hydrogenase 2, 4Fe-4S dicluster domain-containing protein
K32-1_01218	HycB,cooF	4Fe-4S dicluster domain-containing protein
K32-1_02759	HycB	4Fe-4S dicluster domain-containing protein
NADH-quinone oxidoreductase		
K32-1_01102	NuoN,nuoN	NADH-quinone oxidoreductase subunit N
K32-1_01103	NuoM,nuoM	NADH-quinone oxidoreductase subunit M
K32-1_01104	NuoL,nuoL	NADH-quinone oxidoreductase subunit L
K32-1_01105	NuoK,ndhE	NADH-quinone oxidoreductase subunit NuoK
K32-1_01106	NuoJ	NADH-quinone oxidoreductase subunit J
K32-1_01107	NuoI,nuoI	4Fe-4S binding protein/Formate hydrogenlyase subunit 6
K32-1_01108	NuoH,nuoH	NADH-quinone oxidoreductase subunit NuoH
K32-1_01109	NuoD,nuoD	NADH-quinone oxidoreductase subunit D
K32-1_01110	NuoC,nuoC	NADH-quinone oxidoreductase subunit C
K32-1_01111	NuoB,nuoB	NADH-quinone oxidoreductase subunit B
K32-1_01112	NuoA,nuoA	NADH-quinone oxidoreductase subunit A
K32-1_01797	NuoI	4Fe-4S dicluster domain/Formate hydrogenlyase subunit
K32-1_02177	NuoI	4Fe-4S binding protein/Formate hydrogenlyase subunit
Thioredoxin		
K32-1_00126	trxB	TrxB thioredoxin-disulfide reductase
K32-1_00127	trxA, cnoX	TrxA thioredoxin
K32-1_00666	trxA, cnoX	TrxA thioredoxin
K32-1_01890	cnoX, trxA	CnoX Thioredoxin
K32-1_01891	trxB, TRR	TrxB thioredoxin-disulfide reductase
K32-1_01901	cnoX, trxA	CnoX Thioredoxin
K32-1_01902	trxB, TRR	TrxB thioredoxin-disulfide reductase
K32-1_01917	cnoX, trxA	CnoX Thioredoxin

K32-1_01918	trxB, TRR	TrxB thioredoxin-disulfide reductase
K32-1_02477	trxB, TRR	TrxB thioredoxin-disulfide reductase
Cytochrome		
K32-1_00458		S-layer homology domain
K32-1_00963	fdnI	FdnI Prokaryotic cytochrome b561
K32-1_00968	fdnI	FdnI Cytochrome c3
K32-1_00971	fdnI	FdnI Prokaryotic cytochrome b561
K32-1_01197	-	Hypothetical protein
K32-1_01210	norB	Cbb3-type cytochrome c oxidase subunit I
K32-1_01212	nrfA	NrfA Cytochrome c552
K32-1_01213	nrfH	NapC/NirT cytochrome c family, N-terminal region
K32-1_01451	dsbD, ccdA	DsbD Cytochrome C biogenesis protein transmembrane region
K32-1_01716	nrfA	NrfA Cytochrome c552
K32-1_01717	nrfH	NapC/NirT cytochrome c family, N-terminal region
K32-1_01733	nrfA	NrfA Cytochrome c552
K32-1_01743		Hypothetical protein
K32-1_01745	qcrB/petB	QcrB/PetB Cytochrome b(N-terminal)/b6/petB
K32-1_02465	ccmC	CcmC Cytochrome C assembly protein
K32-1_02470	nrfF, ccmH	NrfF Cytochrome C biogenesis protein
K32-1_02471	ccmF	CcmF Cytochrome C assembly protein
K32-1_02574	-	Cytochrome c552
K32-1_03021	appC, cydA	AppC Cytochrome bd terminal oxidase subunit I
K32-1_03022	cydB, appB	CydB cytochrome d ubiquinol oxidase, subunit II
K32-1_03050	-	Doubled CXXCH motif (Paired)
ATPase		
K32-1_02309	atpC, ATPF1E	F0FATP synthase subunit epsilon
K32-1_02310	atpD, ATPF1B	F0FATP synthase subunit beta
K32-1_02311	atpG, ATPF1G	F0FATP synthase subunit gamma
K32-1_02312	atpA, ATPF1A	F0FATP synthase subunit alpha
K32-1_02313	atpH, ATPF1D	F0FATP synthase subunit delta
K32-1_02314	atpF, ATPFB	F0FATP synthase subunit B
K32-1_02315	atpE, ATPFC	ATP synthase F0 subunit C
K32-1_02316	atpB, ATPFA	F0FATP synthase subunit A
K32-1_02317	-	Hypothetical protein
K32-1_02318	atpZ	AtpZ/AtpI family protein
K32-1_02732	-	ATP synthase
Antiporter		
K32-1_00405	nhaC	Na+/H+ antiporter NhaC family protein
K32-1_02330	nhaA	Na+/H+ antiporter NhaA
K32-1_02425	kefB, TC.KEF	Cation:proton antiporter
K32-1_02426	khtT, K07228	Cation:proton antiporter regulatory subunit
Transporter		
K32-1_00011	agcS, alsT	Sodium:alanine symporter family protein

K32-1_01772	benE	Benzoate/H(+) symporter BenE family transporter
K32-1_01792	yfeH	Bile acid:sodium symporter family protein
K32-1_01903	tC.SSS	Sodium:solute symporter family protein
K32-1_02118	benE	Benzoate/H(+) symporter BenE family transporter
K32-1_02121	benE	Benzoate/H(+) symporter BenE family transporter
K32-1_03052	panF, TC.SSS	Sodium:solute symporter

Conclusion

Genomic insights into the subsurface-derived thermophilic formate-utilizing anaerobe *Z. formicivorans* K32 suggested that the genome possesses formate catabolic pathways, including the conventional Wood-Ljungdahl pathway, newly discovered reductive glycine pathway, and a rare methanol-generation pathway in anaerobic bacteria. The possession of multiply electron transfer systems implies that *Z. formicivorans* is capable of performing syntrophic metabolism. The versatile pathways also suggest the flexibility for living in diverse ecosystems. The genetic evidence reveals how syntrophs like strain K32 employ methylotrophic methanogens involved in syntrophic organic matter degradation, which was neglected.

Reference

1. Buckel W & Thauer RK (2018) Flavin-Based Electron Bifurcation, Ferredoxin, Flavodoxin, and Anaerobic Respiration With Protons (Ech) or NAD(+) (Rnf) as Electron Acceptors: A Historical Review. *Front Microbiol* **9**: 401.
2. Buckel W & Thauer RK (2018) Flavin-Based Electron Bifurcation, A New Mechanism of Biological Energy Coupling. *Chem Rev* **118**: 3862-3886.

3. Demmer JK, Huang H, Wang S, Demmer U, Thauer RK & Ermler U (2015) Insights into Flavin-based Electron Bifurcation via the NADH-dependent Reduced Ferredoxin:NADP Oxidoreductase Structure. *J Biol Chem* **290**: 21985-21995.
4. Dolfing J, Jiang B, Henstra AM, Stams AJ & Plugge CM (2008) Syntrophic growth on formate: a new microbial niche in anoxic environments. *Appl Environ Microbiol* **74**: 6126-6131.
5. Jiang B, Henstra AM, Paulo PL, Balk M, van Doesburg W & Stams AJ (2009) Atypical one-carbon metabolism of an acetogenic and hydrogenogenic *Moorella thermoacetica* strain. *Arch Microbiol* **191**: 123-131.
6. Kim YJ, Lee HS, Kim ES*, et al.* (2010) Formate-driven growth coupled with H(2) production. *Nature* **467**: 352-355.
7. Kremp F & Muller V (2021) Methanol and methyl group conversion in acetogenic bacteria: biochemistry, physiology and application. *FEMS Microbiol Rev* **45**: 1-22.
8. Kremp F, Poehlein A, Daniel R & Muller V (2018) Methanol metabolism in the acetogenic bacterium *Acetobacterium woodii*. *Environ Microbiol* **20**: 4369-4384.
9. Lv XM, Yang M, Dai LR*, et al.* (2020) *Zhaonella formicivorans* gen. nov., sp. nov., an anaerobic formate-utilizing bacterium isolated from Shengli oilfield, and proposal of four novel families and Moorellales ord. nov. in the phylum Firmicutes. *Int J Syst Evol Microbiol* **70**: 3361-3373.
10. Lyu Z, Shao N, Akinyemi T & Whitman WB (2018) Methanogenesis. *Curr Biol* **28**: R727-R732.
11. McInerney MJ, Mackie RI & Bryant MP (1981) Syntrophic association of a butyrate-degrading bacterium and methanosarcina enriched from bovine rumen fluid. *Appl Environ Microbiol* **41**: 826-828.

12. Moon J, Donig J, Kramer S, Poehlein A, Daniel R & Muller V (2021) Formate metabolism in the acetogenic bacterium Acetobacterium woodii. *Environ Microbiol* **23**: 4214-4227.
13. Morris BE, Henneberger R, Huber H & Moissl-Eichinger C (2013) Microbial syntrophy: interaction for the common good. *FEMS Microbiol Rev* **37**: 384-406.
14. Muller V (2019) New Horizons in Acetogenic Conversion of One-Carbon Substrates and Biological Hydrogen Storage. *Trends Biotechnol* **37**: 1344-1354.
15. Narihiro T, Nobu MK, Tamaki H, Kamagata Y, Sekiguchi Y & Liu WT (2016) Comparative Genomics of Syntrophic Branched-Chain Fatty Acid Degrading Bacteria. *Microbes Environ* **31**: 288-292.
16. Nobu MK, Narihiro T, Rinke C, Kamagata Y, Tringe SG, Woyke T & Liu WT (2015) Microbial dark matter ecogenomics reveals complex synergistic networks in a methanogenic bioreactor. *ISME J* **9**: 1710-1722.
17. Nobu MK, Narihiro T, Hideyuki T, Qiu YL, Sekiguchi Y, Woyke T, Goodwin L, Davenport KW, Kamagata Y & Liu WT (2015) The genome of *Syntrophorhabdus aromaticivorans* strain UI provides new insights for syntrophic aromatic compound metabolism and electron flow. *Environ Microbiol* **17**: 4861-4872.
18. Paulo PL, Jiang B, Cysneiros D, Stams AJ & Lettinga G (2004) Effect of cobalt on the anaerobic thermophilic conversion of methanol. *Biotechnol Bioeng* **85**: 434-441.
19. Pierce E, Xie G, Barabote RD*, et al.* (2008) The complete genome sequence of Moorella thermoacetica (f. Clostridium thermoaceticum). *Environ Microbiol* **10**: 2550-2573.
20. Sanchez-Andrea I, Guedes IA, Hornung B, Boeren S, Lawson CE, Sousa DZ, Bar-Even A, Claassens NJ & Stams AJM (2020) The reductive glycine pathway allows autotrophic growth of *Desulfovibrio desulfuricans*. *Nat Commun* **11**: 5090.

21. Schink B, Montag D, Keller A & Muller N (2017) Hydrogen or formate: Alternative key players in methanogenic degradation. *Environ Microbiol Rep* **9**: 189-202.
22. Sheik CS, Sieber JR, Badalamenti JP, Carden K & Olson A (2017) Complete Genome Sequence of Desulfovibrio desulfuricans Strain G11, a Model Sulfate-Reducing, Hydrogenotrophic, and Syntrophic Partner Organism. *Genome Announc* **5**.
23. Sieber JR, McInerney MJ & Gunsalus RP (2012) Genomic insights into syntrophy: the paradigm for anaerobic metabolic cooperation. *Annu Rev Microbiol* **66**: 429-452.
24. Sousa DZ, Visser M, van Gelder AH*, et al.* (2018) The deep-subsurface sulfate reducer *Desulfotomaculum kuznetsovii* employs two methanol-degrading pathways. *Nat Commun* **9**: 239.
25. Stams AJ & Plugge CM (2009) Electron transfer in syntrophic communities of anaerobic bacteria and archaea. *Nat Rev Microbiol* **7**: 568-577.
26. Thauer RK, Kaster AK, Seedorf H, Buckel W & Hedderich R (2008) Methanogenic archaea: ecologically relevant differences in energy conservation. *Nat Rev Microbiol* **6**: 579-591.
27. Wang S, Huang H, Moll J & Thauer RK (2010) NADP+ reduction with reduced ferredoxin and NADP+ reduction with NADH are coupled via an electron-bifurcating enzyme complex in Clostridium kluyveri. *J Bacteriol* **192**: 5115-5123.
28. Yishai O, Lindner SN, Gonzalez de la Cruz J, Tenenboim H & Bar-Even A (2016) The formate bio-economy. *Curr Opin Chem Biol* **35**: 1-9.

Chapter 5 Metabolic pathway of formate-driven syntrophic methanogenesis

Introduction

It was known that the typical syntrophic formate degradation was conducted by formate dehydrogenase and hydrogenase for the carbon flow and electron flow, resulting in H_2/CO_2 production and proton gradient-driven ATP synthesis (Dolfing *et al.*, 2008). However, it could not elucidate the metabolic pathway of methanol-mediated syntrophic formate degradation, which needs methanol production via formate reduction and reducing equivalent by formate oxidation. Transcriptomics is an efficient way to look at the gene expression profile for each condition globally. To elucidate the metabolic pathway, RNA sequencing was conducted for the non-syntrophic condition (*i.e.*, yeast extract-fed K32 or methanol-fed ZC-1 monocultures) and the syntrophic lifestyle (formate-fed coculture). Comparative transcriptome results indicated a methanol-mediated syntrophy performed by an unusual metabolic pathway.

Result and discussion

Methylotrophic methanogenesis of *M. shengliensis* ZC-1

Comparative analysis of the gene expression profiles of *M. shengliensis* ZC-1 for the K32/ZC-1 coculture and ZC-1 monoculture showed that methanol was the primary methanogenic precursor in syntrophic conditions. We extracted and sequenced the RNA in formate-fed K32/ZC-1 co-cultures and found that ZC-1 showed a highly similar gene expression pattern in formate-fed and methanol-fed monoculture (Fig. 5.1 and Appendices Supplementary Table 2). The strain ZC-1 highly expressed genes involved in methanol catabolism (*i.e.*, methanol-corrinoid protein co-methyltransferase (ZC1_00056) and methanol-corrinoid protein (ZC1_00058) in top ten of gene

expression level; Fig. 5.1 and Appendices Supplementary Table 2). Genes associated with aceticlastic methanogenesis and CO_2-reducing methanogenesis were expressed relatively much lower. Given that these genes were also highly expressed (top ten) by methanol-grown ZC-1 (Fig. 5.1 and Appendices Supplementary Table 2), the primary energy source for ZC-1 in the K32/ZC-1 co-culture was clearly methanol. In other words, methanol was the primary candidate mediating symbiosis.

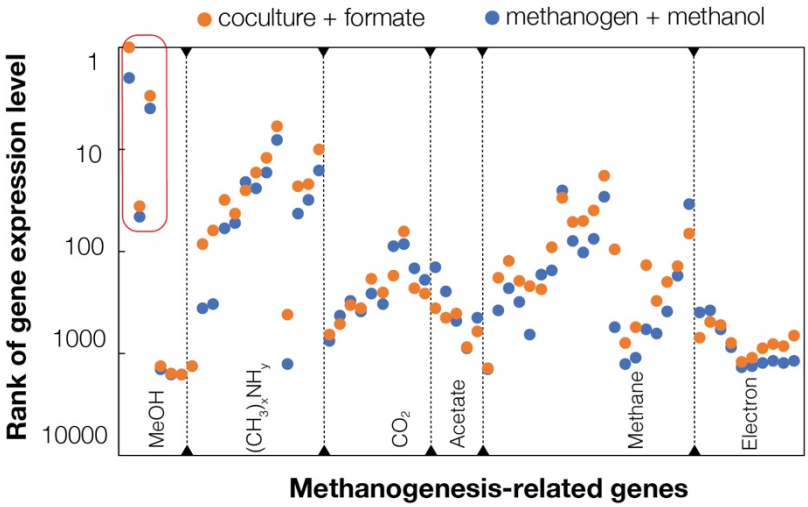

Figure 5.1 Rank of methanogenesis genes in terms of gene expression level by normalized RPKM values for methanol-fed monoculture and formate-fed coculture

Unusual methanol-generating formate disproportionation

In agreement, K32 also highly expressed genes (aldehyde: ferredoxin oxidoreductase [AFOR, K32-1_02760] and alcohol dehydrogenase [ADH, K32-1_00231]) that may support the reduction of formate to methanol via formaldehyde (Ying *et al.*, 2007, Frock *et al.*, 2010, Sousa *et al.*, 2018)

(Fig. 5.2 and Appendices Supplementary Table 3). Although AFOR and ADH can facilitate the reduction of diverse fatty acids to corresponding alcohols (Nissen & Basen, 2019), other fatty acids and alcohols besides formate were undetectable (*e.g.*, ethanol) or only in trace amounts (*e.g.*, acetate) in the formate-fed K32/ZC-1 cocultures. Considering (i) the presence of formate and high expression of ADH and overexpression AFOR in methanol-fed co-cultures of K32 and ZC-1 (Fig. 5.2 and Appendices Supplementary Table 3) and (ii) syntrophic growth of K32 on methanol in co-culture with the formate-utilizing methanogen *Methanothermobacter thermoautotrophicus* TM (Hattori *et al.*, 2000) (Fig. 3.10), it was clear that K32 employs a metabolic relationship between methanol and formate.

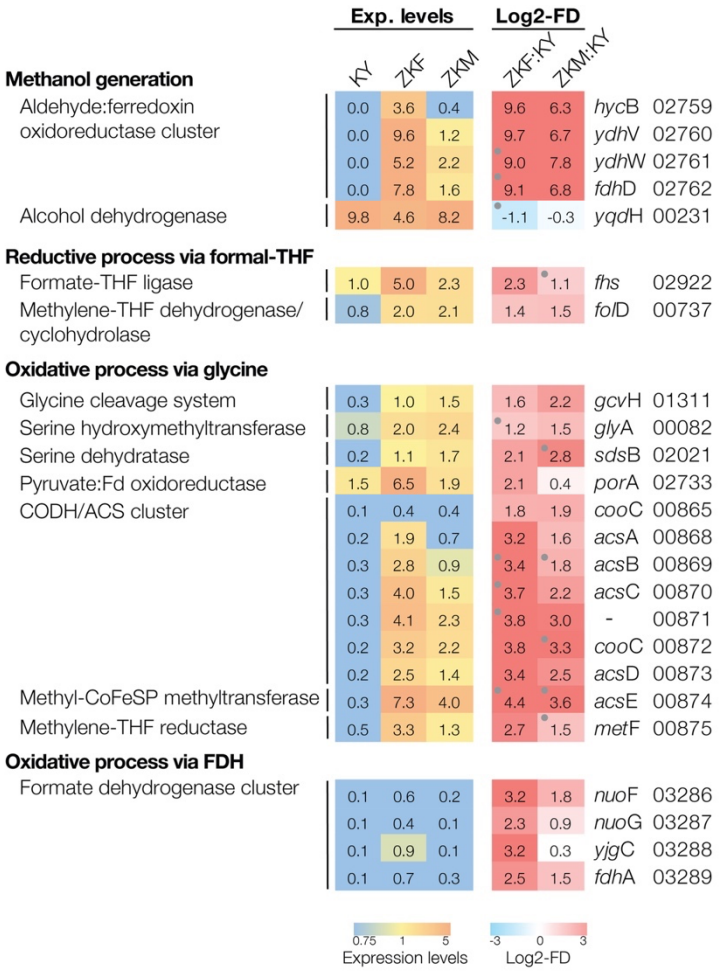

Figure 5.2 Comparison of K32 gene expression in mono-culture growth on yeast extract and co-culture with ZC-1 growth on formate and methanol. Gene expression levels were normalized by RPKM (reads per kilobase transcript per million mapped reads) values plus one to the average ribosomal protein RPKM of each sample. Log2-FD shows the log 2-ratio of averaged normalized RPKM values. p-value < 0.05 are marked with dot. KY, K32 mono-culture growth on yeast extract; ZKF, K32/ZC-1 co-culture growth on formate; ZKM, K32/ZC-1 co-culture growth on methanol.

As methanol generation is a reductive process, K32 must complement this with formate oxidation. Assuming nearly all methane generated in the K32/ZC-1 co-culture was methanol-derived (2.44 mM formate was converted to methanol), all the remaining formate must be oxidized to balance redox. While well-known syntrophic formate-degraders oxidize formate to CO_2 using formate dehydrogenases (Guyot & Brauman, 1986, Dolfing *et al.*, 2008), K32 did not highly express such genes in the formate-fed K32/ZC-1 co-cultures (Fig. 5.2 and Appendices Supplementary Tables 3). Instead, overexpression of the bifunctional CO dehydrogenase/acetyl-CoA synthase (CODH/ACS) and methylenetetrahydrofolate reductase (MTHFR) (K32-1_00865~75) as genes that may support oxidative CO_2 generation was detected (Fig. 5.2 and Fig. 5.3). Although these can alternatively support reductive acetate generation (*i.e.*, acetogenesis), the extremely low concentration of acetate detected in the cultures indicates that these enzymes operate in the acetyl-CoA-oxidizing (*i.e.*, CO_2-yielding) direction. Based on further inspection, K32 highly expressed genes that can support oxidization of formate to CO_2 via acetyl-CoA using a pathway mediated by one-carbon metabolism involving glycine, serine, and pyruvate (Fig. 5.2 and Fig. 5.3): (i) activation of formate with tetrahydrofolate (THF) to formyl-THF and subsequent oxidation to

methylene-THF (FTL and MTCD, K32-1_02922 and K32-1_00737), (ii) sequential condensation of methylene-THF with CO_2 and NH_4^+ to glycine (glycine cleavage system H protein, K32-1_01311) and this glycine with another methylene-THF (discussed later) to serine (serine hydroxymethyltransferase, K32-1_00082), (iii) serine oxidation to acetyl-CoA via pyruvate (serine dehydratase, K32-1_02021; pyruvate: ferredoxin oxidoreductase, K32-1_02733), and (iv) sequential oxidation of acetyl-CoA oxidation to CO_2 and methyl-THF and methyl-THF to methylene-THF, which is recycled for serine formation. Besides the high overexpression of the genes involved, this peculiar one-carbon metabolism mediated by multi-carbon intermediates is further evidenced by the fact that (a) glycine/serine metabolism is one of the very few known metabolic pathways that connect one-carbon metabolism to acetyl-CoA (Yishai *et al.*, 2016, Sanchez-Andrea *et al.*, 2020, Song *et al.*, 2020), (b) aerobic methanotrophs/methylotrophs are known to assimilate formaldehyde via glycine/serine (Hanson & Hanson, 1996), (c) glycine/serine-mediated one-carbon pathways have been proposed for other metabolisms (*Pseudothermotoga lettingae* acetate/methanol catabolism (Nobu *et al.*, 2015)). Besides the overall pathway shown above, an alternative sub-pathway with the methylene-THF generation by the spontaneous reaction of formaldehyde intermediate of formate reduction to methanol with THF may also support the formate oxidizing to CO_2 (Kallen & Jencks, 1966). Overall, such oxidation of formate to CO_2 can be coupled with formate-reducing methanol generation at a 2:1 ratio (Equation 5.1: 3 formate = methanol + 2 CO_2+ H_2O).

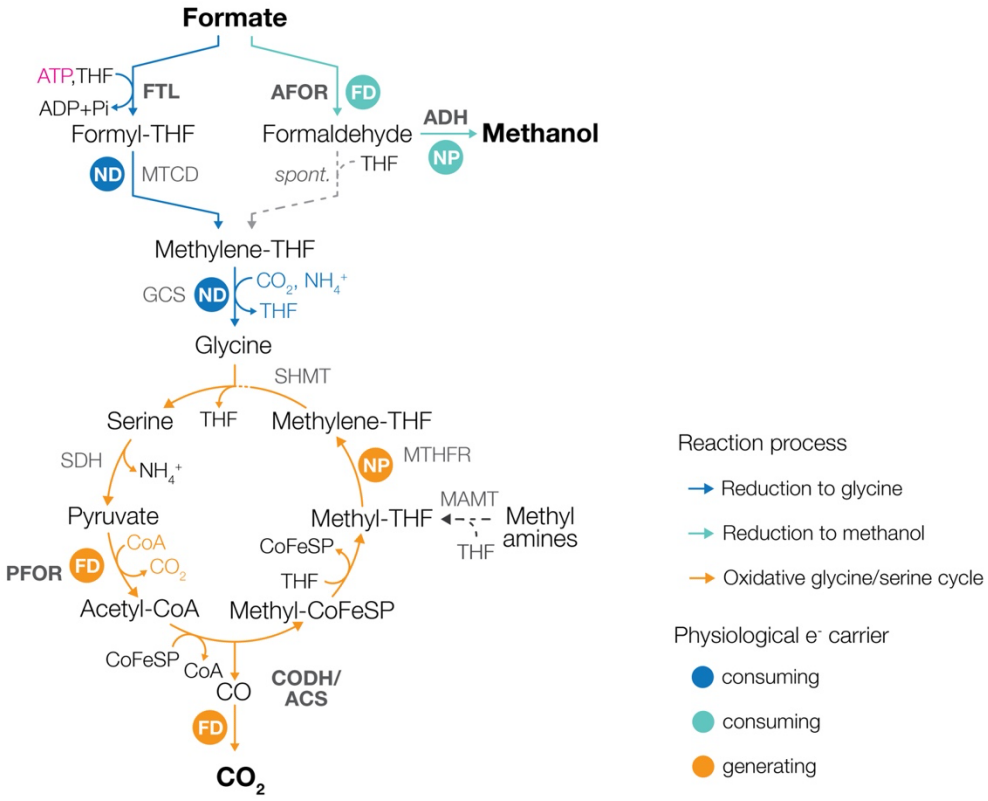

Figure 5.3 Formate disproportionation pathway of *Z. formicivorans* K32. Reductive and oxidative processes are marked with blue and orange lines, respectively. Spontaneous reaction (*Spont.*) and methylated amines metabolism branch are marked with gray and black dash lines, respectively. Dots show the consuming (blue or green) and generating (light orange) of NADH (ND), NADPH (NP), and ferredoxin (FD). Abbreviations: FTL, Formate-THF ligase; MTCD, bifunctional methylene-THF dehydrogenase/cyclohydrolase; GCS, glycine cleavage system; SHMT, serine hydroxymethyltransferase; SDH, serine dehydratase; PFOR, pyruvate: ferredoxin oxidoreductase; CODH/ACS, CO dehydrogenase/acetyl-CoA synthase; MT, methyltetrahydrofolate: corrinoid methyltransferase; MTHFR, methylenetetrahydrofolate reductase; AFOR, aldehyde: ferredoxin oxidoreductase; ADH, alcohol dehydrogenase; MAMT, methylated amines associated methyltransferases.

Energy conservation of K32

The formyl-THF-dependent net pathway converts three formate into one methanol and two CO_2 with the generation of three Fd_{red} and one NADPH and consumption of four NADH and two ATP. Thus, to complete the pathway, electrons must be transferred from the reduced electron carriers (Fd_{red} and NADPH) to NADH. Oxidation of 1 NADPH coupled with reduction of 0.5 NAD^+ and 0.5 Fd_{ox} via electron bifurcation using the NADH-dependent Fd_{red}: $NADP^+$ oxidoreductase NfnAB (K32-1_00735~36) (2 NADPH + NAD^+ + Fd_{ox} = 2 $NADP^+$ + NADH + Fd_{red}^{2-} + H^+) will leave 3.5 Fd_{red} to be oxidized with reduction of 3.5 NAD^+. This redox reaction is coupled with energy generation through extrusion of cations (H^+ or Na^+) via Rnf (Fd_{red}^{2-} + NAD^+ + H^+ + $2X^+_{in}$ = Fd_{ox} + NADH + $2X^+_{out}$ (Buckel & Thauer, 2013, Buckel & Thauer, 2018), but Rnf-lacking syntrophic organisms were thought to utilize an alternative complex (Hdr-Flox complex; K32-1_01374-83) with an unknown reaction mechanism (Nobu *et al.*, 2015, Ramos *et al.*, 2015). Regardless of the reaction mechanism, the electron transfer has a ΔG of −32.8 to −42.5 kJ/mol (based on reduction potentials of −450 to −500 mV for Fd_{ox}/Fd_{red} and −280 mV for NAD^+/NADH) roughly equivalent to translocation of two H^+/Na^+ (−15 to −20 kJ/mol), so we assume that K32 translocates 7 H^+/Na^+, which equates to roughly 2.33 ATP (3 H^+/Na^+ transferred per synthesis of ATP). Thus, the theoretical net ATP yield is 0.33 ATP. Through similar calculations, the formaldehyde-mediated pathway will generate 1 Fd_{red} and 1 NADPH while consuming 2 NADH. The reduction of 1 NADPH results in the generation of 0.5 of each Fd_{red} and NADH via enzyme Nfn, theoretically. In total, 1.5 Fd_{red} will be generated to reduce 1.5 NAD^+ to NADH, resulting in the translation of 3 H^+/Na^+, which will drive ATP synthetase to yield roughly 1 ATP.

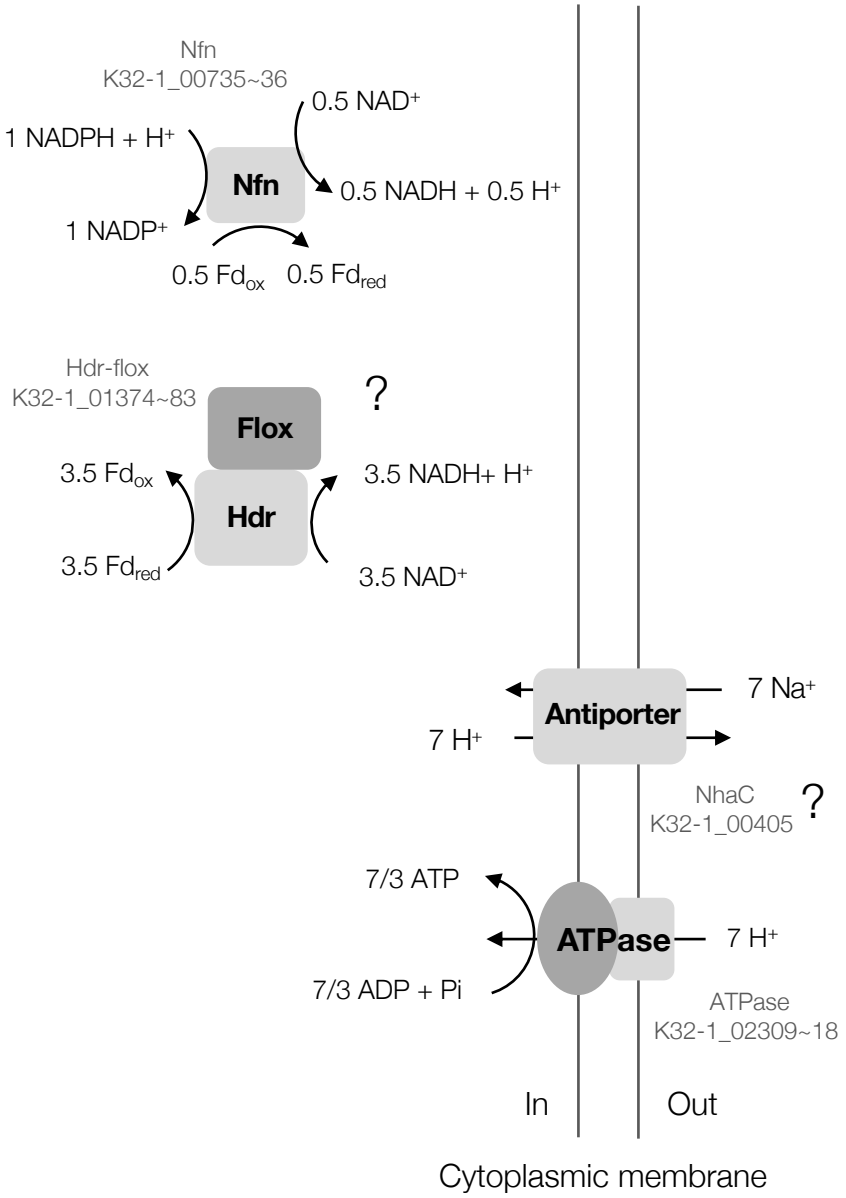

Figure 5.4 Schematic diagram of energy conservation system for *Z. formicivorans*. Values are for the formyl-THF-dependent net pathway.

Conclusion

Gene expression profiles of *M. shengliensis* ZC-1 clearly suggested methanol was the "intermediate" mediating the syntrophic relationship between *M. shengliensis* and *Z. formicivorans.* It is quite unusual to the typical interspecies H_2/formate and direct electron transfer, while it bridges an ecological niche where methylotrophic methanogens were thought to be missing. While utilization of methanol is widespread for anaerobes, especially for acetogens, it is rare that use reductase instead of using methyltransferase that many anaerobes have been reported (Kremp *et al.*, 2018, Sousa *et al.*, 2018, Kremp & Muller, 2021). The employment of AFOR and ADH enables *Z. formicivorans* to generate methanol for the sequential bioprocess – methylotrophic methanogenesis, thus leading the methanol-mediated syntrophy. *Z. formicivorans* conducted formate oxidation via a complex glycine/serine involving reversed Wood- Ljungdahl pathway, while the typical syntrophic formate degradation was performed through simple formate dehydrogenase and hydrogenase. The long pathway may bring more chances to connect the formate catabolism to other necessary metabolisms for the survival of *Z. formicivorans*. In summary, the expression profiles of *Z. formicivorans* and *M. shengliensis* evidenced that the K32/ZC-1 coculture conducted methanol-mediated syntrophy via formate disproportionation to methanol and CO_2. The results also shed light on the diverse metabolism that microorganisms are capable of.

Table 5.1 Electron, reducing equivalents and ATP consumption or generation for each pathway of formate disproportionation

Pathway ID	Pathway	Processes	Electron	Reducing equavilents			ATP	Proton translocation	Net ATP production
				Fd_{red}	NADH	NADPH			
Sub-pathway									
a	Methanol generation	Formate -> Formaldehyde -> Methanol	-4	-1	0	-1	0		
b	Formate reduction to glycine via formaldehyde	Formate -> Formaldehyde -> Methylene-THF -> Glycine	-4	-1	-1	0	0		
c	Formate reduction to glycine via formyl-THF	Formate -> Formyl-THF -> Methylene-THF -> Glycine	-4	0	-2	0	-1		
d	Oxidative glycine-serine cycle	Glycine -> Serine -> pyruvate -> Acetyl-CoA -> Methyl-THF /CO_2	6	2	0	1	0		
Overall pathway									
a+2b+2d	*ATP-high*: formate disproportionation via formaldehyde only	Formate -> Formaldehyde -> Methanol/CO_2	0	1	-2	1	0		
a+2c+2d	*ATP-low*: formate disproportionation via formyl-THF	Formate -> Formyl-THF -> Methanol/CO_2	0	3	-4	1	-2		
a+b+c+2d	*ATP-high* : *ATP-low* = 1:1	Formate -> Formaldehyde/Formyl-THF -> Methanol/CO_2	0	2	-3	1	-1		
Intracellular Electron transfer and energy conservation									
e	Electron bifurcation	2 NADPH + NAD^+ + Fd_{ox} =2 $NADP^+$ + NADH + Fd_{red}^{2-} + H^+	0	0.5	0.5	-1	0		
a+2b+2d+e	*ATP-high*	Formate -> Formaldehyde -> Methanol/CO_2	0	1.5	-1.5	0	0	3	1.00
a+2c+2d+e	*ATP-low*	Formate -> Formyl-THF -> Methanol/CO_2	0	3.5	-3.5	0	-2	7	0.33
a+b+c+2d+e	*ATP-high* : *ATP-high*=1:1	Formate -> Formaldehyde/Formyl-THF -> Methanol/CO_2	0	2.5	-2.5	0	-1	5	0.67

Reference

1. Buckel W & Thauer RK (2013) Energy conservation via electron bifurcating ferredoxin reduction and proton/Na(+) translocating ferredoxin oxidation. *Biochim Biophys Acta* **1827**: 94-113.
2. Buckel W & Thauer RK (2018) Flavin-Based Electron Bifurcation, Ferredoxin, Flavodoxin, and Anaerobic Respiration With Protons (Ech) or NAD(+) (Rnf) as Electron Acceptors: A Historical Review. *Front Microbiol* **9**: 401.
3. Dolfing J, Jiang B, Henstra AM, Stams AJ & Plugge CM (2008) Syntrophic growth on formate: a new microbial niche in anoxic environments. *Appl Environ Microbiol* **74**: 6126-6131.
4. Frock AD, Notey JS & Kelly RM (2010) The genus *Thermotoga*: recent developments. *Environ Technol* **31**: 1169-1181.
5. Guyot JP & Brauman A (1986) Methane Production from Formate by Syntrophic Association of *Methanobacterium bryantii* and *Desulfovibrio vulgaris* JJ. *Appl Environ Microbiol* **52**: 1436-1437.
6. Hanson RS & Hanson TE (1996) Methanotrophic bacteria. *Microbiol Rev* **60**: 439-471.
7. Hattori S, Kamagata Y, Hanada S & Shoun H (2000) *Thermacetogenium phaeum* gen. nov., sp. nov., a strictly anaerobic, thermophilic, syntrophic acetate-oxidizing bacterium. *Int J Syst Evol Microbiol* **50 Pt 4**: 1601-1609.
8. Kallen RG & Jencks WP (1966) The mechanism of the condensation of formaldehyde with tetrahydrofolic acid. *J Biol Chem* **241**: 5851-5863.

9. Kremp F & Muller V (2021) Methanol and methyl group conversion in acetogenic bacteria: biochemistry, physiology and application. *FEMS Microbiol Rev* **45**: 1-22.
10. Kremp F, Poehlein A, Daniel R & Muller V (2018) Methanol metabolism in the acetogenic bacterium *Acetobacterium woodii*. *Environ Microbiol* **20**: 4369-4384.
11. Nissen LS & Basen M (2019) The emerging role of aldehyde:ferredoxin oxidoreductases in microbially-catalyzed alcohol production. *J Biotechnol* **306**: 105-117.
12. Nobu MK, Narihiro T, Rinke C, Kamagata Y, Tringe SG, Woyke T & Liu WT (2015) Microbial dark matter ecogenomics reveals complex synergistic networks in a methanogenic bioreactor. *ISME J* **9**: 1710-1722.
13. Nobu MK, Narihiro T, Hideyuki T, Qiu YL, Sekiguchi Y, Woyke T, Goodwin L, Davenport KW, Kamagata Y & Liu WT (2015) The genome of *Syntrophorhabdus aromaticivorans* strain UI provides new insights for syntrophic aromatic compound metabolism and electron flow. *Environ Microbiol* **17**: 4861-4872.
14. Ramos AR, Grein F, Oliveira GP, Venceslau SS, Keller KL, Wall JD & Pereira IA (2015) The FlxABCD-HdrABC proteins correspond to a novel NADH dehydrogenase/heterodisulfide reductase widespread in anaerobic bacteria and involved in ethanol metabolism in *Desulfovibrio vulgaris* Hildenborough. *Environ Microbiol* **17**: 2288-2305.
15. Sanchez-Andrea I, Guedes IA, Hornung B, Boeren S, Lawson CE, Sousa DZ, Bar-Even A, Claassens NJ & Stams AJM (2020) The reductive glycine pathway allows autotrophic growth of *Desulfovibrio desulfuricans*. *Nat Commun* **11**: 5090.
16. Song Y, Lee JS, Shin J*, et al.* (2020) Functional cooperation of the glycine synthase-reductase and Wood-Ljungdahl pathways for autotrophic growth of Clostridium drakei. *Proc Natl Acad Sci U S A* **117**: 7516-7523.

17. Sousa DZ, Visser M, van Gelder AH*, et al.* (2018) The deep-subsurface sulfate reducer *Desulfotomaculum kuznetsovii* employs two methanol-degrading pathways. *Nat Commun* **9**: 239.
18. Ying X, Wang Y, Badiei HR, Karanassios V & Ma K (2007) Purification and characterization of an iron-containing alcohol dehydrogenase in extremely thermophilic bacterium *Thermotoga* hypogea. *Arch Microbiol* **187**: 499-510.
19. Yishai O, Lindner SN, Gonzalez de la Cruz J, Tenenboim H & Bar-Even A (2016) The formate bio-economy. *Curr Opin Chem Biol* **35**: 1-9.

Chapter 6 Formate-driven syntrophy and its ecological role

Introduction

The growth, metabolism, and interaction of microorganisms can be explained based on the general law of thermodynamics and stoichiometry (Bar-Even *et al.*, 2012, Delattre *et al.*, 2019). Syntrophy is a thermodynamically interdependent lifestyle where microbes work close to thermodynamic equilibrium with a minimum energy dissipation (Leng *et al.*, 2018). Thus, a slight change of reactants and environmental conditions can greatly shift the metabolism. In agreement, syntrophs are flexible to switch their metabolism pattern or establish interactions corresponding to their ecosystem. For instance, *Thermacetogenium phaeum* conducted acetate oxidation or reductive acetogenesis according to the H_2 partial pressure (Schink, 1997, Hattori *et al.*, 2005, Hattori, 2008), and propionate syntrophs in paddy field soils exhibited a distinct biogeographical pattern that was related to the annual temperature and the total sulfur content of soil, *etc* (Jin *et al.*, 2021). Thermodynamics is critical in analyzing and understanding how syntrophs work and respond to the changes in ecosystems by calculating the direction of biochemical processes (González-Cabaleiro *et al.*, 2013), evaluating metabolic routes (Dolfing *et al.*, 2009), predicting the metabolic mechanism (Bar-Even *et al.*, 2012, Dolfing & Hubert, 2017, Veshareh *et al.*, 2021, Wu *et al.*, 2022), interpreting the prevalence of microbes and ecological niches (Dolfing, 2014, Westerholm *et al.*, 2019).

In this study, thermodynamics was applied to elaborate on the syntrophic lifestyle of the formate-utilizing bacterium *Zhaonella formicivorans* and the ecological role of the proposed methanol-mediated syntrophy. The results suggested that the formate syntroph harbor flexible metabolic pathways to perform efficient energy harvest. The results also shed light on the potential ecological niche that methanol-mediated syntrophy has.

Result and discussion

Thermodynamics driven syntrophy

To understand whether the methanol-generating formate disproportionation requires syntrophic interaction with a methylotrophic methanogen, we further evaluate the energetics and thermodynamics of the pathway. The formyl-THF-dependent net pathway is estimated to recover roughly 1/3 ATP (Equation 2: 3 formate + 0.33 ADP + 0.33 Pi = methanol + 2 CO_2 + 1.33 H_2O + 0.33 ATP; $\Delta G^{0`}$ = -7.19 kJ/reaction) through intracellular electron transfer performing by Flox-Hdr complex expressed by K32. (Fig. 5.4 and Appendices Supplementary Table 3) (Nobu *et al.*, 2015, Ramos *et al.*, 2015). Thermodynamic calculations showed that, in order to recover this much energy (~20 kJ/mol for the synthesis of 1/3 mol ATP), the net pathway would require the primary byproduct (methanol) to be maintained at an extremely low concentration (≤ 0.35~11 μM methanol at 1 mM formate, 0.2 atm CO_2, 55 °C, and pH 6.5~7.0; Table 6.1). Thus, the above formate degradation pathway clearly requires a methanol-scavenging partner (*i.e.*, syntrophy).

The energetics and thermodynamics of K32 formate disproportionation may have some flexibility, a feature advantageous for optimizing energy acquisition to dynamic/heterogenous environmental conditions. While K32 highly expressed genes for the reduction of formate to methylene-THF via activation to formyl-THF, the spontaneous formaldehyde-mediated pathway may have an energetic advantage for it does not consume ATP to active the formate catabolism. While seemingly redundant, the two pathways differ in the net thermodynamics and ATP generation, that the latter pathway has a higher ATP yield (Equation 3: 3 formate + ADP + Pi = methanol + 2 CO_2 + 2 H_2O + ATP) (Tables 5.1), but, in exchange, has lower thermodynamic favorability ($\Delta G^{0`}$ = +32.81 kJ/reaction, Tables 6.1). This pathway can recover more energy when thermodynamic

conditions are favorable. Thus, by utilizing the two pathways together, K32 can theoretically flexibly adjust the ATP yield of formate catabolism to adapt to the thermodynamic conditions (*e.g.*, the two pathways can be operated at 5:1 to increase ATP yield by 33% when methanol is extremely low [0.003~0.95 μM at pH 6.5~7.0]; Fig. 6.1). This is a new example of a syntrophic organism possessing two thermodynamic/energetic options for the catabolism (Nobu *et al.*, 2017).

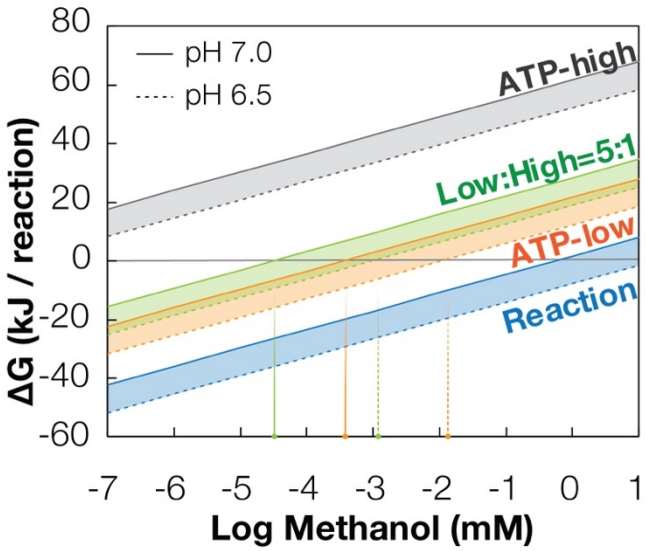

Figure 6.1. Gibbs free-energy changes of formate degradation to methanol and carbon dioxide. Gibbs free energy changes (ΔG) are calculated under a physiological condition with pH of 7.0, CO_2(g) of 0.2 atm, and formate of 1 mM. Reaction, equation 1 in the main text, 3 formate = methanol + 2 CO_2 + H_2O, is the basic reaction of the disproportionation of formate to methanol and CO_2. ATP-low, 3 formate + 0.33 ADP + 0.33 Pi = methanol + 2 CO_2 + 1.33 H_2O + 0.33 ATP (equation 2), indicates the more thermodynamically favorable but low ATP generation pathway when formate is oxidized through formyl-THF-mediated pathway. ATP-high, 3 formate + ADP + Pi = methanol + 2 CO_2 + 2 H_2O + ATP (equation 3), indicates the thermodynamically unfavorable but high ATP generation pathway when formate is oxidized through the formaldehyde-mediated

pathway; The vertical dash lines indicate each equation's threshold methanol concentration when ΔG= 0 KJ/reaction with corresponding colors. ΔG for ATP synthesis ($\Delta G_{ATPsynthesis}$) is assumed to be 60 KJ/mol. ΔG value for other equations are calculated as the $\Delta G_{equation1}$ + (mol ATP generated/reaction) * $\Delta G_{ATPsynthesis}$.

Further inspection of the transcriptome showed that other supplementary electron transfer pathways might also support the K32/ZC-1 symbiosis. ZC-1 expressed methylamine metabolism (mono-, di-, and tri-methylamine methyltransferases) during methanol degradation (both methanol-fed monocultures and formate-fed co-cultures; Fig. 5.3 and Appendices Supplementary Table 3) despite the lack of exogenous methylamines. In accordance with data shown in the previous study that *M. shengliensis* co-expressed methylamine-related genes under the methylated compounds-fed (*i.e.*, methanol and methoxybenzoate) conditions (Kurth *et al.*, 2021). Complementing this, K32 expressed di- and tri-methylamine metabolism in formate-fed co-cultures (Appendices Supplementary Table 3). This suggested that the transfer of methylamines from ZC-1 to K32 may be involved in the symbiotic interaction. The methane generation for the trimethylamine-fed coculture of K32 with a formate-utilizing methanogenic partner (*M. thermoautotrophicus* TM; Fig. 6.2) further confirmed that K32 can symbiotically, though weakly, degrade trimethylamine. Based on thermodynamic calculations, this methylamine exchange may provide supplementary thermodynamic and energetic advantages in driving syntrophic formate degradation (Tables 6.1).

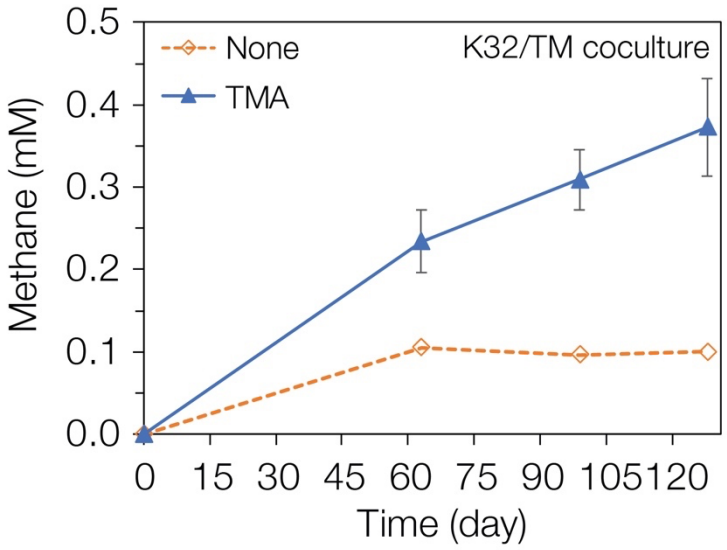

Figure 6.2 Growth of co-culture of *Z. formicivorans* K32 and *M. thermautotrophicus* TM on trimethylamine. TMA, trimethylamine. Error bars represent the standard deviation of the triplicates.

Table 6.1 Gibbs free energy yield (ΔG) for formate-based syntrophy

Note	Reaction	pH 7.0 or CH_4 = 0.2 atm				pH 6.5 or CH_4 = 0.002 atm			
		ΔG^0	$\Delta G^{0'}$	$\Delta G^{1'}$	MeOH/H_2 threshold	ΔG^0	$\Delta G^{0'}$	$\Delta G^{1'}$	MeOH/H_2 threshold
Syntrophic formate disproportionation to methanol and CO_2									
Basic Reaction	3 formate + $3H^+$ = methanol + 2 CO_2 + H_2O	-28.54	-27.19	20.52		-37.10	-36.62	11.14	
ATP-low	3 formate + $3H^+$ + 1/3 ADP + 1/3 Pi = *methanol* + 2 CO_2 + 4/3 H_2O + 1/3 ATP	-8.54	-7.19	40.52	0.35 μM	-17.10	-16.62	31.14	11 μM
ATP-high	3 formate + $3H^+$ + ADP + Pi = methanol + 2 CO_2 + 2 H_2O + ATP	31.46	32.81	80.52		22.90	23.38	71.14	
ATP-low : ATP-high=5:1	3 formate + $3H^+$ + 4/9 ADP + 4/9 Pi = *methanol* + 2 CO_2 + 13/9 H_2O + 4/9 ATP	-1.87	-0.52	47.19	0.003 μM	-10.43	-9.95	37.81	0.95 μM
Typical syntrophic formate oxidation									
	Formate + H^+ = H_2 + CO_2	-3.45	-7.02	7.43	0.03 μM (4.3 pa)	-6.30	-10.16	4.29	0.1 μM (13.5 pa)
Methanogenesis									
H2-dependent	4 H_2+CO_2 = CH_4 + H_2O	-130.8	-118.51	-118.51	0.09 μM (12.0 pa)	-130.8	-118.51	-131.08	0.03 μM (3.8 pa)
Methanol-dependent	4 *Methanol* = 3 CH_4 + CO_2 +2 H_2O	-319.6	-331.04	-348.6	0.8 nM	-319.6	-331.04	-386.3	0.025 nM
Methylated amines involved syntrophic formate degradation									
Methylamine	3 formate + 4 H^+ + methylamine = 2 methanol + 2 CO_2 + $NH4^+$	-26.88	-25.05	-33.83		-38.30	-37.62	-46.28	
Dimethylamine	3 formate + 3 H^+ + dimethylamine = 3 methanol + 2 CO_2 + methylamine	-3.94	-4.17	-19.24		-12.50	-13.60	-26.19	
Trimethylamine	3 formate + 3 H^+ + trimethylamine = 3 methanol + 2 CO_2 + dimethylamine	-1.84	-2.37	-17.43		-10.40	-11.79	-24.09	
Trimethylamine	6 formate + 6 H^+ + trimethylamine = 4 methanol + 4 CO_2 + methylamine	-5.78	-6.54	-36.67		-22.90	-25.39	-50.27	
Trimethylamine	9 formate + 10 H^+ + trimethylamine = 6 methanol + 6 CO_2 + $NH4^+$	-32.66	-31.59	-70.5		-61.20	-63.00	-96.55	

Notes: ΔG^0 was calculated at standard conditions (pH7.0 or pH 6.5). $\Delta G_{0'}$ was calculated at 328K otherwise at standard conditions (pH7.0 or pH 6.5). $\Delta G^{1'}$ was calculated at pH of 7.0 or 6.5, CO_2 (g) of 0.2 atm, formate of 1 mM, otherwise at standard conditions. Methanol or H_2 threshold shows the maximum (formate degradation) or minimum (methanogenesis) methanol concentration or H_2 partial pressure for $\Delta G^{1'}$ meeting the minimal energy quantum to generate ATP (1/3 ATP, one proton for formate degradation and H_2-dependent methanogenesis, six protons for methanol-dependent methanogenesis). $\Delta G^{1'}$ for methylated amines related reactions were calculated under condition of methylamines and methanol of 0.01 mM, NH_4^+ of 0.1 mM, CO_2 (g) of 0.2 atm and pH 7.0 or 6.5.

Thermodynamic/energetic advantages of methanol-mediated syntrophy

The formate disproportionation pathway used by K32 has thermodynamic/energetic advantages over typical syntrophic formate oxidation (coupled with reductive H_2 production; $HCOO^- + H^+ = CO_2 + H_2$, $\Delta G^{0'} = -7.02$ kJ/reaction, Fig. 6.3 and Tables 6.1). The latter metabolism requires H_2 to be at extremely low concentrations (0.03~0.1 µM assuming 1 mM formate, 0.2 atm CO_2, 55 °C, pH 6.5~7.0, and 1/3 ATP gained per formate) near the thermodynamic limit of H_2-utilizing methanogenesis (0.03~0.09 µM H_2 at 0.002~0.2 atm CH_4, 0.2 atm CO_2, pH 6.5~7.0 and 55 °C; Fig. 6.3 and Table 6.1). Moreover, this metabolism is likely subject to thermodynamic inhibition from other H_2-generating processes, which are ubiquitous. On the other hand, methanol-generating formate disproportionation only necessitates methanol concentrations well above the thermodynamic limit of their partners (0.8 nM at 0.2 atm CO_2 and CH_4, 55 °C, and pH 6.5~7; Fig. 6.1b), is unencumbered by thermodynamic competition (*i.e.*, no other common methanol-generating processes), and has the capacity to adapt its energetics to the immediate thermodynamic conditions.

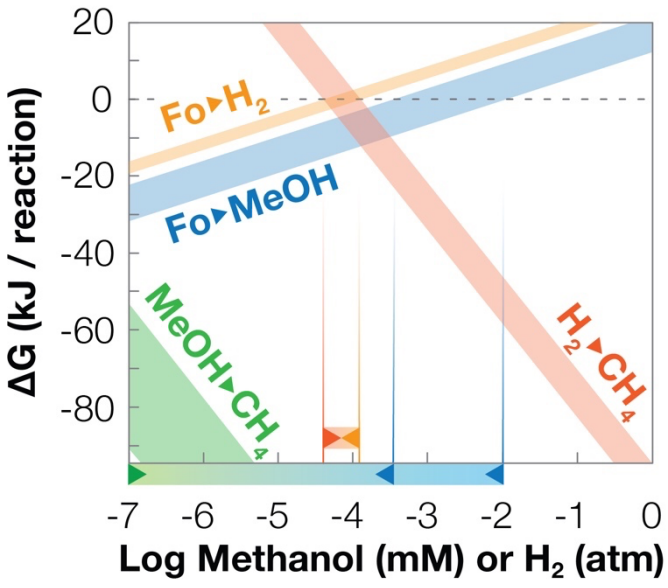

Fig.6.3 Comparison of Gibbs free-energy changes of formate-based syntrophy. ΔG is calculated at CO_2 (g) of 0.2 atm and formate of 1 mM. Fo→MeOH, syntrophic formate degradation to methanol and CO_2 as showing in (a); Fo→H_2, syntrophic formate degradation to H_2 and CO_2 ($HCOO^- + H^+ = H_2 + CO_2$); H_2→CH_4, hydrogenotrophic methanogenesis ($4H_2+CO_2 = CH_4 + H_2O$); MeOH→CH_4, methylotrophic methanogenesis ($4CH_3OH= 3CH_4 + CO_2 +2H_2O$). For syntrophic metabolism, the relationship between ΔG and MeOH/H_2 concentration is shown for pH 6.5 (lower boundary) to 7.0 (upper). For methanogenic metabolism, the relationship is shown for 0.002 atm (lower boundary) to 0.2 atm (upper) CH_4. The vertical lines indicate each equation's threshold methanol concentration or hydrogen partial pressure to generate minimal ATP (1/3 ATP, one proton for Fo→H_2, Fo→MeOH, and H_2→CH_4, six protons for MeOH→CH_4 (Kurth *et al.*, 2021)) with corresponding arrows. The MeOH/H_2 concentration range at which metabolic syntrophy is viable is indicated.

Conclusion

Thermodynamics shows that the methanol-mediated interaction between *Z. formicivorans* and *M. shengliensis* takes place close to thermodynamic equilibrium, confirming that the symbiosis is thermodynamically interdependent (*i.e.*, syntrophy). *Z. formicivorans* possesses two parallel metabolic pathways for its syntrophic lifestyle, which enable the syntroph to have the flexibility to combat thermodynamic restriction with the maximum energy conservation. This finding suggests the underestimation of the metabolic diversity and the adaption strategies that syntrophs have. Taking the advantages that methylated compounds have, methanol-mediated syntrophy

shows thermodynamic and energetic superiority for encountering no thermodynamic limitation from its partner methanogens and no competition from other methanol generation bioprocesses. This may make syntrophic formate oxidation coupled to methylotrophic methanogens as a significant anaerobic pathway in some scenarios like methanogenic organics degradation in the deep subsurface.

Reference

1. Bar-Even A, Flamholz A, Noor E & Milo R (2012) Thermodynamic constraints shape the structure of carbon fixation pathways. *Biochim Biophys Acta* **1817**: 1646-1659.
2. Delattre H, Desmond-Le Quemener E, Duquennoi C, Filali A & Bouchez T (2019) Consistent microbial dynamics and functional community patterns derived from first principles. *ISME J* **13**: 263-276.
3. Dolfing J (2014) Thermodynamic constraints on syntrophic acetate oxidation. *Appl Environ Microbiol* **80**: 1539-1541.
4. Dolfing J & Hubert CRJ (2017) Using Thermodynamics to Predict the Outcomes of Nitrate-Based Oil Reservoir Souring Control Interventions. *Front Microbiol* **8**: 2575.
5. Dolfing J, Xu A, Gray ND, Larter SR & Head IM (2009) The thermodynamic landscape of methanogenic PAH degradation. *Microb Biotechnol* **2**: 566-574.
6. González-Cabaleiro R, Lema JM, Rodríguez J & Kleerebezem R (2013) Linking thermodynamics and kinetics to assess pathway reversibility in anaerobic bioprocesses. *Energy & Environmental Science* **6**.

7. Hattori S (2008) Syntrophic acetate-oxidizing microbes in methanogenic environments. *Microbes Environ* **23**: 118-127.
8. Hattori S, Galushko AS, Kamagata Y & Schink B (2005) Operation of the CO dehydrogenase/acetyl coenzyme A pathway in both acetate oxidation and acetate formation by the syntrophically acetate-oxidizing bacterium Thermacetogenium phaeum. *J Bacteriol* **187**: 3471-3476.
9. Jin Y, Jiao S, Dolfing J & Lu Y (2021) Thermodynamics shapes the biogeography of propionate-oxidizing syntrophs in paddy field soils. *Environ Microbiol Rep* **13**: 684-695.
10. Kurth JM, Nobu MK, Tamaki H*, et al.* (2021) Methanogenic archaea use a bacteria-like methyltransferase system to demethoxylate aromatic compounds. *ISME J* **15**: 3549-3565.
11. Leng L, Yang P, Singh S*, et al.* (2018) A review on the bioenergetics of anaerobic microbial metabolism close to the thermodynamic limits and its implications for digestion applications. *Bioresour Technol* **247**: 1095-1106.
12. Nobu MK, Narihiro T, Liu M, Kuroda K, Mei R & Liu WT (2017) Thermodynamically diverse syntrophic aromatic compound catabolism. *Environ Microbiol* **19**: 4576-4586.
13. Nobu MK, Narihiro T, Hideyuki T, Qiu YL, Sekiguchi Y, Woyke T, Goodwin L, Davenport KW, Kamagata Y & Liu WT (2015) The genome of *Syntrophorhabdus aromaticivorans* strain UI provides new insights for syntrophic aromatic compound metabolism and electron flow. *Environ Microbiol* **17**: 4861-4872.
14. Ramos AR, Grein F, Oliveira GP, Venceslau SS, Keller KL, Wall JD & Pereira IA (2015) The FlxABCD-HdrABC proteins correspond to a novel NADH dehydrogenase/heterodisulfide reductase widespread in anaerobic bacteria and involved in ethanol metabolism in *Desulfovibrio vulgaris* Hildenborough. *Environ Microbiol* **17**: 2288-2305.

15. Schink B (1997) Energetics of syntrophic cooperation in methanogenic degradation. *Microbiol Mol Biol Rev* **61**: 262-280.
16. Veshareh MJ, Dolfing J & Nick HM (2021) Importance of thermodynamics dependent kinetic parameters in nitrate-based souring mitigation studies. *Water Res* **206**: 117673.
17. Westerholm M, Dolfing J & Schnurer A (2019) Growth Characteristics and Thermodynamics of Syntrophic Acetate Oxidizers. *Environ Sci Technol* **53**: 5512-5520.
18. Wu D, Li L, Zhen F, Liu H, Xiao F, Sun Y, Peng X, Li Y & Wang X (2022) Thermodynamics of volatile fatty acid degradation during anaerobic digestion under organic overload stress: The potential to better identify process stability. *Water Res* **214**: 118187.

Chapter 7 General Conclusion

Syntrophy is a well-known and critical survival strategy for microorganisms living in oligotrophic conditions. Syntrophic metabolism is a crucial step for decomposing organic matter into methane and carbon dioxide when inorganic electron acceptors are insufficient or absent (Stams & Plugge, 2009). The typical methanogenic syntrophy is established depending on interspecies H_2/formate and direct electron transfer (Stams & Plugge, 2009, Morris *et al.*, 2013, Lovley, 2017, Nozhevnikova *et al.*, 2020). However, none take advantage of one of the most thermodynamically favorable substrates utilizable by methanogens – methylated compounds (Nobu *et al.*, 2020).

In this study, a hitherto overlooked methanol-mediated symbiotic interaction was discovered through the establishment of cocultures between the anaerobic formate-utilizing bacterium *Zhaonella formicivorans* K32 (Lv *et al.*, 2020) and obligate methylotrophic archaea *Methermicoccus shengliensis* ZC-1 and AmaM (Cheng et al., 2007, Mayumi et al., 2016). The novel syntrophic interaction was proposed as the fourth mode of syntrophy involving methylotrophic methanogens hitherto unassociated with symbiosis. Unlike conventional electron carriers for syntrophy (*i.e.*, hydrogen, formate, and electron-conducting proteins) that only function as an electron donor for the methanogenic partner, methanol serves three purposes (electron donor, highly favorable electron acceptor, and carbon source), making methanol exchange uniquely a multidimensional mutualistic interaction. The generation of an electron acceptor for symbiotic partners is unprecedented and remarkable, given that it resolves one of the characteristic challenges of living in methanogenic environments, the lack of favorable electron acceptors.

Through the synthesis of cultivation- and transcriptomics-based analyses of *Z. formicivorans* and *M. shengliensis* cocultures, a novel methanol-generating metabolism was proposed. The formate

was disproportionated into methanol and CO_2 through unusual oxidoreductase and dehydrogenase involved methanol generation pathway and glycine/serine mediated reversed Wood-Ljungdahl pathway, respectively. This metabolism may serve as a rare biological source of methanol, providing insight into the enigmatic prevalence of methylotrophic methanogens despite the lack of endogenous sources of methanol (Yanagawa *et al.*, 2016, Sousa *et al.*, 2018). For instance, it may be one of the endogenous methylated compounds generation processes in subsurface ecosystems (*i.e.*, the oil reservoirs where *Z. formicivorans* and *M. shengliensis* strains were isolated from) that are rich in methylotrophic methanogens (*i.e.*, high proportions of *Methermicoccus*, *Methanosarcina*, *Methanolobus*, and *Methanomethylovorans* rRNA sequences in the SILVA v138 database are derived from oil reservoirs [8.3, 29.4, 34.7, and 43.4%]) despite the low availability of methylated compounds *in situ* (Mesle *et al.*, 2013).

Thermodynamics-based analyses suggested a versatile syntrophic mechanism that *Z. formicivorans* and *M. shengliensis* may employ, including the adjustment of pathways and performing other molecule exchanges. It indicates complex and diverse interactions that microbes may perform to adapt to the diverse ecosystem. The thermodynamics also showed the importance of methanol-mediated syntrophy and methyl compounds in anaerobic global carbon cycling. This not only reveals an overlooked symbiotic interaction and branch of carbon flow in subsurface environments, but also a bridge between two carbon cycles typically thought as independent of each other – syntrophic organics degradation and methylotrophic methanogenesis. Methanol-mediated syntrophy remarkably consumes formate that can thermodynamically inhibit conventional syntrophic processes.

Reference

1. Cheng L, Qiu TL, Yin XB, Wu XL, Hu GQ, Deng Y & Zhang H (2007) *Methermicoccus shengliensis* gen. nov., sp. nov., a thermophilic, methylotrophic methanogen isolated from oil-production water, and proposal of Methermicoccaceae fam. nov. *Int J Syst Evol Microbiol* **57**: 2964-2969.
2. Lovley DR (2017) Syntrophy Goes Electric: Direct Interspecies Electron Transfer. *Annu Rev Microbiol* **71**: 643-664.
3. Lv XM, Yang M, Dai LR*, et al.* (2020) *Zhaonella formicivorans* gen. nov., sp. nov., an anaerobic formate-utilizing bacterium isolated from Shengli oilfield, and proposal of four novel families and Moorellales ord. nov. in the phylum Firmicutes. *Int J Syst Evol Microbiol* **70**: 3361-3373.
4. Mayumi D, Mochimaru H, Tamaki H, Yamamoto K, Yoshioka H, Suzuki Y, Kamagata Y & Sakata S (2016) Methane production from coal by a single methanogen. *Science* **354**: 222-225.
5. Mesle M, Dromart G & Oger P (2013) Microbial methanogenesis in subsurface oil and coal. *Res Microbiol* **164**: 959-972.
6. Morris BE, Henneberger R, Huber H & Moissl-Eichinger C (2013) Microbial syntrophy: interaction for the common good. *FEMS Microbiol Rev* **37**: 384-406.
7. Nobu MK, Narihiro T, Mei R, Kamagata Y, Lee PKH, Lee PH, McInerney MJ & Liu WT (2020) Catabolism and interactions of uncultured organisms shaped by eco-thermodynamics in methanogenic bioprocesses. *Microbiome* **8**: 111.
8. Nozhevnikova AN, Russkova YI, Litti YV, Parshina SN, Zhuravleva EA & Nikitina AA (2020) Syntrophy and Interspecies Electron Transfer in Methanogenic Microbial Communities. *Microbiology* **89**: 129-147.

9. Sousa DZ, Visser M, van Gelder AH*, et al.* (2018) The deep-subsurface sulfate reducer *Desulfotomaculum kuznetsovii* employs two methanol-degrading pathways. *Nat Commun* **9**: 239.
10. Stams AJ & Plugge CM (2009) Electron transfer in syntrophic communities of anaerobic bacteria and archaea. *Nat Rev Microbiol* **7**: 568-577.
11. Yanagawa K, Tani A, Yamamoto N, Hachikubo A, Kano A, Matsumoto R & Suzuki Y (2016) Biogeochemical Cycle of Methanol in Anoxic Deep-Sea Sediments. *Microbes Environ* **31**: 190-193.

Appendices

Supplementary Table 1 *Z. formicivorans* strain K32 genes related to general functions.

Supplementary Table 2 Gene expression levels of methanogenesis-related genes of *M. shengliensis* ZC-1.

Supplementary Table 3 Gene expression levels for formate degradation, electron transduction, and energy conservation of *Z. formicivorans*.

Supplementary Table1 *Z. formicivorans* strain K32 genes related to general functions

Locus_Tag	Gene	Description
Carbohydrate metabolism		
Glycolysis / Gluconeogenesis		
K32-1_00095	yiaY	alcohol dehydrogenase
K32-1_00319	pfkA, PFK	6-phosphofructokinase 1
K32-1_00320	PK, pyk	pyruvate kinase
K32-1_00342	K16306	fructose-bisphosphate aldolase / 2-amino-3,7-dideoxy-D-threo-hept-6-ulosonate synthase
K32-1_00364	ACSS1_2, acs	acetyl-CoA synthetase
K32-1_00377	porC, porG	pyruvate ferredoxin oxidoreductase gamma subunit
K32-1_00378	porD	pyruvate ferredoxin oxidoreductase delta subunit
K32-1_00379	porA	pyruvate ferredoxin oxidoreductase alpha subunit
K32-1_00380	porB	pyruvate ferredoxin oxidoreductase beta subunit
K32-1_00579	DLD, lpd, pdhD	dihydrolipoamide dehydrogenase
K32-1_01495	glk	glucokinase
K32-1_01554	ppdK	pyruvate, orthophosphate dikinase
K32-1_01753	pgi1	glucose-6-phosphate isomerase, archaeal
K32-1_01761	acdB	acetate---CoA ligase (ADP-forming) subunit beta
K32-1_01762	acdA	acetate---CoA ligase (ADP-forming) subunit alpha
K32-1_01763	porB	pyruvate ferredoxin oxidoreductase beta subunit
K32-1_01764	porA	pyruvate ferredoxin oxidoreductase alpha subunit
K32-1_01765	porD	pyruvate ferredoxin oxidoreductase delta subunit
K32-1_01766	porC, porG	pyruvate ferredoxin oxidoreductase gamma subunit
K32-1_01805	GPI, pgi	glucose-6-phosphate isomerase
K32-1_01847	korB, oorB, oforB	2-oxoglutarate/2-oxoacid ferredoxin oxidoreductase subunit beta
K32-1_01848	korA, oorA, oforA	2-oxoglutarate/2-oxoacid ferredoxin oxidoreductase subunit alpha
K32-1_01976	PGK, pgk	phosphoglycerate kinase
K32-1_01977	gap2	glyceraldehyde-3-phosphate dehydrogenase (NAD(P))
K32-1_01978	DLD, lpd, pdhD	dihydrolipoamide dehydrogenase
K32-1_01979	DLAT, aceF, pdhC	pyruvate dehydrogenase E2 component (dihydrolipoamide acetyltransferase)
K32-1_01988	pps, ppsA	pyruvate, water dikinase
K32-1_02131	ENO, eno	enolase
K32-1_02132	gpmI	2,3-bisphosphoglycerate-independent phosphoglycerate mutase
K32-1_02133	TPI, tpiA	triosephosphate isomerase (TIM)
K32-1_02134	PGK, pgk	phosphoglycerate kinase
K32-1_02135	GAPDH, gapA	glyceraldehyde 3-phosphate dehydrogenase (phosphorylating)
K32-1_02339	glpX	fructose-1,6-bisphosphatase II
K32-1_02343	FBA, fbaA	fructose-bisphosphate aldolase, class II
K32-1_02733	korA, oorA, oforA	2-oxoglutarate/2-oxoacid ferredoxin oxidoreductase subunit alpha
K32-1_02734	korB, oorB, oforB	2-oxoglutarate/2-oxoacid ferredoxin oxidoreductase subunit beta
K32-1_03246	korB, oorB, oforB	2-oxoglutarate/2-oxoacid ferredoxin oxidoreductase subunit beta
K32-1_03247	korA, oorA, oforA	2-oxoglutarate/2-oxoacid ferredoxin oxidoreductase subunit alpha
Citrate cycle (TCA cycle)		
K32-1_00244	IDH1, IDH2, icd	isocitrate dehydrogenase
K32-1_00279	ACO, acnA	aconitate hydratase
K32-1_00377	porC, porG	pyruvate ferredoxin oxidoreductase gamma subunit
K32-1_00378	porD	pyruvate ferredoxin oxidoreductase delta subunit
K32-1_00379	porA	pyruvate ferredoxin oxidoreductase alpha subunit
K32-1_00380	porB	pyruvate ferredoxin oxidoreductase beta subunit
K32-1_00579	DLD, lpd, pdhD	dihydrolipoamide dehydrogenase
K32-1_00891	E4.2.1.2AA, fumA	fumarate hydratase subunit alpha
K32-1_00892	E4.2.1.2AB, fumB	fumarate hydratase subunit beta
K32-1_01763	porB	pyruvate ferredoxin oxidoreductase beta subunit
K32-1_01764	porA	pyruvate ferredoxin oxidoreductase alpha subunit
K32-1_01765	porD	pyruvate ferredoxin oxidoreductase delta subunit
K32-1_01766	porC, porG	pyruvate ferredoxin oxidoreductase gamma subunit
K32-1_01846	korC, oorC	2-oxoglutarate ferredoxin oxidoreductase subunit gamma
K32-1_01847	korB, oorB, oforB	2-oxoglutarate/2-oxoacid ferredoxin oxidoreductase subunit beta
K32-1_01848	korA, oorA, oforA	2-oxoglutarate/2-oxoacid ferredoxin oxidoreductase subunit alpha
K32-1_01978	DLD, lpd, pdhD	dihydrolipoamide dehydrogenase
K32-1_01979	DLAT, aceF, pdhC	pyruvate dehydrogenase E2 component (dihydrolipoamide acetyltransferase)
K32-1_02733	korA, oorA, oforA	2-oxoglutarate/2-oxoacid ferredoxin oxidoreductase subunit alpha
K32-1_02734	korB, oorB, oforB	2-oxoglutarate/2-oxoacid ferredoxin oxidoreductase subunit beta
K32-1_02735	korC, oorC	2-oxoglutarate ferredoxin oxidoreductase subunit gamma
K32-1_02736	korD, oorD	2-oxoglutarate ferredoxin oxidoreductase subunit delta
K32-1_03245	korC, oorC	2-oxoglutarate ferredoxin oxidoreductase subunit gamma
K32-1_03246	korB, oorB, oforB	2-oxoglutarate/2-oxoacid ferredoxin oxidoreductase subunit beta
K32-1_03247	korA, oorA, oforA	2-oxoglutarate/2-oxoacid ferredoxin oxidoreductase subunit alpha
K32-1_03248	korD, oorD	2-oxoglutarate ferredoxin oxidoreductase subunit delta
Pentose phosphate pathway		
K32-1_00034	aor	aldehyde:ferredoxin oxidoreductase
K32-1_00094	aor	aldehyde:ferredoxin oxidoreductase
K32-1_00252	deoC, DERA	deoxyribose-phosphate aldolase
K32-1_00319	pfkA, PFK	6-phosphofructokinase 1
K32-1_00342	K16306	fructose-bisphosphate aldolase / 2-amino-3,7-dideoxy-D-threo-hept-6-ulosonate synthase
K32-1_00767	deoB	phosphopentomutase
K32-1_01235	rpe, RPE	ribulose-phosphate 3-epimerase
K32-1_01525	aor	aldehyde:ferredoxin oxidoreductase
K32-1_01753	pgi1	glucose-6-phosphate isomerase, archaeal
K32-1_01803	E2.2.1.1, tktA, tktB	transketolase
K32-1_01804	E2.2.1.1, tktA, tktB	transketolase
K32-1_01805	GPI, pgi	glucose-6-phosphate isomerase
K32-1_01855	eda	2-dehydro-3-deoxyphosphogluconate aldolase / (4S)-4-hydroxy-2-oxoglutarate aldolase
K32-1_01856	kdgK	2-dehydro-3-deoxygluconokinase
K32-1_01857	eda	2-dehydro-3-deoxyphosphogluconate aldolase / (4S)-4-hydroxy-2-oxoglutarate aldolase
K32-1_01861	aor	aldehyde:ferredoxin oxidoreductase
K32-1_02174	E2.2.1.1, tktA, tktB	transketolase
K32-1_02175	E2.2.1.1, tktA, tktB	transketolase
K32-1_02325	rpiB	ribose 5-phosphate isomerase B
K32-1_02339	glpX	fructose-1,6-bisphosphatase II
K32-1_02340	E2.2.1.2, talA, talB	transaldolase
K32-1_02343	FBA, fbaA	fructose-bisphosphate aldolase, class II
K32-1_02879	PRPS, prsA	ribose-phosphate pyrophosphokinase
K32-1_03089	rbsK, RBKS	ribokinase
K32-1_03130	aor	aldehyde:ferredoxin oxidoreductase
Pentose and glucuronate interconversions		
K32-1_00343	SORD, gutB	L-iditol 2-dehydrogenase
K32-1_00344	xylB, XYLB	xylulokinase
K32-1_00837	UGP2, galU, galF	UTP--glucose-1-phosphate uridylyltransferase
K32-1_01235	rpe, RPE	ribulose-phosphate 3-epimerase
K32-1_02059	uxaA2	altronate dehydratase large subunit
K32-1_02060	uxaA1	altronate dehydratase small subunit
K32-1_02144	SORD, gutB	L-iditol 2-dehydrogenase
K32-1_02214	fucA	L-fuculose-phosphate aldolase
Fructose and mannose metabolism		
K32-1_00120	K16881	mannose-1-phosphate guanylyltransferase / phosphomannomutase
K32-1_00319	pfkA, PFK	6-phosphofructokinase 1
K32-1_00342	K16306	fructose-bisphosphate aldolase / 2-amino-3,7-dideoxy-D-threo-hept-6-ulosonate synthase
K32-1_00343	SORD, gutB	L-iditol 2-dehydrogenase
K32-1_02133	TPI, tpiA	triosephosphate isomerase (TIM)
K32-1_02144	SORD, gutB	L-iditol 2-dehydrogenase
K32-1_02146	manZ	mannose PTS system EIID component
K32-1_02147	manY	mannose PTS system EIIC component
K32-1_02149	manXa	mannose PTS system EIIA component
K32-1_02214	fucA	L-fuculose-phosphate aldolase
K32-1_02325	rpiB	ribose 5-phosphate isomerase B
K32-1_02339	glpX	fructose-1,6-bisphosphatase II
K32-1_02343	FBA, fbaA	fructose-bisphosphate aldolase, class II
Galactose metabolism		
K32-1_00319	pfkA, PFK	6-phosphofructokinase 1
K32-1_00385	galE, GALE	UDP-glucose 4-epimerase

K32-1_00837	UGP2, galU, galF	UTP--glucose-1-phosphate uridylyltransferase
K32-1_01495	glk	glucokinase
K32-1_02085	lacC	tagatose 6-phosphate kinase
K32-1_02086	gatY-kbaY	tagatose 1,6-diphosphate aldolase GatY/KbaY
K32-1_02087	fk	tagatose kinase
K32-1_02256	galE, GALE	UDP-glucose 4-epimerase
K32-1_02257	galE, GALE	UDP-glucose 4-epimerase
Starch and sucrose metabolism		
K32-1_00128	K16149	1,4-alpha-glucan branching enzyme
K32-1_00755	TPS	trehalose 6-phosphate synthase/phosphatase
K32-1_00756	otsB	trehalose 6-phosphate phosphatase
K32-1_00837	UGP2, galU, galF	UTP--glucose-1-phosphate uridylyltransferase
K32-1_01495	glk	glucokinase
K32-1_01753	pgi1	glucose-6-phosphate isomerase, archaeal
K32-1_01805	GPI, pgi	glucose-6-phosphate isomerase
Amino sugar and nucleotide sugar metabolism		
K32-1_00120	K16881	mannose-1-phosphate guanylyltransferase / phosphomannomutase
K32-1_00385	galE, GALE	UDP-glucose 4-epimerase
K32-1_00837	UGP2, galU, galF	UTP--glucose-1-phosphate uridylyltransferase
K32-1_01334	murA	UDP-N-acetylglucosamine 1-carboxyvinyltransferase
K32-1_01335	murB	UDP-N-acetylmuramate dehydrogenase
K32-1_01495	glk	glucokinase
K32-1_01753	pgi1	glucose-6-phosphate isomerase, archaeal
K32-1_01805	GPI, pgi	glucose-6-phosphate isomerase
K32-1_02146	manZ	mannose PTS system EIID component
K32-1_02147	manY	mannose PTS system EIIC component
K32-1_02149	manXa	mannose PTS system EIIA component
K32-1_02256	galE, GALE	UDP-glucose 4-epimerase
K32-1_02257	galE, GALE	UDP-glucose 4-epimerase
K32-1_02267	legF, ptmB	CMP-N,N'-diacetyllegionaminic acid synthase
K32-1_02271	legG, neuC2	GDP/UDP-N,N'-diacetylbacillosamine 2-epimerase (hydrolysing)
K32-1_02272	per, rfbE	perosamine synthetase
K32-1_02307	murA	UDP-N-acetylglucosamine 1-carboxyvinyltransferase
K32-1_02319	wecB	UDP-N-acetylglucosamine 2-epimerase (non-hydrolysing)
K32-1_02454	murA	UDP-N-acetylglucosamine 1-carboxyvinyltransferase
K32-1_02878	glmU	bifunctional UDP-N-acetylglucosamine pyrophosphorylase / glucosamine-1-phosphate N-acetyltransferase
K32-1_03190	glmM	phosphoglucosamine mutase
K32-1_03191	glmS, GFPT	glutamine---fructose-6-phosphate transaminase (isomerizing)
Pyruvate metabolism		
K32-1_00095	yiaY	alcohol dehydrogenase
K32-1_00113	nifV	homocitrate synthase NifV
K32-1_00320	PK, pyk	pyruvate kinase
K32-1_00364	ACSS1_2, acs	acetyl-CoA synthetase
K32-1_00377	porC, porG	pyruvate ferredoxin oxidoreductase gamma subunit
K32-1_00378	porD	pyruvate ferredoxin oxidoreductase delta subunit
K32-1_00379	porA	pyruvate ferredoxin oxidoreductase alpha subunit
K32-1_00380	porB	pyruvate ferredoxin oxidoreductase beta subunit
K32-1_00395	ACAT, atoB	acetyl-CoA C-acetyltransferase
K32-1_00441	accD	acetyl-CoA carboxylase carboxyl transferase subunit beta
K32-1_00442	accA	acetyl-CoA carboxylase carboxyl transferase subunit alpha
K32-1_00531	larA	lactate racemase
K32-1_00579	DLD, lpd, pdhD	dihydrolipoamide dehydrogenase
K32-1_00659	gloB, gloC, HAGH	hydroxyacylglutathione hydrolase
K32-1_00728	oadA	oxaloacetate decarboxylase (Na+ extruding) subunit alpha
K32-1_00729	accC	acetyl-CoA carboxylase, biotin carboxylase subunit
K32-1_00885	K15024	putative phosphotransacetylase
K32-1_00891	E4.2.1.2AA, fumA	fumarate hydratase subunit alpha
K32-1_00892	E4.2.1.2AB, fumB	fumarate hydratase subunit beta
K32-1_01142	ackA	acetate kinase
K32-1_01310	K15024	putative phosphotransacetylase
K32-1_01554	ppdK	pyruvate, orthophosphate dikinase
K32-1_01654	larA	lactate racemase
K32-1_01761	acdB	acetate---CoA ligase (ADP-forming) subunit beta
K32-1_01762	acdA	acetate---CoA ligase (ADP-forming) subunit alpha
K32-1_01763	porB	pyruvate ferredoxin oxidoreductase beta subunit
K32-1_01764	porA	pyruvate ferredoxin oxidoreductase alpha subunit
K32-1_01765	porD	pyruvate ferredoxin oxidoreductase delta subunit
K32-1_01766	porC, porG	pyruvate ferredoxin oxidoreductase gamma subunit
K32-1_01847	korB, oorB, oforB	2-oxoglutarate/2-oxoacid ferredoxin oxidoreductase subunit beta
K32-1_01848	korA, oorA, oforA	2-oxoglutarate/2-oxoacid ferredoxin oxidoreductase subunit alpha
K32-1_01974	ME2, sfcA, maeA	malate dehydrogenase (oxaloacetate-decarboxylating)
K32-1_01975	larA	lactate racemase
K32-1_01978	DLD, lpd, pdhD	dihydrolipoamide dehydrogenase
K32-1_01979	DLAT, aceF, pdhC	pyruvate dehydrogenase E2 component (dihydrolipoamide acetyltransferase)
K32-1_01988	pps, ppsA	pyruvate, water dikinase
K32-1_02108	ACAT, atoB	acetyl-CoA C-acetyltransferase
K32-1_02113	ACAT, atoB	acetyl-CoA C-acetyltransferase
K32-1_02577	K15024	putative phosphotransacetylase
K32-1_02578	E1.2.1.10	acetaldehyde dehydrogenase (acetylating)
K32-1_02733	korA, oorA, oforA	2-oxoglutarate/2-oxoacid ferredoxin oxidoreductase subunit alpha
K32-1_02734	korB, oorB, oforB	2-oxoglutarate/2-oxoacid ferredoxin oxidoreductase subunit beta
K32-1_03175	leuA, IMS	2-isopropylmalate synthase
K32-1_03179	leuA, IMS	2-isopropylmalate synthase
K32-1_03246	korB, oorB, oforB	2-oxoglutarate/2-oxoacid ferredoxin oxidoreductase subunit beta
K32-1_03247	korA, oorA, oforA	2-oxoglutarate/2-oxoacid ferredoxin oxidoreductase subunit alpha
Glyoxylate and dicarboxylate metabolism		
K32-1_00032	glyA, SHMT	glycine hydroxymethyltransferase
K32-1_00082	glyA, SHMT	glycine hydroxymethyltransferase
K32-1_00242	glnA, GLUL	glutamine synthetase
K32-1_00279	ACO, acnA	aconitate hydratase
K32-1_00364	ACSS1_2, acs	acetyl-CoA synthetase
K32-1_00395	ACAT, atoB	acetyl-CoA C-acetyltransferase
K32-1_00502	glnA, GLUL	glutamine synthetase
K32-1_00569	glnA, GLUL	glutamine synthetase
K32-1_00571	glnA, GLUL	glutamine synthetase
K32-1_00579	DLD, lpd, pdhD	dihydrolipoamide dehydrogenase
K32-1_01204	fdoH, fdsB	formate dehydrogenase iron-sulfur subunit
K32-1_01311	gcvH, GCSH	glycine cleavage system H protein
K32-1_01855	eda	2-dehydro-3-deoxyphosphogluconate aldolase / (4S)-4-hydroxy-2-oxoglutarate aldolase
K32-1_01857	eda	2-dehydro-3-deoxyphosphogluconate aldolase / (4S)-4-hydroxy-2-oxoglutarate aldolase
K32-1_01978	DLD, lpd, pdhD	dihydrolipoamide dehydrogenase
K32-1_02108	ACAT, atoB	acetyl-CoA C-acetyltransferase
K32-1_02113	ACAT, atoB	acetyl-CoA C-acetyltransferase
K32-1_02116	glcF	glycolate oxidase iron-sulfur subunit
K32-1_02600	gph	phosphoglycolate phosphatase
K32-1_02767	glxK, garK	glycerate 2-kinase
K32-1_02768	gyaR, GOR1	glyoxylate reductase
K32-1_02828	gcvT, AMT	aminomethyltransferase
K32-1_02829	gcvH, GCSH	glycine cleavage system H protein
K32-1_02830	gcvPA	glycine dehydrogenase subunit 1
K32-1_02831	gcvPB	glycine dehydrogenase subunit 2
K32-1_03156	glmS, mutS, mamA	methylaspartate mutase sigma subunit
K32-1_03158	glmE, mutE, mamB	methylaspartate mutase epsilon subunit
K32-1_03159	mal	methylaspartate ammonia-lyase
K32-1_03249	glcF	glycolate oxidase iron-sulfur subunit
K32-1_03250	glcD	glycolate oxidase
Propanoate metabolism		
K32-1_00231	yqhD	NADP-dependent alcohol dehydrogenase
K32-1_00364	ACSS1_2, acs	acetyl-CoA synthetase
K32-1_00377	porC, porG	pyruvate ferredoxin oxidoreductase gamma subunit
K32-1_00378	porD	pyruvate ferredoxin oxidoreductase delta subunit
K32-1_00379	porA	pyruvate ferredoxin oxidoreductase alpha subunit
K32-1_00380	porB	pyruvate ferredoxin oxidoreductase beta subunit
K32-1_00441	accD	acetyl-CoA carboxylase carboxyl transferase subunit beta
K32-1_00442	accA	acetyl-CoA carboxylase carboxyl transferase subunit alpha
K32-1_00579	DLD, lpd, pdhD	dihydrolipoamide dehydrogenase
K32-1_00729	accC	acetyl-CoA carboxylase, biotin carboxylase subunit
K32-1_00885	K15024	putative phosphotransacetylase
K32-1_01142	ackA	acetate kinase
K32-1_01310	K15024	putative phosphotransacetylase
K32-1_01761	acdB	acetate---CoA ligase (ADP-forming) subunit beta
K32-1_01762	acdA	acetate---CoA ligase (ADP-forming) subunit alpha
K32-1_01763	porB	pyruvate ferredoxin oxidoreductase beta subunit
K32-1_01764	porA	pyruvate ferredoxin oxidoreductase alpha subunit

K32-1_01765	porD	pyruvate ferredoxin oxidoreductase delta subunit
K32-1_01766	porC, porG	pyruvate ferredoxin oxidoreductase gamma subunit
K32-1_01978	DLD, lpd, pdhD	dihydrolipoamide dehydrogenase
K32-1_02577	K15024	putative phosphotransacetylase
K32-1_02621	mgsA	methylglyoxal synthase
K32-1_03232	gldA	glycerol dehydrogenase
Butanoate metabolism		
K32-1_00377	porC, porG	pyruvate ferredoxin oxidoreductase gamma subunit
K32-1_00378	porD	pyruvate ferredoxin oxidoreductase delta subunit
K32-1_00379	porA	pyruvate ferredoxin oxidoreductase alpha subunit
K32-1_00380	porB	pyruvate ferredoxin oxidoreductase beta subunit
K32-1_00394	crt	enoyl-CoA hydratase
K32-1_00395	ACAT, atoB	acetyl-CoA C-acetyltransferase
K32-1_00396	paaH, hbd, fadB, mmgB	3-hydroxybutyryl-CoA dehydrogenase
K32-1_00407	atoD	acetate CoA/acetoacetate CoA-transferase alpha subunit
K32-1_00408	atoA	acetate CoA/acetoacetate CoA-transferase beta subunit
K32-1_01466	nicE, maiA	maleate isomerase
K32-1_01763	porB	pyruvate ferredoxin oxidoreductase beta subunit
K32-1_01764	porA	pyruvate ferredoxin oxidoreductase alpha subunit
K32-1_01765	porD	pyruvate ferredoxin oxidoreductase delta subunit
K32-1_01766	porC, porG	pyruvate ferredoxin oxidoreductase gamma subunit
K32-1_01845	buk	butyrate kinase
K32-1_01847	korB, oorB, oforB	2-oxoglutarate/2-oxoacid ferredoxin oxidoreductase subunit beta
K32-1_01848	korA, oorA, oforA	2-oxoglutarate/2-oxoacid ferredoxin oxidoreductase subunit alpha
K32-1_01991	paaH, hbd, fadB, mmgB	3-hydroxybutyryl-CoA dehydrogenase
K32-1_02108	ACAT, atoB	acetyl-CoA C-acetyltransferase
K32-1_02111	paaH, hbd, fadB, mmgB	3-hydroxybutyryl-CoA dehydrogenase
K32-1_02113	ACAT, atoB	acetyl-CoA C-acetyltransferase
K32-1_02558	E2.2.1.6S, ilvH, ilvN	acetolactate synthase I/III small subunit
K32-1_02578	E1.2.1.10	acetaldehyde dehydrogenase (acetylating)
K32-1_02733	korA, oorA, oforA	2-oxoglutarate/2-oxoacid ferredoxin oxidoreductase subunit alpha
K32-1_02734	korB, oorB, oforB	2-oxoglutarate/2-oxoacid ferredoxin oxidoreductase subunit beta
K32-1_03172	E2.2.1.6L, ilvB, ilvG, ilvI	acetolactate synthase I/II/III large subunit
K32-1_03173	E2.2.1.6S, ilvH, ilvN	acetolactate synthase I/III small subunit
K32-1_03174	E2.2.1.6L, ilvB, ilvG, ilvI	acetolactate synthase I/II/III large subunit
K32-1_03246	korB, oorB, oforB	2-oxoglutarate/2-oxoacid ferredoxin oxidoreductase subunit beta
K32-1_03247	korA, oorA, oforA	2-oxoglutarate/2-oxoacid ferredoxin oxidoreductase subunit alpha
C5-Branched dibasic acid metabolism		
K32-1_02558	E2.2.1.6S, ilvH, ilvN	acetolactate synthase I/III small subunit
K32-1_03156	glmS, mutS, mamA	methylaspartate mutase sigma subunit
K32-1_03158	glmE, mutE, mamB	methylaspartate mutase epsilon subunit
K32-1_03159	mal	methylaspartate ammonia-lyase
K32-1_03172	E2.2.1.6L, ilvB, ilvG, ilvI	acetolactate synthase I/II/III large subunit
K32-1_03173	E2.2.1.6S, ilvH, ilvN	acetolactate synthase I/III small subunit
K32-1_03174	E2.2.1.6L, ilvB, ilvG, ilvI	acetolactate synthase I/II/III large subunit
K32-1_03176	leuC, IPMI-L	3-isopropylmalate/(R)-2-methylmalate dehydratase large subunit
K32-1_03177	leuD, IPMI-S	3-isopropylmalate/(R)-2-methylmalate dehydratase small subunit
K32-1_03178	leuB, IMDH	3-isopropylmalate dehydrogenase
Energy metabolism		
Oxidative phosphorylation		
K32-1_00063	ppaC	manganese-dependent inorganic pyrophosphatase
K32-1_00609	nuoF	NADH-quinone oxidoreductase subunit F
K32-1_00977	ppaX	pyrophosphatase PpaX
K32-1_01102	nuoN	NADH-quinone oxidoreductase subunit N
K32-1_01103	nuoM	NADH-quinone oxidoreductase subunit M
K32-1_01104	nuoL	NADH-quinone oxidoreductase subunit L
K32-1_01105	ndhE	NAD(P)H-quinone oxidoreductase subunit 4L
K32-1_01107	nuoI	NADH-quinone oxidoreductase subunit I
K32-1_01108	nuoH	NADH-quinone oxidoreductase subunit H
K32-1_01109	nuoD	NADH-quinone oxidoreductase subunit D
K32-1_01110	nuoC	NADH-quinone oxidoreductase subunit C
K32-1_01111	nuoB	NADH-quinone oxidoreductase subunit B
K32-1_02309	ATPF1E, atpC	F-type H+-transporting ATPase subunit epsilon
K32-1_02310	ATPF1B, atpD	F-type H+/Na+-transporting ATPase subunit beta
K32-1_02311	ATPF1G, atpG	F-type H+-transporting ATPase subunit gamma
K32-1_02312	ATPF1A, atpA	F-type H+/Na+-transporting ATPase subunit alpha
K32-1_02313	ATPF1D, atpH	F-type H+-transporting ATPase subunit delta
K32-1_02314	ATPF0B, atpF	F-type H+-transporting ATPase subunit b
K32-1_02315	ATPF0C, atpE	F-type H+-transporting ATPase subunit c
K32-1_02316	ATPF0A, atpB	F-type H+-transporting ATPase subunit a
K32-1_02854	nuoE	NADH-quinone oxidoreductase subunit E
K32-1_02855	nuoF	NADH-quinone oxidoreductase subunit F
K32-1_03021	cydA	cytochrome bd ubiquinol oxidase subunit I
K32-1_03022	cydB	cytochrome bd ubiquinol oxidase subunit II
K32-1_03285	nuoE	NADH-quinone oxidoreductase subunit E
K32-1_03286	nuoF	NADH-quinone oxidoreductase subunit F
Carbon fixation pathways in prokaryotes		
K32-1_00244	IDH1, IDH2, icd	isocitrate dehydrogenase
K32-1_00279	ACO, acnA	aconitate hydratase
K32-1_00364	ACSS1_2, acs	acetyl-CoA synthetase
K32-1_00377	porC, porG	pyruvate ferredoxin oxidoreductase gamma subunit
K32-1_00378	porD	pyruvate ferredoxin oxidoreductase delta subunit
K32-1_00379	porA	pyruvate ferredoxin oxidoreductase alpha subunit
K32-1_00380	porB	pyruvate ferredoxin oxidoreductase beta subunit
K32-1_00395	ACAT, atoB	acetyl-CoA C-acetyltransferase
K32-1_00441	accD	acetyl-CoA carboxylase carboxyl transferase subunit beta
K32-1_00442	accA	acetyl-CoA carboxylase carboxyl transferase subunit alpha
K32-1_00576	cooF	anaerobic carbon-monoxide dehydrogenase iron sulfur subunit
K32-1_00729	accC	acetyl-CoA carboxylase, biotin carboxylase subunit
K32-1_00737	folD	methylenetetrahydrofolate dehydrogenase (NADP+) / methenyltetrahydrofolate cyclohydrolase
K32-1_00738	fchA	methenyltetrahydrofolate cyclohydrolase
K32-1_00868	cooS, acsA	anaerobic carbon-monoxide dehydrogenase catalytic subunit
K32-1_00869	acsB	acetyl-CoA synthase
K32-1_00870	cdhE, acsC	acetyl-CoA decarbonylase/synthase, CODH/ACS complex subunit gamma
K32-1_00873	cdhD, acsD	acetyl-CoA decarbonylase/synthase, CODH/ACS complex subunit delta
K32-1_00874	acsE	5-methyltetrahydrofolate corrinoid/iron sulfur protein methyltransferase
K32-1_00875	metF, MTHFR	methylenetetrahydrofolate reductase (NADH)
K32-1_00885	K15024	putative phosphotransacetylase
K32-1_00891	E4.2.1.2AA, fumA	fumarate hydratase subunit alpha
K32-1_00892	E4.2.1.2AB, fumB	fumarate hydratase subunit beta
K32-1_01142	ackA	acetate kinase
K32-1_01215	fchA	methenyltetrahydrofolate cyclohydrolase
K32-1_01218	cooF	anaerobic carbon-monoxide dehydrogenase iron sulfur subunit
K32-1_01219	cooS, acsA	anaerobic carbon-monoxide dehydrogenase catalytic subunit
K32-1_01310	K15024	putative phosphotransacetylase
K32-1_01489	cooS, acsA	anaerobic carbon-monoxide dehydrogenase catalytic subunit
K32-1_01554	ppdK	pyruvate, orthophosphate dikinase
K32-1_01763	porB	pyruvate ferredoxin oxidoreductase beta subunit
K32-1_01764	porA	pyruvate ferredoxin oxidoreductase alpha subunit
K32-1_01765	porD	pyruvate ferredoxin oxidoreductase delta subunit
K32-1_01766	porC, porG	pyruvate ferredoxin oxidoreductase gamma subunit
K32-1_01777	tfrA	fumarate reductase (CoM/CoB) subunit A
K32-1_01846	korC, oorC	2-oxoglutarate ferredoxin oxidoreductase subunit gamma
K32-1_01847	korB, oorB, oforB	2-oxoglutarate/2-oxoacid ferredoxin oxidoreductase subunit beta
K32-1_01848	korA, oorA, oforA	2-oxoglutarate/2-oxoacid ferredoxin oxidoreductase subunit alpha
K32-1_01926	acsE	5-methyltetrahydrofolate corrinoid/iron sulfur protein methyltransferase
K32-1_01971	cooS, acsA	anaerobic carbon-monoxide dehydrogenase catalytic subunit
K32-1_01988	pps, ppsA	pyruvate, water dikinase
K32-1_02108	ACAT, atoB	acetyl-CoA C-acetyltransferase
K32-1_02113	ACAT, atoB	acetyl-CoA C-acetyltransferase
K32-1_02364	acsE	5-methyltetrahydrofolate corrinoid/iron sulfur protein methyltransferase
K32-1_02397	acsE	5-methyltetrahydrofolate corrinoid/iron sulfur protein methyltransferase
K32-1_02449	cooS, acsA	anaerobic carbon-monoxide dehydrogenase catalytic subunit
K32-1_02450	cooF	anaerobic carbon-monoxide dehydrogenase iron sulfur subunit
K32-1_02577	K15024	putative phosphotransacetylase
K32-1_02733	korA, oorA, oforA	2-oxoglutarate/2-oxoacid ferredoxin oxidoreductase subunit alpha
K32-1_02734	korB, oorB, oforB	2-oxoglutarate/2-oxoacid ferredoxin oxidoreductase subunit beta
K32-1_02735	korC, oorC	2-oxoglutarate ferredoxin oxidoreductase subunit gamma
K32-1_02736	korD, oorD	2-oxoglutarate ferredoxin oxidoreductase subunit delta
K32-1_02858	metF, MTHFR	methylenetetrahydrofolate reductase (NADH)
K32-1_02922	fhs	formate--tetrahydrofolate ligase
K32-1_03138	fchA	methenyltetrahydrofolate cyclohydrolase
K32-1_03245	korC, oorC	2-oxoglutarate ferredoxin oxidoreductase subunit gamma
K32-1_03246	korB, oorB, oforB	2-oxoglutarate/2-oxoacid ferredoxin oxidoreductase subunit beta
K32-1_03247	korA, oorA, oforA	2-oxoglutarate/2-oxoacid ferredoxin oxidoreductase subunit alpha

K32-1_03248	korD, oorD	2-oxoglutarate ferredoxin oxidoreductase subunit delta
K32-1_03299	fchA	methenyltetrahydrofolate cyclohydrolase
Nitrogen metabolism		
K32-1_00104	arcC	carbamate kinase
K32-1_00242	glnA, GLUL	glutamine synthetase
K32-1_00383	cynT, can	carbonic anhydrase
K32-1_00495	GLUD1_2, gdhA	glutamate dehydrogenase (NAD(P)+)
K32-1_00502	glnA, GLUL	glutamine synthetase
K32-1_00509	arcC	carbamate kinase
K32-1_00569	glnA, GLUL	glutamine synthetase
K32-1_00571	glnA, GLUL	glutamine synthetase
K32-1_00736	gltD	glutamate synthase (NADPH) small chain
K32-1_01132	ncd2, npd	nitronate monooxygenase
K32-1_01212	nrfA	nitrite reductase (cytochrome c-552)
K32-1_01213	nrfH	cytochrome c nitrite reductase small subunit
K32-1_01716	nrfA	nitrite reductase (cytochrome c-552)
K32-1_01717	nrfH	cytochrome c nitrite reductase small subunit
K32-1_01811	arcC	carbamate kinase
K32-1_02033	hcp	hydroxylamine reductase
K32-1_03057	cynS	cyanate lyase
K32-1_03252	cynT, can	carbonic anhydrase
Sulfur metabolism		
K32-1_00075	cysK	cysteine synthase
K32-1_00460	doxD	thiosulfate dehydrogenase (quinone) large subunit
K32-1_00525	ssuA	sulfonate transport system substrate-binding protein
K32-1_00526	ssuC	sulfonate transport system permease protein
K32-1_00634	cysK	cysteine synthase
K32-1_01069	nrnA	bifunctional oligoribonuclease and PAP phosphatase NrnA
K32-1_01216	asrC	anaerobic sulfite reductase subunit C
K32-1_01490	cysK	cysteine synthase
K32-1_01512	doxD	thiosulfate dehydrogenase (quinone) large subunit
K32-1_01725	dmsC	dimethyl sulfoxide reductase membrane subunit
K32-1_01726	dmsB	dimethyl sulfoxide reductase iron-sulfur subunit
K32-1_01748	ttrB	tetrathionate reductase subunit B
K32-1_01749	phsA, psrA	thiosulfate reductase / polysulfide reductase chain A
K32-1_01999	TST, MPST, sseA	thiosulfate/3-mercaptopyruvate sulfurtransferase
K32-1_02373	metB	cystathionine gamma-synthase
K32-1_02380	metA	homoserine O-succinyltransferase/O-acetyltransferase
K32-1_02499	sir	sulfite reductase (ferredoxin)
K32-1_02840	dmsB	dimethyl sulfoxide reductase iron-sulfur subunit
K32-1_02841	dmsC	dimethyl sulfoxide reductase membrane subunit
K32-1_02951	cysE	serine O-acetyltransferase
Other energy metabolism		
K32-1_00021	serA, PHGDH	D-3-phosphoglycerate dehydrogenase / 2-oxoglutarate reductase
K32-1_00032	glyA, SHMT	glycine hydroxymethyltransferase
K32-1_00082	glyA, SHMT	glycine hydroxymethyltransferase
K32-1_00289	mttB	trimethylamine---corrinoid protein Co-methyltransferase
K32-1_00291	mttB	trimethylamine---corrinoid protein Co-methyltransferase
K32-1_00319	pfkA, PFK	6-phosphofructokinase 1
K32-1_00342	K16306	fructose-bisphosphate aldolase / 2-amino-3,7-dideoxy-D-threo-hept-6-ulosonate synthase
K32-1_00364	ACSS1_2, acs	acetyl-CoA synthetase
K32-1_00377	porC, porG	pyruvate ferredoxin oxidoreductase gamma subunit
K32-1_00378	porD	pyruvate ferredoxin oxidoreductase delta subunit
K32-1_00379	porA	pyruvate ferredoxin oxidoreductase alpha subunit
K32-1_00380	porB	pyruvate ferredoxin oxidoreductase beta subunit
K32-1_00404	mttB	trimethylamine---corrinoid protein Co-methyltransferase
K32-1_00409	mtbB	dimethylamine---corrinoid protein Co-methyltransferase
K32-1_00411	mttC	trimethylamine corrinoid protein
K32-1_00412	mttB	trimethylamine---corrinoid protein Co-methyltransferase
K32-1_00413	mttB	trimethylamine---corrinoid protein Co-methyltransferase
K32-1_00433	mch	methenyltetrahydromethanopterin cyclohydrolase
K32-1_00434	mch	methenyltetrahydromethanopterin cyclohydrolase
K32-1_00576	cooF	anaerobic carbon-monoxide dehydrogenase iron sulfur subunit
K32-1_00686	mgsC	methylamine---glutamate N-methyltransferase subunit C
K32-1_00868	cooS, acsA	anaerobic carbon-monoxide dehydrogenase catalytic subunit
K32-1_00870	cdhE, acsC	acetyl-CoA decarbonylase/synthase, CODH/ACS complex subunit gamma
K32-1_00873	cdhD, acsD	acetyl-CoA decarbonylase/synthase, CODH/ACS complex subunit delta
K32-1_01142	ackA	acetate kinase
K32-1_01204	fdoH, fdsB	formate dehydrogenase iron-sulfur subunit
K32-1_01218	cooF	anaerobic carbon-monoxide dehydrogenase iron sulfur subunit
K32-1_01219	cooS, acsA	anaerobic carbon-monoxide dehydrogenase catalytic subunit
K32-1_01376	fdhB	formate dehydrogenase (coenzyme F420) beta subunit
K32-1_01377	mvhD, vhuD, vhcD	F420-non-reducing hydrogenase iron-sulfur subunit
K32-1_01378	hdrA2	heterodisulfide reductase subunit A2
K32-1_01379	hdrA2	heterodisulfide reductase subunit A2
K32-1_01380	hdrB2	heterodisulfide reductase subunit B2
K32-1_01381	hdrC2	heterodisulfide reductase subunit C2
K32-1_01489	cooS, acsA	anaerobic carbon-monoxide dehydrogenase catalytic subunit
K32-1_01763	porB	pyruvate ferredoxin oxidoreductase beta subunit
K32-1_01764	porA	pyruvate ferredoxin oxidoreductase alpha subunit
K32-1_01765	porD	pyruvate ferredoxin oxidoreductase delta subunit
K32-1_01766	porC, porG	pyruvate ferredoxin oxidoreductase gamma subunit
K32-1_01933	mttB	trimethylamine---corrinoid protein Co-methyltransferase
K32-1_01935	mttB	trimethylamine---corrinoid protein Co-methyltransferase
K32-1_01971	cooS, acsA	anaerobic carbon-monoxide dehydrogenase catalytic subunit
K32-1_01988	pps, ppsA	pyruvate, water dikinase
K32-1_02131	ENO, eno	enolase
K32-1_02132	gpmI	2,3-bisphosphoglycerate-independent phosphoglycerate mutase
K32-1_02179	mttB	trimethylamine---corrinoid protein Co-methyltransferase
K32-1_02181	mttB	trimethylamine---corrinoid protein Co-methyltransferase
K32-1_02182	mttB	trimethylamine---corrinoid protein Co-methyltransferase
K32-1_02339	glpX	fructose-1,6-bisphosphatase II
K32-1_02343	FBA, fbaA	fructose-bisphosphate aldolase, class II
K32-1_02410	mtaB	methanol---5-hydroxybenzimidazolylcobamide Co-methyltransferase
K32-1_02449	cooS, acsA	anaerobic carbon-monoxide dehydrogenase catalytic subunit
K32-1_02450	cooF	anaerobic carbon-monoxide dehydrogenase iron sulfur subunit
K32-1_02525	comB	2-phosphosulfolactate phosphatase
K32-1_02526	comA	phosphosulfolactate synthase
K32-1_02601	mttB	trimethylamine---corrinoid protein Co-methyltransferase
K32-1_02606	mttB	trimethylamine---corrinoid protein Co-methyltransferase
K32-1_02607	mttB	trimethylamine---corrinoid protein Co-methyltransferase
K32-1_02827	mgsC	methylamine---glutamate N-methyltransferase subunit C
K32-1_02851	mttB	trimethylamine---corrinoid protein Co-methyltransferase
K32-1_02852	mttB	trimethylamine---corrinoid protein Co-methyltransferase
K32-1_02897	mttB	trimethylamine---corrinoid protein Co-methyltransferase
K32-1_02898	mttB	trimethylamine---corrinoid protein Co-methyltransferase
K32-1_03132	mttB	trimethylamine---corrinoid protein Co-methyltransferase
K32-1_03133	mttB	trimethylamine---corrinoid protein Co-methyltransferase
K32-1_03145	mttB	trimethylamine---corrinoid protein Co-methyltransferase
K32-1_03146	mttB	trimethylamine---corrinoid protein Co-methyltransferase
K32-1_00670	iscU, nifU	nitrogen fixation protein NifU and related proteins
K32-1_00773	K09165	dodecin
K32-1_01383	fdhD	FdhD protein
K32-1_01817	fdrA	FdrA protein
K32-1_01880	fixX	ferredoxin like protein
K32-1_02046	iscU, nifU	nitrogen fixation protein NifU and related proteins
K32-1_02540	fer	ferredoxin
K32-1_02550	napH	ferredoxin-type protein NapH
K32-1_02762	fdhD	FdhD protein
K32-1_02813	fixA, etfB	electron transfer flavoprotein beta subunit
K32-1_02816	fixX	ferredoxin like protein
Lipid metabolism		
Fatty acid biosynthesis		
K32-1_00441	accD	acetyl-CoA carboxylase carboxyl transferase subunit beta
K32-1_00442	accA	acetyl-CoA carboxylase carboxyl transferase subunit alpha
K32-1_00729	accC	acetyl-CoA carboxylase, biotin carboxylase subunit
K32-1_01131	fabF, OXSM, CEM1	3-oxoacyl-[acyl-carrier-protein] synthase II
K32-1_01133	acpP	acyl carrier protein
K32-1_01134	fabG, OAR1	3-oxoacyl-[acyl-carrier protein] reductase
K32-1_01135	fabD, MCAT, MCT1	[acyl-carrier-protein] S-malonyltransferase
K32-1_01136	fabK	enoyl-[acyl-carrier protein] reductase II
K32-1_01137	fabH	3-oxoacyl-[acyl-carrier-protein] synthase III
K32-1_02110	fabG, OAR1	3-oxoacyl-[acyl-carrier protein] reductase
K32-1_02207	fabZ	3-hydroxyacyl-[acyl-carrier-protein] dehydratase
K32-1_00095	yiaY	alcohol dehydrogenase

K32-1_00395	ACAT, atoB	acetyl-CoA C-acetyltransferase
K32-1_02108	ACAT, atoB	acetyl-CoA C-acetyltransferase
K32-1_02109	fadB	enoyl-CoA hydratase
K32-1_02113	ACAT, atoB	acetyl-CoA C-acetyltransferase
Glycerolipid metabolism		
K32-1_00293	glpK, GK	glycerol kinase
K32-1_00978	mgs, bgsB	1,2-diacylglycerol 3-alpha-glucosyltransferase
K32-1_01138	plsX	phosphate acyltransferase
K32-1_01149	ugtP	processive 1,2-diacylglycerol beta-glucosyltransferase
K32-1_01296	ltaS	lipoteichoic acid synthase
K32-1_01565	dgkA, DGK	diacylglycerol kinase (ATP)
K32-1_01921	plsY	acyl phosphate:glycerol-3-phosphate acyltransferase
K32-1_02515	plsC	1-acyl-sn-glycerol-3-phosphate acyltransferase
K32-1_02767	glxK, garK	glycerate 2-kinase
K32-1_03019	plsC	1-acyl-sn-glycerol-3-phosphate acyltransferase
K32-1_03232	gldA	glycerol dehydrogenase
Glycerophospholipid metabolism		
K32-1_00284	glpA, glpD	glycerol-3-phosphate dehydrogenase
K32-1_00285	glpB	glycerol-3-phosphate dehydrogenase subunit B
K32-1_00286	glpC	glycerol-3-phosphate dehydrogenase subunit C
K32-1_00825	gpsA	glycerol-3-phosphate dehydrogenase (NAD(P)+)
K32-1_01042	pgsA, PGS1	CDP-diacylglycerol---glycerol-3-phosphate 3-phosphatidyltransferase
K32-1_01083	E2.7.7.41, CDS1, CDS2, cdsA	phosphatidate cytidylyltransferase
K32-1_01154	pcrB	heptaprenylglyceryl phosphate synthase
K32-1_01565	dgkA, DGK	diacylglycerol kinase (ATP)
K32-1_01921	plsY	acyl phosphate:glycerol-3-phosphate acyltransferase
K32-1_02138	yvoF	heptaprenylglycerol acetyltransferase
K32-1_02515	plsC	1-acyl-sn-glycerol-3-phosphate acyltransferase
K32-1_02589	eutA	ethanolamine utilization protein EutA
K32-1_02590	eutC	ethanolamine ammonia-lyase small subunit
K32-1_02591	eutB	ethanolamine ammonia-lyase large subunit
K32-1_02594	eutC	ethanolamine ammonia-lyase small subunit
K32-1_02595	eutB	ethanolamine ammonia-lyase large subunit
K32-1_03019	plsC	1-acyl-sn-glycerol-3-phosphate acyltransferase
K32-1_03238	UGCG	ceramide glucosyltransferase
Arginine biosynthesis		
K32-1_00104	arcC	carbamate kinase
K32-1_00242	glnA, GLUL	glutamine synthetase
K32-1_00495	GLUD1_2, gdhA	glutamate dehydrogenase (NAD(P)+)
K32-1_00502	glnA, GLUL	glutamine synthetase
K32-1_00507	OTC, argF, argI	ornithine carbamoyltransferase
K32-1_00509	arcC	carbamate kinase
K32-1_00569	glnA, GLUL	glutamine synthetase
K32-1_00571	glnA, GLUL	glutamine synthetase
K32-1_01806	OTC, argF, argI	ornithine carbamoyltransferase
K32-1_01811	arcC	carbamate kinase
K32-1_02769	aspB	aspartate aminotransferase
K32-1_03034	argC	N-acetyl-gamma-glutamyl-phosphate reductase
K32-1_03036	argJ	glutamate N-acetyltransferase / amino-acid N-acetyltransferase
K32-1_03037	argB	acetylglutamate kinase
K32-1_03038	argD	acetylornithine/N-succinyldiaminopimelate aminotransferase
K32-1_03039	argG, ASS1	argininosuccinate synthase
K32-1_03040	argH, ASL	argininosuccinate lyase
K32-1_03181	aspB	aspartate aminotransferase
Alanine, aspartate and glutamate metabolism		
K32-1_00013	ald	alanine dehydrogenase
K32-1_00040	purB, ADSL	adenylosuccinate lyase
K32-1_00042	purF, PPAT	amidophosphoribosyltransferase
K32-1_00242	glnA, GLUL	glutamine synthetase
K32-1_00495	GLUD1_2, gdhA	glutamate dehydrogenase (NAD(P)+)
K32-1_00502	glnA, GLUL	glutamine synthetase
K32-1_00569	glnA, GLUL	glutamine synthetase
K32-1_00571	glnA, GLUL	glutamine synthetase
K32-1_00573	asnB, ASNS	asparagine synthase (glutamine-hydrolysing)
K32-1_00736	gltD	glutamate synthase (NADPH) small chain
K32-1_00765	ald	alanine dehydrogenase
K32-1_00982	NIT2, yafV	omega-amidase
K32-1_01293	pyrB, PYR2	aspartate carbamoyltransferase catalytic subunit
K32-1_01648	carB, CPA2	carbamoyl-phosphate synthase large subunit
K32-1_01649	carA, CPA1	carbamoyl-phosphate synthase small subunit
K32-1_01738	purF, PPAT	amidophosphoribosyltransferase
K32-1_01904	ala	alanine dehydrogenase
K32-1_02487	purA, ADSS	adenylosuccinate synthase
K32-1_02769	aspB	aspartate aminotransferase
K32-1_03033	purF, PPAT	amidophosphoribosyltransferase
K32-1_03039	argG, ASS1	argininosuccinate synthase
K32-1_03040	argH, ASL	argininosuccinate lyase
K32-1_03181	aspB	aspartate aminotransferase
K32-1_03191	glmS, GFPT	glutamine---fructose-6-phosphate transaminase (isomerizing)
Glycine, serine and threonine metabolism		
K32-1_00021	serA, PHGDH	D-3-phosphoglycerate dehydrogenase / 2-oxoglutarate reductase
K32-1_00028	doeA	ectoine hydrolase
K32-1_00032	glyA, SHMT	glycine hydroxymethyltransferase
K32-1_00076	E4.3.1.17, sdaA, sdaB, tdcG	L-serine dehydratase
K32-1_00077	E4.3.1.17, sdaA, sdaB, tdcG	L-serine dehydratase
K32-1_00082	glyA, SHMT	glycine hydroxymethyltransferase
K32-1_00102	thrC	threonine synthase
K32-1_00114	ltaE	threonine aldolase
K32-1_00294	mtgB	glycine betaine---corrinoid protein Co-methyltransferase
K32-1_00415	thrC	threonine synthase
K32-1_00419	trpB	tryptophan synthase beta chain
K32-1_00579	DLD, lpd, pdhD	dihydrolipoamide dehydrogenase
K32-1_00828	hom	homoserine dehydrogenase
K32-1_00829	thrB	homoserine kinase
K32-1_00830	lysC	aspartate kinase
K32-1_01051	lysC	aspartate kinase
K32-1_01052	asd	aspartate-semialdehyde dehydrogenase
K32-1_01311	gcvH, GCSH	glycine cleavage system H protein
K32-1_01868	trpA	tryptophan synthase alpha chain
K32-1_01869	trpB	tryptophan synthase beta chain
K32-1_01876	mtgB	glycine betaine---corrinoid protein Co-methyltransferase
K32-1_01978	DLD, lpd, pdhD	dihydrolipoamide dehydrogenase
K32-1_02132	gpmI	2,3-bisphosphoglycerate-independent phosphoglycerate mutase
K32-1_02604	thrB2	homoserine kinase type II
K32-1_02767	glxK, garK	glycerate 2-kinase
K32-1_02828	gcvT, AMT	aminomethyltransferase
K32-1_02829	gcvH, GCSH	glycine cleavage system H protein
K32-1_02830	gcvPA	glycine dehydrogenase subunit 1
K32-1_02831	gcvPB	glycine dehydrogenase subunit 2
K32-1_02847	E3.5.3.3	creatinase
Cysteine and methionine metabolism		
K32-1_00021	serA, PHGDH	D-3-phosphoglycerate dehydrogenase / 2-oxoglutarate reductase
K32-1_00075	cysK	cysteine synthase
K32-1_00076	E4.3.1.17, sdaA, sdaB, tdcG	L-serine dehydratase
K32-1_00077	E4.3.1.17, sdaA, sdaB, tdcG	L-serine dehydratase
K32-1_00088	mtaD	5-methylthioadenosine/S-adenosylhomocysteine deaminase
K32-1_00101	mtaD	5-methylthioadenosine/S-adenosylhomocysteine deaminase
K32-1_00106	mtaD	5-methylthioadenosine/S-adenosylhomocysteine deaminase
K32-1_00250	mtaD	5-methylthioadenosine/S-adenosylhomocysteine deaminase
K32-1_00292	E4.4.1.11	methionine-gamma-lyase
K32-1_00330	mtaD	5-methylthioadenosine/S-adenosylhomocysteine deaminase
K32-1_00345	mtaD	5-methylthioadenosine/S-adenosylhomocysteine deaminase
K32-1_00373	mtnX	2-hydroxy-3-keto-5-methylthiopentenyl-1-phosphate phosphatase
K32-1_00475	speE, SRM, SPE3	spermidine synthase
K32-1_00634	cysK	cysteine synthase
K32-1_00828	hom	homoserine dehydrogenase
K32-1_00830	lysC	aspartate kinase
K32-1_00833	speD, AMD1	S-adenosylmethionine decarboxylase
K32-1_01051	lysC	aspartate kinase
K32-1_01052	asd	aspartate-semialdehyde dehydrogenase
K32-1_01125	mtaD	5-methylthioadenosine/S-adenosylhomocysteine deaminase
K32-1_01276	metK, MAT	S-adenosylmethionine synthetase

K32-1_01282	E3.3.1.1, ahcY	adenosylhomocysteinase
K32-1_01490	cysK	cysteine synthase
K32-1_01839	mtaD	5-methylthioadenosine/S-adenosylhomocysteine deaminase
K32-1_01963	metY	O-acetylhomoserine (thiol)-lyase
K32-1_01999	TST, MPST, sseA	thiosulfate/3-mercaptopyruvate sulfurtransferase
K32-1_02216	mtaP, MTAP	5'-methylthioadenosine phosphorylase
K32-1_02219	mtnA	methylthioribose-1-phosphate isomerase
K32-1_02373	metB	cystathionine gamma-synthase
K32-1_02374	metC	cysteine-S-conjugate beta-lyase
K32-1_02380	metA	homoserine O-succinyltransferase/O-acetyltransferase
K32-1_02562	dcyD	D-cysteine desulfhydrase
K32-1_02769	aspB	aspartate aminotransferase
K32-1_02868	metH, MTR	5-methyltetrahydrofolate--homocysteine methyltransferase
K32-1_02951	cysE	serine O-acetyltransferase
K32-1_03030	speD, AMD1	S-adenosylmethionine decarboxylase
K32-1_03124	DNMT1, dcm	DNA (cytosine-5)-methyltransferase 1
K32-1_03170	E2.6.1.42, ilvE	branched-chain amino acid aminotransferase
K32-1_03181	aspB	aspartate aminotransferase
Valine, leucine and isoleucine degradation		
K32-1_00395	ACAT, atoB	acetyl-CoA C-acetyltransferase
K32-1_00579	DLD, lpd, pdhD	dihydrolipoamide dehydrogenase
K32-1_01849	E1.4.1.9	leucine dehydrogenase
K32-1_01978	DLD, lpd, pdhD	dihydrolipoamide dehydrogenase
K32-1_02108	ACAT, atoB	acetyl-CoA C-acetyltransferase
K32-1_02113	ACAT, atoB	acetyl-CoA C-acetyltransferase
K32-1_03170	E2.6.1.42, ilvE	branched-chain amino acid aminotransferase
K32-1_00803	ilvC	ketol-acid reductoisomerase
K32-1_01849	E1.4.1.9	leucine dehydrogenase
K32-1_02558	E2.2.1.6S, ilvH, ilvN	acetolactate synthase I/III small subunit
K32-1_03170	E2.6.1.42, ilvE	branched-chain amino acid aminotransferase
K32-1_03171	ilvD	dihydroxy-acid dehydratase
K32-1_03172	E2.2.1.6L, ilvB, ilvG, ilvI	acetolactate synthase I/II/III large subunit
K32-1_03173	E2.2.1.6S, ilvH, ilvN	acetolactate synthase I/III small subunit
K32-1_03174	E2.2.1.6L, ilvB, ilvG, ilvI	acetolactate synthase I/II/III large subunit
K32-1_03175	leuA, IMS	2-isopropylmalate synthase
K32-1_03176	leuC, IPMI-L	3-isopropylmalate/(R)-2-methylmalate dehydratase large subunit
K32-1_03177	leuD, IPMI-S	3-isopropylmalate/(R)-2-methylmalate dehydratase small subunit
K32-1_03178	leuB, IMDH	3-isopropylmalate dehydrogenase
K32-1_03179	leuA, IMS	2-isopropylmalate synthase
Lysine biosynthesis		
K32-1_00690	pylB	methylornithine synthase
K32-1_00691	pylC	3-methylornithine--L-lysine ligase
K32-1_00692	pylD	3-methylornithyl-N6-L-lysine dehydrogenase
K32-1_00790	lysA	diaminopimelate decarboxylase
K32-1_00828	hom	homoserine dehydrogenase
K32-1_00830	lysC	aspartate kinase
K32-1_01029	E2.6.1.83	LL-diaminopimelate aminotransferase
K32-1_01050	dapA	4-hydroxy-tetrahydrodipicolinate synthase
K32-1_01051	lysC	aspartate kinase
K32-1_01052	asd	aspartate-semialdehyde dehydrogenase
K32-1_01055	dapB	4-hydroxy-tetrahydrodipicolinate reductase
K32-1_01283	E2.6.1.83	LL-diaminopimelate aminotransferase
K32-1_01284	dapF	diaminopimelate epimerase
K32-1_01341	murF	UDP-N-acetylmuramoyl-tripeptide--D-alanyl-D-alanine ligase
K32-1_01342	murE	UDP-N-acetylmuramoyl-L-alanyl-D-glutamate--2,6-diaminopimelate ligase
K32-1_01796	dapE	succinyl-diaminopimelate desuccinylase
K32-1_03038	argD	acetylornithine/N-succinyldiaminopimelate aminotransferase
K32-1_03058	dapE	succinyl-diaminopimelate desuccinylase
K32-1_00395	ACAT, atoB	acetyl-CoA C-acetyltransferase
K32-1_00397	kdd	L-erythro-3,5-diaminohexanoate dehydrogenase
K32-1_00400	kamD	beta-lysine 5,6-aminomutase alpha subunit
K32-1_00401	kamE	beta-lysine 5,6-aminomutase beta subunit
K32-1_00402	kal	3-aminobutyryl-CoA ammonia-lyase
K32-1_00403	kce	3-keto-5-aminohexanoate cleavage enzyme
K32-1_00406	kamA	lysine 2,3-aminomutase
K32-1_00407	atoD	acetate CoA/acetoacetate CoA-transferase alpha subunit
K32-1_00408	atoA	acetate CoA/acetoacetate CoA-transferase beta subunit
K32-1_00561	patA	putrescine aminotransferase

K32-1_00579	DLD, lpd, pdhD	dihydrolipoamide dehydrogenase
K32-1_01978	DLD, lpd, pdhD	dihydrolipoamide dehydrogenase
K32-1_02108	ACAT, atoB	acetyl-CoA C-acetyltransferase
K32-1_02113	ACAT, atoB	acetyl-CoA C-acetyltransferase
Arginine and proline metabolism		
K32-1_00426	codA	cytosine/creatinine deaminase
K32-1_00475	speE, SRM, SPE3	spermidine synthase
K32-1_00476	speB	agmatinase
K32-1_00561	patA	putrescine aminotransferase
K32-1_00625	E3.5.1.4, amiE	amidase
K32-1_00833	speD, AMD1	S-adenosylmethionine decarboxylase
K32-1_01317	proC	pyrroline-5-carboxylate reductase
K32-1_01603	proA	glutamate-5-semialdehyde dehydrogenase
K32-1_01604	proB	glutamate 5-kinase
K32-1_01778	E3.5.2.10	creatinine amidohydrolase
K32-1_02752	speA	arginine decarboxylase
K32-1_02769	aspB	aspartate aminotransferase
K32-1_02847	E3.5.3.3	creatinase
K32-1_02848	E3.5.2.10	creatinine amidohydrolase
K32-1_03030	speD, AMD1	S-adenosylmethionine decarboxylase
K32-1_03031	pdaD	arginine decarboxylase
K32-1_03065	speA	arginine decarboxylase
K32-1_03080	speA	arginine decarboxylase
K32-1_03181	aspB	aspartate aminotransferase
Histidine metabolism		
K32-1_00053	hisZ	ATP phosphoribosyltransferase regulatory subunit
K32-1_00054	hisG	ATP phosphoribosyltransferase
K32-1_00055	hisD	histidinol dehydrogenase
K32-1_00056	hisB	imidazoleglycerol-phosphate dehydratase
K32-1_00057	hisH	imidazole glycerol-phosphate synthase subunit HisH
K32-1_00058	hisA	phosphoribosylformimino-5-aminoimidazole carboxamide ribotide isomerase
K32-1_00059	hisF	imidazole glycerol-phosphate synthase subunit HisF
K32-1_00060	hisIE	phosphoribosyl-AMP cyclohydrolase / phosphoribosyl-ATP pyrophosphohydrolase
K32-1_01373	E3.1.3.15B	histidinol-phosphatase (PHP family)
K32-1_01682	hisC	histidinol-phosphate aminotransferase
K32-1_03134	hutH, HAL	histidine ammonia-lyase
K32-1_03135	hutU, UROC1	urocanate hydratase
K32-1_03136	hutI, AMDHD1	imidazolonepropionase
K32-1_03137	fctD	glutamate formiminotransferase / 5-formyltetrahydrofolate cyclo-ligase
K32-1_03298	fctD	glutamate formiminotransferase / 5-formyltetrahydrofolate cyclo-ligase
Tyrosine metabolism		
K32-1_00095	yiaY	alcohol dehydrogenase
K32-1_01682	hisC	histidinol-phosphate aminotransferase
K32-1_02769	aspB	aspartate aminotransferase
K32-1_03181	aspB	aspartate aminotransferase
K32-1_03233	E4.1.99.2	tyrosine phenol-lyase
Phenylalanine metabolism		
K32-1_00396	paaH, hbd, fadB, mmgB	3-hydroxybutyryl-CoA dehydrogenase
K32-1_00625	E3.5.1.4, amiE	amidase
K32-1_01682	hisC	histidinol-phosphate aminotransferase
K32-1_01684	paaK	phenylacetate-CoA ligase
K32-1_01991	paaH, hbd, fadB, mmgB	3-hydroxybutyryl-CoA dehydrogenase
K32-1_02111	paaH, hbd, fadB, mmgB	3-hydroxybutyryl-CoA dehydrogenase
K32-1_02769	aspB	aspartate aminotransferase
K32-1_03053	paaK	phenylacetate-CoA ligase
K32-1_03181	aspB	aspartate aminotransferase
K32-1_03241	paaI	acyl-CoA thioesterase
Tryptophan metabolism		
K32-1_00395	ACAT, atoB	acetyl-CoA C-acetyltransferase
K32-1_00579	DLD, lpd, pdhD	dihydrolipoamide dehydrogenase
K32-1_00625	E3.5.1.4, amiE	amidase
K32-1_01978	DLD, lpd, pdhD	dihydrolipoamide dehydrogenase
K32-1_02108	ACAT, atoB	acetyl-CoA C-acetyltransferase
K32-1_02113	ACAT, atoB	acetyl-CoA C-acetyltransferase
Phenylalanine, tyrosine and tryptophan biosynthesis		
K32-1_00342	K16306	fructose-bisphosphate aldolase / 2-amino-3,7-dideoxy-D-threo-hept-6-ulosonate synthase
K32-1_00419	trpB	tryptophan synthase beta chain

K32-1_00694	aroE	shikimate dehydrogenase
K32-1_00696	aroC	chorismate synthase
K32-1_00697	aroK, aroL	shikimate kinase
K32-1_00698	aroB	3-dehydroquinate synthase
K32-1_00714	aroQ, qutE	3-dehydroquinate dehydratase II
K32-1_00808	aroH	chorismate mutase
K32-1_00809	trpF	phosphoribosylanthranilate isomerase
K32-1_00810	AROA2, aroA	3-deoxy-7-phosphoheptulonate synthase
K32-1_00811	pheA2	prephenate dehydratase
K32-1_00812	tyrA2	prephenate dehydrogenase
K32-1_00813	aroA	3-phosphoshikimate 1-carboxyvinyltransferase
K32-1_00827	pheB	chorismate mutase
K32-1_01181	trpF	phosphoribosylanthranilate isomerase
K32-1_01182	trpC	indole-3-glycerol phosphate synthase
K32-1_01183	trpD	anthranilate phosphoribosyltransferase
K32-1_01185	trpE	anthranilate synthase component I
K32-1_01186	trpE	anthranilate synthase component I
K32-1_01682	hisC	histidinol-phosphate aminotransferase
K32-1_01868	trpA	tryptophan synthase alpha chain
K32-1_01869	trpB	tryptophan synthase beta chain
K32-1_01870	trpF	phosphoribosylanthranilate isomerase
K32-1_01871	trpC	indole-3-glycerol phosphate synthase
K32-1_01872	trpD	anthranilate phosphoribosyltransferase
K32-1_02355	AROA2, aroA	3-deoxy-7-phosphoheptulonate synthase
K32-1_02769	aspB	aspartate aminotransferase
K32-1_03181	aspB	aspartate aminotransferase
beta-Alanine metabolism		
K32-1_00103	DPYS, dht, hydA	dihydropyrimidinase
K32-1_01464	preA	dihydropyrimidine dehydrogenase (NAD+) subunit PreA
K32-1_02864	panC	pantoate--beta-alanine ligase
K32-1_02865	panD	aspartate 1-decarboxylase
Taurine and hypotaurine metabolism		
K32-1_00013	ald	alanine dehydrogenase
K32-1_00765	ald	alanine dehydrogenase
K32-1_00885	K15024	putative phosphotransacetylase
K32-1_01142	ackA	acetate kinase
K32-1_01310	K15024	putative phosphotransacetylase
K32-1_01904	ala	alanine dehydrogenase
K32-1_02577	K15024	putative phosphotransacetylase
Selenocompound metabolism		
K32-1_00126	trxB, TRR	thioredoxin reductase (NADPH)
K32-1_00292	E4.4.1.11	methionine-gamma-lyase
K32-1_00508	ygfK	putative selenate reductase
K32-1_01891	trxB, TRR	thioredoxin reductase (NADPH)
K32-1_01902	trxB, TRR	thioredoxin reductase (NADPH)
K32-1_01918	trxB, TRR	thioredoxin reductase (NADPH)
K32-1_02373	metB	cystathionine gamma-synthase
K32-1_02374	metC	cysteine-S-conjugate beta-lyase
K32-1_02477	trxB, TRR	thioredoxin reductase (NADPH)
K32-1_02521	selD, SEPHS	selenide, water dikinase
K32-1_02652	selA	L-seryl-tRNA(Ser) seleniumtransferase
K32-1_02764	MARS, metG	methionyl-tRNA synthetase
K32-1_02868	metH, MTR	5-methyltetrahydrofolate--homocysteine methyltransferase
Cyanoamino acid metabolism		
K32-1_00032	glyA, SHMT	glycine hydroxymethyltransferase
K32-1_00082	glyA, SHMT	glycine hydroxymethyltransferase
D-Amino acid metabolism		
K32-1_00400	kamD	beta-lysine 5,6-aminomutase alpha subunit
K32-1_00401	kamE	beta-lysine 5,6-aminomutase beta subunit
K32-1_00790	lysA	diaminopimelate decarboxylase
K32-1_00961	ddl	D-alanine-D-alanine ligase
K32-1_01284	dapF	diaminopimelate epimerase
K32-1_01339	murD	UDP-N-acetylmuramoylalanine--D-glutamate ligase
K32-1_01679	murI	glutamate racemase
K32-1_02348	alr	alanine racemase
K32-1_02562	dcyD	D-cysteine desulfhydrase
K32-1_03266	alr	alanine racemase
Glutathione metabolism		
K32-1_00244	IDH1, IDH2, icd	isocitrate dehydrogenase
K32-1_00475	speE, SRM, SPE3	spermidine synthase
Other amino acids metabolism		
K32-1_01319	yggS, PROSC	PLP dependent protein
K32-1_02580	eutM	ethanolamine utilization protein EutM
K32-1_02581	eutQ	ethanolamine utilization protein EutQ
K32-1_02584	eutN	ethanolamine utilization protein EutN
K32-1_02586	eutJ	ethanolamine utilization protein EutJ
K32-1_02588	eutL	ethanolamine utilization protein EutL
K32-1_02592	eutP	ethanolamine utilization protein EutP
K32-1_02593	eutS	ethanolamine utilization protein EutS
Metabolism of cofactors and vitamins		
Ubiquinone and other terpenoid-quinone biosynthesis		
K32-1_00835	ubiE	demethylmenaquinone methyltransferase / 2-methoxy-6-polyprenyl-1,4-benzoquinol methylase
K32-1_00836	ubiX, bsdB, PAD1	flavin prenyltransferase
K32-1_01659	ubiA	4-hydroxybenzoate polyprenyltransferase
K32-1_01660	ubiD	4-hydroxy-3-polyprenylbenzoate decarboxylase
K32-1_02620	NQO1	NAD(P)H dehydrogenase (quinone)
K32-1_02703	menA	1,4-dihydroxy-2-naphthoate polyprenyltransferase
One carbon pool by folate		
K32-1_00032	glyA, SHMT	glycine hydroxymethyltransferase
K32-1_00044	purN	phosphoribosylglycinamide formyltransferase 1
K32-1_00045	purH	phosphoribosylaminoimidazolecarboxamide formyltransferase / IMP cyclohydrolase
K32-1_00082	glyA, SHMT	glycine hydroxymethyltransferase
K32-1_00737	folD	methylenetetrahydrofolate dehydrogenase (NADP+) / methenyltetrahydrofolate cyclohydrolase
K32-1_00738	fchA	methenyltetrahydrofolate cyclohydrolase
K32-1_00875	metF, MTHFR	methylenetetrahydrofolate reductase (NADH)
K32-1_01215	fchA	methenyltetrahydrofolate cyclohydrolase
K32-1_01250	MTFMT, fmt	methionyl-tRNA formyltransferase
K32-1_02828	gcvT, AMT	aminomethyltransferase
K32-1_02858	metF, MTHFR	methylenetetrahydrofolate reductase (NADH)
K32-1_02868	metH, MTR	5-methyltetrahydrofolate--homocysteine methyltransferase
K32-1_02922	fhs	formate--tetrahydrofolate ligase
K32-1_02954	thyX, thy1	thymidylate synthase (FAD)
K32-1_03137	fctD	glutamate formiminotransferase / 5-formyltetrahydrofolate cyclo-ligase
K32-1_03138	fchA	methenyltetrahydrofolate cyclohydrolase
K32-1_03282	MTHFS	5-formyltetrahydrofolate cyclo-ligase
K32-1_03298	fctD	glutamate formiminotransferase / 5-formyltetrahydrofolate cyclo-ligase
K32-1_03299	fchA	methenyltetrahydrofolate cyclohydrolase
Thiamine metabolism		
K32-1_00370	thiG	thiazole synthase
K32-1_00371	thiH	2-iminoacetate synthase
K32-1_00372	thiE	thiamine-phosphate pyrophosphorylase
K32-1_00485	thiD	hydroxymethylpyrimidine/phosphomethylpyrimidine kinase
K32-1_00487	thiM	hydroxyethylthiazole kinase
K32-1_00600	thiH	2-iminoacetate synthase
K32-1_00669	iscS, NFS1	cysteine desulfurase
K32-1_00743	dxs	1-deoxy-D-xylulose-5-phosphate synthase
K32-1_01236	rsgA, engC	ribosome biogenesis GTPase / thiamine phosphate phosphatase
K32-1_01571	thiN, TPK1, THI80	thiamine pyrophosphokinase
K32-1_02995	adk, AK	adenylate kinase
K32-1_03032	thiC	phosphomethylpyrimidine synthase
Riboflavin metabolism		
K32-1_00487	thiM	hydroxyethylthiazole kinase
K32-1_00762	nudF	ADP-ribose pyrophosphatase
K32-1_00836	ubiX, bsdB, PAD1	flavin prenyltransferase
K32-1_01067	ribF	riboflavin kinase / FMN adenylyltransferase
K32-1_02859	ribD	diaminohydroxyphosphoribosylaminopyrimidine deaminase / 5-amino-6-(5-phosphoribosylamino)uracil reductase
K32-1_02860	ribE, RIB5	riboflavin synthase
K32-1_02861	ribBA	3,4-dihydroxy 2-butanone 4-phosphate synthase / GTP cyclohydrolase II
K32-1_02862	ribH, RIB4	6,7-dimethyl-8-ribityllumazine synthase
Vitamin B6 metabolism		
K32-1_00102	thrC	threonine synthase
K32-1_00415	thrC	threonine synthase
K32-1_00528	pdxT, pdx2	pyridoxal 5'-phosphate synthase pdxT subunit
K32-1_00529	pdxS, pdx1	pyridoxal 5'-phosphate synthase pdxS subunit

Nicotinate and nicotinamide metabolism		
K32-1_00327	ndhL	nicotinate dehydrogenase large molybdopterin subunit
K32-1_00354	pncB, NAPRT1	nicotinate phosphoribosyltransferase
K32-1_00635	nadE	NAD+ synthase
K32-1_00746	ppnK, NADK	NAD+ kinase
K32-1_00768	punA, PNP	purine-nucleoside phosphorylase
K32-1_00902	surE	5'-nucleotidase
K32-1_01214	npdA	NAD-dependent deacetylase
K32-1_01460	ndhL	nicotinate dehydrogenase large molybdopterin subunit
K32-1_01466	nicE, maiA	maleate isomerase
K32-1_01602	nadD	nicotinate-nucleotide adenylyltransferase
K32-1_02204	pncC	nicotinamide-nucleotide amidase
K32-1_02821	dml	2,3-dimethylmalate lyase
Pantothenate and CoA biosynthesis		
K32-1_00103	DPYS, dht, hydA	dihydropyrimidinase
K32-1_00295	panB	3-methyl-2-oxobutanoate hydroxymethyltransferase
K32-1_00316	E2.7.7.3A, coaD, kdtB	pantetheine-phosphate adenylyltransferase
K32-1_00352	coaE	dephospho-CoA kinase
K32-1_00803	ilvC	ketol-acid reductoisomerase
K32-1_01277	coaBC, dfp	phosphopantothenoylcysteine decarboxylase / phosphopantothenate---cysteine ligase
K32-1_01464	preA	dihydropyrimidine dehydrogenase (NAD+) subunit PreA
K32-1_02558	E2.2.1.6S, ilvH, ilvN	acetolactate synthase I/III small subunit
K32-1_02863	panB	3-methyl-2-oxobutanoate hydroxymethyltransferase
K32-1_02864	panC	pantoate--beta-alanine ligase
K32-1_02865	panD	aspartate 1-decarboxylase
K32-1_02926	coaX	type III pantothenate kinase
K32-1_03170	E2.6.1.42, ilvE	branched-chain amino acid aminotransferase
K32-1_03171	ilvD	dihydroxy-acid dehydratase
K32-1_03172	E2.2.1.6L, ilvB, ilvG, ilvI	acetolactate synthase I/II/III large subunit
K32-1_03173	E2.2.1.6S, ilvH, ilvN	acetolactate synthase I/III small subunit
K32-1_03174	E2.2.1.6L, ilvB, ilvG, ilvI	acetolactate synthase I/II/III large subunit
K32-1_03264	acpS	holo-[acyl-carrier protein] synthase
Biotin metabolism		
K32-1_00597	bioB	biotin synthase
K32-1_01131	fabF, OXSM, CEM1	3-oxoacyl-[acyl-carrier-protein] synthase II
K32-1_01134	fabG, OAR1	3-oxoacyl-[acyl-carrier protein] reductase
K32-1_01180	bioB	biotin synthase
K32-1_02001	bioB	biotin synthase
K32-1_02110	fabG, OAR1	3-oxoacyl-[acyl-carrier protein] reductase
K32-1_02207	fabZ	3-hydroxyacyl-[acyl-carrier-protein] dehydratase
K32-1_02924	birA	BirA family transcriptional regulator, biotin operon repressor / biotin---[acetyl-CoA-carboxylase] ligase
Lipoic acid metabolism		
K32-1_00580	lipA, LIAS, LIP1, LIP5	lipoyl synthase
K32-1_01196	lplA, lplJ, lipL1	lipoate---protein ligase
K32-1_02832	lipM	lipoyl(octanoyl) transferase
Folate biosynthesis		
K32-1_00005	moeA	molybdopterin molybdotransferase
K32-1_00006	moeA	molybdopterin molybdotransferase
K32-1_00007	moaA, CNX2	GTP 3',8-cyclase
K32-1_00008	moaC, CNX3	cyclic pyranopterin monophosphate synthase
K32-1_00010	mogA	molybdopterin adenylyltransferase
K32-1_00079	mocA	molybdenum cofactor cytidylyltransferase
K32-1_00436	folB	7,8-dihydroneopterin aldolase/epimerase/oxygenase
K32-1_01646	folC	dihydrofolate synthase / folylpolyglutamate synthase
K32-1_01721	moeA	molybdopterin molybdotransferase
K32-1_01722	mobA	molybdenum cofactor guanylyltransferase
K32-1_01787	sulD	dihydroneopterin aldolase / 2-amino-4-hydroxy-6-hydroxymethyldihydropteridine diphosphokinase
K32-1_01788	folP	dihydropteroate synthase
K32-1_01789	GCH1, folE	GTP cyclohydrolase IA
K32-1_02039	K06897	7,8-dihydropterin-6-yl-methyl-4-(beta-D-ribofuranosyl)aminobenzene 5'-phosphate synthase
K32-1_02114	mobA	molybdenum cofactor guanylyltransferase
K32-1_02428	queF	7-cyano-7-deazaguanine reductase
K32-1_02861	ribBA	3,4-dihydroxy 2-butanone 4-phosphate synthase / GTP cyclohydrolase II
Porphyrin metabolism		
K32-1_00019	hemE, UROD	uroporphyrinogen decarboxylase
K32-1_00414	hemL	glutamate-1-semialdehyde 2,1-aminomutase
K32-1_00660	hemN, hemZ	oxygen-independent coproporphyrinogen III oxidase
K32-1_00801	cobA, btuR	cob(I)alamin adenosyltransferase
K32-1_00841	sirC	precorrin-2 dehydrogenase
K32-1_00842	hemA	glutamyl-tRNA reductase
K32-1_00843	hemC, HMBS	hydroxymethylbilane synthase
K32-1_00844	cobA-hemD	uroporphyrinogen III methyltransferase / synthase
K32-1_00845	ahbC	Fe-coproporphyrin III synthase
K32-1_00846	hemB, ALAD	porphobilinogen synthase
K32-1_00847	ahbD	AdoMet-dependent heme synthase
K32-1_00848	ahbAB	siroheme decarboxylase
K32-1_00849	ahbAB	siroheme decarboxylase
K32-1_00850	hemL	glutamate-1-semialdehyde 2,1-aminomutase
K32-1_01011	cobD	threonine-phosphate decarboxylase
K32-1_01012	pduX	L-threonine kinase
K32-1_01013	E2.7.8.26, cobS, cobV	adenosylcobinamide-GDP ribazoletransferase
K32-1_01014	cobB-cbiA	cobyrinic acid a,c-diamide synthase
K32-1_01015	cbiB, cobD	adenosylcobinamide-phosphate synthase
K32-1_01016	cobQ, cbiP	adenosylcobyric acid synthase
K32-1_01017	cobH-cbiC	precorrin-8X/cobalt-precorrin-8 methylmutase
K32-1_01019	cobK-cbiJ	precorrin-6A/cobalt-precorrin-6A reductase
K32-1_01020	cobJ, cbiH	precorrin-3B C17-methyltransferase / cobalt-factor III methyltransferase
K32-1_01021	cbiG	cobalt-precorrin 5A hydrolase
K32-1_01022	cobM, cbiF	precorrin-4/cobalt-precorrin-4 C11-methyltransferase
K32-1_01023	cobI-cbiL	precorrin-2/cobalt-factor-2 C20-methyltransferase
K32-1_01024	cbiT	cobalt-precorrin-6B (C15)-methyltransferase
K32-1_01025	cbiE	cobalt-precorrin-7 (C5)-methyltransferase
K32-1_01026	cbiD	cobalt-precorrin-5B (C1)-methyltransferase
K32-1_01027	cobP, cobU	adenosylcobinamide kinase / adenosylcobinamide-phosphate guanylyltransferase
K32-1_01499	hemE, UROD	uroporphyrinogen decarboxylase
K32-1_01503	hemE, UROD	uroporphyrinogen decarboxylase
K32-1_01734	bzaE	5-methoxy-6-methylbenzimidazole methyltransferase
K32-1_01735	bzaD	5-methoxybenzimidazole methyltransferase
K32-1_01736	bzaC	5-hydroxybenzimidazole methyltransferase
K32-1_01737	E2.4.2.21, cobU, cobT	nicotinate-nucleotide--dimethylbenzimidazole phosphoribosyltransferase
K32-1_01739	E2.7.8.26, cobS, cobV	adenosylcobinamide-GDP ribazoletransferase
K32-1_01740	bzaA_B	5-hydroxybenzimidazole synthase
K32-1_01741	bzaA_B	5-hydroxybenzimidazole synthase
K32-1_01785	E2.4.2.21, cobU, cobT	nicotinate-nucleotide--dimethylbenzimidazole phosphoribosyltransferase
K32-1_01850	hemE, UROD	uroporphyrinogen decarboxylase
K32-1_01969	cobK-cbiJ	precorrin-6A/cobalt-precorrin-6A reductase
K32-1_02024	cobA, btuR	cob(I)alamin adenosyltransferase
K32-1_02025	chlD, bchD	magnesium chelatase subunit D
K32-1_02026	chlI, bchI	magnesium chelatase subunit I
K32-1_02027	cobN	cobaltochelatase CobN
K32-1_02028	cbiZ	adenosylcobinamide hydrolase
K32-1_02438	hemG	menaquinone-dependent protoporphyrinogen oxidase
K32-1_02587	eutT	ethanolamine utilization cobalamin adenosyltransferase
Other Cofactor metabolism		
K32-1_00642	mobB	molybdopterin-guanine dinucleotide biosynthesis adapter protein
K32-1_01720	mobB	molybdopterin-guanine dinucleotide biosynthesis adapter protein
K32-1_02184	ubiB, aarF	ubiquinone biosynthesis protein
K32-1_02358	ubiB, aarF	ubiquinone biosynthesis protein
Xenobiotics biodegradation and metabolism		
Benzoate degradation		
K32-1_00313	praC, xylH	4-oxalocrotonate tautomerase
K32-1_00395	ACAT, atoB	acetyl-CoA C-acetyltransferase
K32-1_00396	paaH, hbd, fadB, mmgB	3-hydroxybutyryl-CoA dehydrogenase
K32-1_01482	pcaC	4-carboxymuconolactone decarboxylase
K32-1_01553	praC, xylH	4-oxalocrotonate tautomerase
K32-1_01991	paaH, hbd, fadB, mmgB	3-hydroxybutyryl-CoA dehydrogenase
K32-1_02108	ACAT, atoB	acetyl-CoA C-acetyltransferase
K32-1_02109	fadB	enoyl-CoA hydratase
K32-1_02111	paaH, hbd, fadB, mmgB	3-hydroxybutyryl-CoA dehydrogenase
K32-1_02113	ACAT, atoB	acetyl-CoA C-acetyltransferase
K32-1_02557	dmpP, poxF, tomA5	phenol/toluene 2-monooxygenase (NADH) P5/A5
Aminobenzoate degradation		
K32-1_00407	atoD	acetate CoA/acetoacetate CoA-transferase alpha subunit
K32-1_00408	atoA	acetate CoA/acetoacetate CoA-transferase beta subunit

K32-1_00449	lpdD	gallate decarboxylase subunit D
K32-1_00625	E3.5.1.4, amiE	amidase
K32-1_00836	ubiX, bsdB, PAD1	flavin prenyltransferase
K32-1_02122	abmG	2-aminobenzoate-CoA ligase
Folding, sorting and degradation		
Protein export		
K32-1_00051	tatA	sec-independent protein translocase protein TatA
K32-1_00650	yajC	preprotein translocase subunit YajC
K32-1_00652	secD	preprotein translocase subunit SecD
K32-1_00653	secF	preprotein translocase subunit SecF
K32-1_01117	lepB	signal peptidase I
K32-1_01123	SRP54, ffh	signal recognition particle subunit SRP54
K32-1_01126	ftsY	fused signal recognition particle receptor
K32-1_01198	tatC	sec-independent protein translocase protein TatC
K32-1_01199	tatA	sec-independent protein translocase protein TatA
K32-1_01304	lspA	signal peptidase II
K32-1_02130	secG	preprotein translocase subunit SecG
K32-1_02188	secA	preprotein translocase subunit SecA
K32-1_02686	lepB	signal peptidase I
K32-1_02693	yidC, spoIIIJ, OXA1, ccfA	YidC/Oxa1 family membrane protein insertase
K32-1_02706	tatA	sec-independent protein translocase protein TatA
K32-1_02707	tatC	sec-independent protein translocase protein TatC
K32-1_02994	secY	preprotein translocase subunit SecY
Sulfur relay system		
K32-1_00007	moaA, CNX2	GTP 3',8-cyclase
K32-1_00008	moaC, CNX3	cyclic pyranopterin monophosphate synthase
K32-1_00010	mogA	molybdopterin adenylyltransferase
K32-1_00035	thiS	sulfur carrier protein
K32-1_00091	moaD, cysO	sulfur-carrier protein
K32-1_00369	thiS	sulfur carrier protein
K32-1_00669	iscS, NFS1	cysteine desulfurase
K32-1_00671	mnmA, trmU	tRNA-uridine 2-sulfurtransferase
K32-1_01351	moeB	molybdopterin-synthase adenylyltransferase
K32-1_01859	moaD, cysO	sulfur-carrier protein
K32-1_01995	ynjE	molybdopterin synthase sulfurtransferase
K32-1_01999	TST, MPST, sseA	thiosulfate/3-mercaptopyruvate sulfurtransferase
K32-1_02015	tusA, sirA	tRNA 2-thiouridine synthesizing protein A
K32-1_02498	mec	[CysO sulfur-carrier protein]-S-L-cysteine hydrolase
Membrane transport		
ABC transporters		
K32-1_00047	metQ	D-methionine transport system substrate-binding protein
K32-1_00048	metI	D-methionine transport system permease protein
K32-1_00049	metN	D-methionine transport system ATP-binding protein
K32-1_00086	nupB	general nucleoside transport system permease protein
K32-1_00087	nupC	general nucleoside transport system permease protein
K32-1_00089	bmpA, bmpB, tmpC	basic membrane protein A and related proteins
K32-1_00092	nupA	general nucleoside transport system ATP-binding protein
K32-1_00093	bmpA, bmpB, tmpC	basic membrane protein A and related proteins
K32-1_00097	bmpA, bmpB, tmpC	basic membrane protein A and related proteins
K32-1_00098	nupA	general nucleoside transport system ATP-binding protein
K32-1_00099	nupB	general nucleoside transport system permease protein
K32-1_00100	nupC	general nucleoside transport system permease protein
K32-1_00246	bmpA, bmpB, tmpC	basic membrane protein A and related proteins
K32-1_00247	nupA	general nucleoside transport system ATP-binding protein
K32-1_00248	nupB	general nucleoside transport system permease protein
K32-1_00249	nupC	general nucleoside transport system permease protein
K32-1_00338	bmpA, bmpB, tmpC	basic membrane protein A and related proteins
K32-1_00339	nupA	general nucleoside transport system ATP-binding protein
K32-1_00340	nupB	general nucleoside transport system permease protein
K32-1_00341	nupC	general nucleoside transport system permease protein
K32-1_00365	bmpA, bmpB, tmpC	basic membrane protein A and related proteins
K32-1_00366	nupA	general nucleoside transport system ATP-binding protein
K32-1_00367	nupB	general nucleoside transport system permease protein
K32-1_00368	nupC	general nucleoside transport system permease protein
K32-1_00437	bmpA, bmpB, tmpC	basic membrane protein A and related proteins
K32-1_00438	nupB	general nucleoside transport system permease protein
K32-1_00439	nupC	general nucleoside transport system permease protein
K32-1_00440	nupA	general nucleoside transport system ATP-binding protein
K32-1_00444	pstS	phosphate transport system substrate-binding protein
K32-1_00445	pstC	phosphate transport system permease protein
K32-1_00446	pstA	phosphate transport system permease protein
K32-1_00447	pstB	phosphate transport system ATP-binding protein
K32-1_00450	tupB, vupB	tungstate transport system permease protein
K32-1_00451	tupC, vupC	tungstate transport system ATP-binding protein
K32-1_00462	oppA, mppA	oligopeptide transport system substrate-binding protein
K32-1_00463	oppB	oligopeptide transport system permease protein
K32-1_00464	oppC	oligopeptide transport system permease protein
K32-1_00465	oppD	oligopeptide transport system ATP-binding protein
K32-1_00466	oppF	oligopeptide transport system ATP-binding protein
K32-1_00525	ssuA	sulfonate transport system substrate-binding protein
K32-1_00526	ssuC	sulfonate transport system permease protein
K32-1_01155	bmpA, bmpB, tmpC	basic membrane protein A and related proteins
K32-1_01179	bioY	biotin transport system substrate-specific component
K32-1_01297	nodJ	lipooligosaccharide transport system permease protein
K32-1_01298	nodI	lipooligosaccharide transport system ATP-binding protein
K32-1_01468	cbiO	cobalt/nickel transport system ATP-binding protein
K32-1_01469	cbiQ	cobalt/nickel transport system permease protein
K32-1_01471	cbiN	cobalt/nickel transport protein
K32-1_01472	cbiM	cobalt/nickel transport system permease protein
K32-1_01473	tupA, vupA	tungstate transport system substrate-binding protein
K32-1_01500	rbsB	ribose transport system substrate-binding protein
K32-1_01501	xylG	D-xylose transport system ATP-binding protein
K32-1_01502	rbsC	ribose transport system permease protein
K32-1_01826	nupC	general nucleoside transport system permease protein
K32-1_01827	nupB	general nucleoside transport system permease protein
K32-1_01828	nupA	general nucleoside transport system ATP-binding protein
K32-1_01829	bmpA, bmpB, tmpC	basic membrane protein A and related proteins
K32-1_01851	rbsC	ribose transport system permease protein
K32-1_01852	rbsA	ribose transport system ATP-binding protein
K32-1_01853	rbsB	ribose transport system substrate-binding protein
K32-1_01965	cbiO	cobalt/nickel transport system ATP-binding protein
K32-1_01966	cbiQ	cobalt/nickel transport system permease protein
K32-1_01967	cbiN	cobalt/nickel transport protein
K32-1_01968	cbiM	cobalt/nickel transport system permease protein
K32-1_02005	phnE	phosphonate transport system permease protein
K32-1_02006	phnE	phosphonate transport system permease protein
K32-1_02007	phnC	phosphonate transport system ATP-binding protein
K32-1_02008	phnD	phosphonate transport system substrate-binding protein
K32-1_02018	modA	molybdate transport system substrate-binding protein
K32-1_02019	modB	molybdate transport system permease protein
K32-1_02020	modC	molybdate transport system ATP-binding protein
K32-1_02035	znuA	zinc transport system substrate-binding protein
K32-1_02036	znuC	zinc transport system ATP-binding protein
K32-1_02037	znuB	zinc transport system permease protein
K32-1_02067	livF	branched-chain amino acid transport system ATP-binding protein
K32-1_02068	livG	branched-chain amino acid transport system ATP-binding protein
K32-1_02069	livM	branched-chain amino acid transport system permease protein
K32-1_02070	livH	branched-chain amino acid transport system permease protein
K32-1_02071	livK	branched-chain amino acid transport system substrate-binding protein
K32-1_02088	rbsC	ribose transport system permease protein
K32-1_02090	rbsB	ribose transport system substrate-binding protein
K32-1_02093	nupC	general nucleoside transport system permease protein
K32-1_02094	nupB	general nucleoside transport system permease protein
K32-1_02095	nupA	general nucleoside transport system ATP-binding protein
K32-1_02096	bmpA, bmpB, tmpC	basic membrane protein A and related proteins
K32-1_02152	bmpA, bmpB, tmpC	basic membrane protein A and related proteins
K32-1_02167	ftsX	cell division transport system permease protein
K32-1_02168	ftsE	cell division transport system ATP-binding protein
K32-1_02194	glnQ	glutamine transport system ATP-binding protein
K32-1_02195	glnP	glutamine transport system permease protein
K32-1_02196	glnH	glutamine transport system substrate-binding protein
K32-1_02217	ecfT	energy-coupling factor transport system permease protein
K32-1_02221	lysY	putative lysine transport system ATP-binding protein
K32-1_02222	lysX2	putative lysine transport system permease protein
K32-1_02223	lysX1	putative lysine transport system substrate-binding protein

K32-1_02429	afuC, fbpC	iron(III) transport system ATP-binding protein
K32-1_02430	afuB, fbpB	iron(III) transport system permease protein
K32-1_02431	afuA, fbpA	iron(III) transport system substrate-binding protein
K32-1_02465	ccmC	heme exporter protein C
K32-1_02466	ccmB	heme exporter protein B
K32-1_02467	ccmA	heme exporter protein A
K32-1_02529	livF	branched-chain amino acid transport system ATP-binding protein
K32-1_02530	livG	branched-chain amino acid transport system ATP-binding protein
K32-1_02531	livM	branched-chain amino acid transport system permease protein
K32-1_02532	livH	branched-chain amino acid transport system permease protein
K32-1_02533	livK	branched-chain amino acid transport system substrate-binding protein
K32-1_02654	livF	branched-chain amino acid transport system ATP-binding protein
K32-1_02655	livG	branched-chain amino acid transport system ATP-binding protein
K32-1_02656	livM	branched-chain amino acid transport system permease protein
K32-1_02657	livH	branched-chain amino acid transport system permease protein
K32-1_02658	livK	branched-chain amino acid transport system substrate-binding protein
K32-1_03005	ecfA1	energy-coupling factor transport system ATP-binding protein
K32-1_03006	ecfA2	energy-coupling factor transport system ATP-binding protein
K32-1_03007	ecfT	energy-coupling factor transport system permease protein
K32-1_03023	cydD	ATP-binding cassette, subfamily C, bacterial CydD
K32-1_03024	cydC	ATP-binding cassette, subfamily C, bacterial CydC
K32-1_03090	bmpA, bmpB, tmpC	basic membrane protein A and related proteins
K32-1_03091	nupA	general nucleoside transport system ATP-binding protein
K32-1_03092	nupB	general nucleoside transport system permease protein
K32-1_03093	nupC	general nucleoside transport system permease protein
K32-1_03106	mdlB, smdB	ATP-binding cassette, subfamily B, multidrug efflux pump
K32-1_03107	mdlA, smdA	ATP-binding cassette, subfamily B, multidrug efflux pump
K32-1_03125	opuBD	osmoprotectant transport system permease protein
K32-1_03126	opuA	osmoprotectant transport system ATP-binding protein
K32-1_03127	opuBD	osmoprotectant transport system permease protein
K32-1_03128	opuC	osmoprotectant transport system substrate-binding protein
K32-1_03149	opuC	osmoprotectant transport system substrate-binding protein
K32-1_03150	opuA	osmoprotectant transport system ATP-binding protein
K32-1_03153	opuA	osmoprotectant transport system ATP-binding protein
K32-1_03155	opuBD	osmoprotectant transport system permease protein
K32-1_03228	bmpA, bmpB, tmpC	basic membrane protein A and related proteins
K32-1_03229	nupB	general nucleoside transport system permease protein
K32-1_03230	nupC	general nucleoside transport system permease protein
K32-1_03231	nupA	general nucleoside transport system ATP-binding protein
K32-1_03263	pstS	phosphate transport system substrate-binding protein
K32-1_03293	livK	branched-chain amino acid transport system substrate-binding protein
K32-1_03294	livH	branched-chain amino acid transport system permease protein
K32-1_03295	livM	branched-chain amino acid transport system permease protein
K32-1_03296	livG	branched-chain amino acid transport system ATP-binding protein
K32-1_03297	livF	branched-chain amino acid transport system ATP-binding protein
Phosphotransferase system (PTS)		
K32-1_02142	ptsI	phosphoenolpyruvate-protein phosphotransferase (PTS system enzyme I)
K32-1_02143	ptsH	phosphocarrier protein HPr
K32-1_02146	manZ	mannose PTS system EIID component
K32-1_02147	manY	mannose PTS system EIIC component
K32-1_02149	manXa	mannose PTS system EIIA component
Bacterial secretion system		
K32-1_00051	tatA	sec-independent protein translocase protein TatA
K32-1_00218	virD4, lvhD4	type IV secretion system protein VirD4
K32-1_00650	yajC	preprotein translocase subunit YajC
K32-1_00652	secD	preprotein translocase subunit SecD
K32-1_00653	secF	preprotein translocase subunit SecF
K32-1_00702	gspG	general secretion pathway protein G
K32-1_00933	virD4, lvhD4	type IV secretion system protein VirD4
K32-1_01123	SRP54, ffh	signal recognition particle subunit SRP54
K32-1_01126	ftsY	fused signal recognition particle receptor
K32-1_01198	tatC	sec-independent protein translocase protein TatC
K32-1_01199	tatA	sec-independent protein translocase protein TatA
K32-1_02130	secG	preprotein translocase subunit SecG
K32-1_02188	secA	preprotein translocase subunit SecA
K32-1_02693	yidC, spoIIIJ, OXA1, ccfA	YidC/Oxa1 family membrane protein insertase
K32-1_02706	tatA	sec-independent protein translocase protein TatA
K32-1_02707	tatC	sec-independent protein translocase protein TatC
K32-1_02994	secY	preprotein translocase subunit SecY
Signal transduction		
Two-component system		
K32-1_00030	dctM	C4-dicarboxylate transporter, DctM subunit
K32-1_00068	agrB	accessory gene regulator B
K32-1_00242	glnA, GLUL	glutamine synthetase
K32-1_00395	ACAT, atoB	acetyl-CoA C-acetyltransferase
K32-1_00407	atoD	acetate CoA/acetoacetate CoA-transferase alpha subunit
K32-1_00408	atoA	acetate CoA/acetoacetate CoA-transferase beta subunit
K32-1_00444	pstS	phosphate transport system substrate-binding protein
K32-1_00496	mcp	methyl-accepting chemotaxis protein
K32-1_00502	glnA, GLUL	glutamine synthetase
K32-1_00569	glnA, GLUL	glutamine synthetase
K32-1_00571	glnA, GLUL	glutamine synthetase
K32-1_00751	spo0A	two-component system, response regulator, stage 0 sporulation protein A
K32-1_00785	cssR	two-component system, OmpR family, response regulator CssR
K32-1_00786	cssS	two-component system, OmpR family, sensor histidine kinase CssS
K32-1_00989	baeS, smeS	two-component system, OmpR family, sensor histidine kinase BaeS
K32-1_01100	mcp	methyl-accepting chemotaxis protein
K32-1_01202	barA, gacS, varS	two-component system, NarL family, sensor histidine kinase BarA
K32-1_01221	crp	CRP/FNR family transcriptional regulator, cyclic AMP receptor protein
K32-1_01386	mcp	methyl-accepting chemotaxis protein
K32-1_01389	cheY	two-component system, chemotaxis family, chemotaxis protein CheY
K32-1_01391	cheR	chemotaxis protein methyltransferase CheR
K32-1_01397	fliA, whiG	RNA polymerase sigma factor FliA
K32-1_01410	motA	chemotaxis protein MotA
K32-1_01434	fliC, hag	flagellin
K32-1_01440	csrA	carbon storage regulator
K32-1_01445	flgM	negative regulator of flagellin synthesis FlgM
K32-1_01446	cheB	two-component system, chemotaxis family, protein-glutamate methylesterase/glutaminase
K32-1_01447	cheA	two-component system, chemotaxis family, sensor kinase CheA
K32-1_01448	cheW	purine-binding chemotaxis protein CheW
K32-1_01456	dctM	C4-dicarboxylate transporter, DctM subunit
K32-1_01457	dctQ	C4-dicarboxylate transporter, DctQ subunit
K32-1_01458	dctP	C4-dicarboxylate-binding protein DctP
K32-1_01539	degU	two-component system, NarL family, response regulator DegU
K32-1_01540	degS	two-component system, NarL family, sensor histidine kinase DegS
K32-1_01594	lytT, lytR	two-component system, LytTR family, response regulator LytT
K32-1_01595	lytS	two-component system, LytTR family, sensor histidine kinase LytS
K32-1_01719	barA, gacS, varS	two-component system, NarL family, sensor histidine kinase BarA
K32-1_01748	ttrB	tetrathionate reductase subunit B
K32-1_01878	yesN	two-component system, response regulator YesN
K32-1_01924	yesN	two-component system, response regulator YesN
K32-1_01930	yesN	two-component system, response regulator YesN
K32-1_01945	mprA	two-component system, OmpR family, response regulator MprA
K32-1_01947	degP, htrA	serine protease Do
K32-1_01974	ME2, sfcA, maeA	malate dehydrogenase (oxaloacetate-decarboxylating)
K32-1_02072	mcp	methyl-accepting chemotaxis protein
K32-1_02097	yesN	two-component system, response regulator YesN
K32-1_02098	yesM	two-component system, sensor histidine kinase YesM
K32-1_02108	ACAT, atoB	acetyl-CoA C-acetyltransferase
K32-1_02113	ACAT, atoB	acetyl-CoA C-acetyltransferase
K32-1_02136	rpoN	RNA polymerase sigma-54 factor
K32-1_02154	glnB	nitrogen regulatory protein P-II 1
K32-1_02159	mprF, fmtC	phosphatidylglycerol lysyltransferase
K32-1_02306	mcp	methyl-accepting chemotaxis protein
K32-1_02319	wecB	UDP-N-acetylglucosamine 2-epimerase (non-hydrolysing)
K32-1_02345	spo0F	two-component system, response regulator, stage 0 sporulation protein F
K32-1_02366	yesN	two-component system, response regulator YesN
K32-1_02406	divK	two-component system, cell cycle response regulator DivK
K32-1_02409	yesN	two-component system, response regulator YesN
K32-1_02452	degP, htrA	serine protease Do
K32-1_02481	kdpE	two-component system, OmpR family, KDP operon response regulator KdpE
K32-1_02679	crp	CRP/FNR family transcriptional regulator, cyclic AMP receptor protein
K32-1_02696	dnaA	chromosomal replication initiator protein
K32-1_02722	mcp	methyl-accepting chemotaxis protein

K32-1_02835	phoB1, phoP	two-component system, OmpR family, alkaline phosphatase synthesis response regulator PhoP
K32-1_02836	phoR	two-component system, OmpR family, phosphate regulon sensor histidine kinase PhoR
K32-1_02895	yesN	two-component system, response regulator YesN
K32-1_03014	mcp	methyl-accepting chemotaxis protein
K32-1_03021	cydA	cytochrome bd ubiquinol oxidase subunit I
K32-1_03022	cydB	cytochrome bd ubiquinol oxidase subunit II
K32-1_03071	mcp	methyl-accepting chemotaxis protein
K32-1_03072	cheW	purine-binding chemotaxis protein CheW
K32-1_03073	cheB	two-component system, chemotaxis family, protein-glutamate methylesterase/glutaminase
K32-1_03074	cheR	chemotaxis protein methyltransferase CheR
K32-1_03075	cheA	two-component system, chemotaxis family, sensor kinase CheA
K32-1_03077	mcp	methyl-accepting chemotaxis protein
K32-1_03078	cheY	two-component system, chemotaxis family, chemotaxis protein CheY
K32-1_03079	degU	two-component system, NarL family, response regulator DegU
K32-1_03225	resD	two-component system, OmpR family, response regulator ResD
K32-1_03226	resE	two-component system, OmpR family, sensor histidine kinase ResE
K32-1_03260	mcp	methyl-accepting chemotaxis protein
K32-1_03262	phoB1, phoP	two-component system, OmpR family, alkaline phosphatase synthesis response regulator PhoP
K32-1_03263	pstS	phosphate transport system substrate-binding protein
K32-1_03272	spo0F	two-component system, response regulator, stage 0 sporulation protein F
K32-1_03277	kinE	two-component system, sporulation sensor kinase E
HIF-1 signaling pathway		
K32-1_00319	pfkA, PFK	6-phosphofructokinase 1
K32-1_01976	PGK, pgk	phosphoglycerate kinase
K32-1_02131	ENO, eno	enolase
K32-1_02134	PGK, pgk	phosphoglycerate kinase
K32-1_02135	GAPDH, gapA	glyceraldehyde 3-phosphate dehydrogenase (phosphorylating)
Phosphatidylinositol signaling system		
K32-1_01083	E2.7.7.41, CDS1, CDS2, cdsA	phosphatidate cytidylyltransferase
K32-1_01565	dgkA, DGK	diacylglycerol kinase (ATP)
K32-1_01565	dgkA, DGK	diacylglycerol kinase (ATP)
AMPK signaling pathway		
K32-1_00319	pfkA, PFK	6-phosphofructokinase 1
Peroxisome		
K32-1_00244	IDH1, IDH2, icd	isocitrate dehydrogenase
Other transport		
K32-1_00011	TC.AGCS	alanine or glycine:cation symporter, AGCS family
K32-1_00384	TC.CIC	chloride channel protein, CIC family
K32-1_00624	TC.APA	basic amino acid/polyamine antiporter, APA family
K32-1_01792	TC.BASS	bile acid:Na+ symporter, BASS family
K32-1_01903	TC.SSS	solute:Na+ symporter, SSS family
K32-1_02073	TC.PIT	inorganic phosphate transporter, PiT family
K32-1_02178	TC.BCT	betaine/carnitine transporter, BCCT family
K32-1_02213	TC.CIC	chloride channel protein, CIC family
K32-1_02234	TC.HAE1	hydrophobic/amphiphilic exporter-1 (mainly G- bacteria), HAE1 family
K32-1_02425	TC.KEF	monovalent cation:H+ antiporter-2, CPA2 family
K32-1_03052	TC.SSS	solute:Na+ symporter, SSS family
Cell motility		
Bacterial chemotaxis		
K32-1_00496	mcp	methyl-accepting chemotaxis protein
K32-1_01100	mcp	methyl-accepting chemotaxis protein
K32-1_01386	mcp	methyl-accepting chemotaxis protein
K32-1_01387	fliN	flagellar motor switch protein FliN
K32-1_01388	fliM	flagellar motor switch protein FliM
K32-1_01389	cheY	two-component system, chemotaxis family, chemotaxis protein CheY
K32-1_01390	cheC	chemotaxis protein CheC
K32-1_01391	cheR	chemotaxis protein methyltransferase CheR
K32-1_01392	cheD	chemotaxis protein CheD
K32-1_01407	fliN	flagellar motor switch protein FliN
K32-1_01409	motB	chemotaxis protein MotB
K32-1_01410	motA	chemotaxis protein MotA
K32-1_01419	fliG	flagellar motor switch protein FliG
K32-1_01446	cheB	two-component system, chemotaxis family, protein-glutamate methylesterase/glutaminase
K32-1_01447	cheA	two-component system, chemotaxis family, sensor kinase CheA
K32-1_01448	cheW	purine-binding chemotaxis protein CheW
K32-1_01500	rbsB	ribose transport system substrate-binding protein
K32-1_01853	rbsB	ribose transport system substrate-binding protein
K32-1_02072	mcp	methyl-accepting chemotaxis protein
K32-1_02090	rbsB	ribose transport system substrate-binding protein
K32-1_02306	mcp	methyl-accepting chemotaxis protein
K32-1_02722	mcp	methyl-accepting chemotaxis protein
K32-1_03014	mcp	methyl-accepting chemotaxis protein
K32-1_03071	mcp	methyl-accepting chemotaxis protein
K32-1_03072	cheW	purine-binding chemotaxis protein CheW
K32-1_03073	cheB	two-component system, chemotaxis family, protein-glutamate methylesterase/glutaminase
K32-1_03074	cheR	chemotaxis protein methyltransferase CheR
K32-1_03075	cheA	two-component system, chemotaxis family, sensor kinase CheA
K32-1_03077	mcp	methyl-accepting chemotaxis protein
K32-1_03078	cheY	two-component system, chemotaxis family, chemotaxis protein CheY
K32-1_03109	cheX	chemotaxis protein CheX
K32-1_03260	mcp	methyl-accepting chemotaxis protein
Flagellar assembly		
K32-1_01387	fliN	flagellar motor switch protein FliN
K32-1_01388	fliM	flagellar motor switch protein FliM
K32-1_01393	flgG	flagellar basal-body rod protein FlgG
K32-1_01394	flgF	flagellar basal-body rod protein FlgF
K32-1_01397	fliA, whiG	RNA polymerase sigma factor FliA
K32-1_01401	flhA	flagellar biosynthesis protein FlhA
K32-1_01402	flhB	flagellar biosynthesis protein FlhB
K32-1_01403	fliR	flagellar biosynthesis protein FliR
K32-1_01404	fliQ	flagellar biosynthesis protein FliQ
K32-1_01405	fliP	flagellar biosynthesis protein FliP
K32-1_01406	fliO, fliZ	flagellar protein FliO/FliZ
K32-1_01407	fliN	flagellar motor switch protein FliN
K32-1_01408	fliL	flagellar protein FliL
K32-1_01409	motB	chemotaxis protein MotB
K32-1_01410	motA	chemotaxis protein MotA
K32-1_01412	flgE	flagellar hook protein FlgE
K32-1_01414	flgD	flagellar basal-body rod modification protein FlgD
K32-1_01416	fliJ	flagellar protein FliJ
K32-1_01417	fliI	flagellum-specific ATP synthase
K32-1_01418	fliH	flagellar assembly protein FliH
K32-1_01419	fliG	flagellar motor switch protein FliG
K32-1_01420	fliF	flagellar M-ring protein FliF
K32-1_01421	fliE	flagellar hook-basal body complex protein FliE
K32-1_01422	flgC	flagellar basal-body rod protein FlgC
K32-1_01423	flgB	flagellar basal-body rod protein FlgB
K32-1_01424	fliS	flagellar secretion chaperone FliS
K32-1_01427	fliD	flagellar hook-associated protein 2
K32-1_01434	fliC, hag	flagellin
K32-1_01442	flgL	flagellar hook-associated protein 3 FlgL
K32-1_01443	flgK	flagellar hook-associated protein 1
K32-1_01445	flgM	negative regulator of flagellin synthesis FlgM
K32-1_01549	rpoD	RNA polymerase primary sigma factor
K32-1_02136	rpoN	RNA polymerase sigma-54 factor
Cell growth		
K32-1_00197	spoIVCA	site-specific DNA recombinase
K32-1_00198	spoIVCA	site-specific DNA recombinase
K32-1_00256	spoVR	stage V sporulation protein R
K32-1_00491	gerKC	spore germination protein KC
K32-1_00492	gerKA	spore germination protein KA
K32-1_00647	spoIID	stage II sporulation protein D
K32-1_00720	spoIIAA	stage III sporulation protein AA
K32-1_00721	spoIIAB	stage III sporulation protein AB
K32-1_00722	spoIIAC	stage III sporulation protein AC
K32-1_00723	spoIIAD	stage III sporulation protein AD
K32-1_00724	spoIIAE	stage III sporulation protein AE
K32-1_00725	spoIIAF	stage III sporulation protein AF
K32-1_00726	spoIIAG	stage III sporulation protein AG
K32-1_00727	spoIIAH	stage III sporulation protein AH
K32-1_00764	spoIIM	stage II sporulation protein M
K32-1_00770	spoIIAA	stage II sporulation protein AA (anti-sigma F factor antagonist)

K32-1_00775	spoVAC	stage V sporulation protein AC
K32-1_00776	spoVAD	stage V sporulation protein AD
K32-1_00777	spoVAE	stage V sporulation protein AE
K32-1_00778	spoVAE	stage V sporulation protein AE
K32-1_00779	spoVAF	stage V sporulation protein AF
K32-1_00787	cotJC	spore coat protein JC
K32-1_00788	cotJB	spore coat protein JB
K32-1_00797	spmA	spore maturation protein A
K32-1_00798	spmB	spore maturation protein B
K32-1_00818	spoIIP	stage II sporulation protein P
K32-1_00826	spoIVA	stage IV sporulation protein A
K32-1_00865	cooC	CO dehydrogenase maturation factor
K32-1_00872	cooC	CO dehydrogenase maturation factor
K32-1_00994	spoVK	stage V sporulation protein K
K32-1_01032	spoVS	stage V sporulation protein S
K32-1_01053	spoVFB	dipicolinate synthase subunit B
K32-1_01054	spoVFA	dipicolinate synthase subunit A
K32-1_01129	spoVS	stage V sporulation protein S
K32-1_01326	spoIIR	stage II sporulation protein R
K32-1_01385	sspF	small acid-soluble spore protein F (minor alpha/beta-type SASP)
K32-1_01569	yqfD	similar to stage IV sporulation protein
K32-1_01588	spoIIP	stage II sporulation protein P
K32-1_01681	gerM	germination protein M
K32-1_01685	spoVR	stage V sporulation protein R
K32-1_02050	gerKC	spore germination protein KC
K32-1_02051	gerKA	spore germination protein KA
K32-1_02301	spoIID	stage II sporulation protein D
K32-1_02372	sspH	small acid-soluble spore protein H (minor)
K32-1_02496	yaaH	spore germination protein
K32-1_02692	jag	spoIIIJ-associated protein
K32-1_02731	bofA	inhibitor of the pro-sigma K processing machinery
K32-1_02795	yabG	spore coat assemly protein
K32-1_02810	ypeB	spore germination protein
K32-1_02877	spoVG	stage V sporulation protein G
K32-1_02881	yndD	spore germination protein
K32-1_02883	yndF	spore germination protein
K32-1_02894	spoIID	stage II sporulation protein D
K32-1_03258	gerM	germination protein M
Cellular community - prokaryotes		
Quorum sensing		
K32-1_00068	agrB	accessory gene regulator B
K32-1_00355	ABC.PE.S	peptide/nickel transport system substrate-binding protein
K32-1_00462	oppA, mppA	oligopeptide transport system substrate-binding protein
K32-1_00463	oppB	oligopeptide transport system permease protein
K32-1_00464	oppC	oligopeptide transport system permease protein
K32-1_00465	oppD	oligopeptide transport system ATP-binding protein
K32-1_00466	oppF	oligopeptide transport system ATP-binding protein
K32-1_00501	phzF	trans-2,3-dihydro-3-hydroxyanthranilate isomerase
K32-1_00650	yajC	preprotein translocase subunit YajC
K32-1_00751	spo0A	two-component system, response regulator, stage 0 sporulation protein A
K32-1_00995	hfq	host factor-I protein
K32-1_01123	SRP54, ffh	signal recognition particle subunit SRP54
K32-1_01126	ftsY	fused signal recognition particle receptor
K32-1_01185	trpE	anthranilate synthase component I
K32-1_01186	trpE	anthranilate synthase component I
K32-1_01221	crp	CRP/FNR family transcriptional regulator, cyclic AMP receptor protein
K32-1_01539	degU	two-component system, NarL family, response regulator DegU
K32-1_01814	TC.BAT2	bacterial/archaeal transporter family-2 protein
K32-1_02067	livF	branched-chain amino acid transport system ATP-binding protein
K32-1_02068	livG	branched-chain amino acid transport system ATP-binding protein
K32-1_02069	livM	branched-chain amino acid transport system permease protein
K32-1_02070	livH	branched-chain amino acid transport system permease protein
K32-1_02071	livK	branched-chain amino acid transport system substrate-binding protein
K32-1_02130	secG	preprotein translocase subunit SecG
K32-1_02188	secA	preprotein translocase subunit SecA
K32-1_02345	spo0F	two-component system, response regulator, stage 0 sporulation protein F
K32-1_02481	kdpE	two-component system, OmpR family, KDP operon response regulator KdpE
K32-1_02529	livF	branched-chain amino acid transport system ATP-binding protein
K32-1_02530	livG	branched-chain amino acid transport system ATP-binding protein
K32-1_02531	livM	branched-chain amino acid transport system permease protein
K32-1_02532	livH	branched-chain amino acid transport system permease protein
K32-1_02533	livK	branched-chain amino acid transport system substrate-binding protein
K32-1_02654	livF	branched-chain amino acid transport system ATP-binding protein
K32-1_02655	livG	branched-chain amino acid transport system ATP-binding protein
K32-1_02656	livM	branched-chain amino acid transport system permease protein
K32-1_02657	livH	branched-chain amino acid transport system permease protein
K32-1_02658	livK	branched-chain amino acid transport system substrate-binding protein
K32-1_02679	crp	CRP/FNR family transcriptional regulator, cyclic AMP receptor protein
K32-1_02693	yidC, spoIIIJ, OXA1, ccfA	YidC/Oxa1 family membrane protein insertase
K32-1_02859	ribD	diaminohydroxyphosphoribosylaminopyrimidine deaminase / 5-amino-6-(5-phosphoribosylamino)uracil reductase
K32-1_02911	TC.BAT2	bacterial/archaeal transporter family-2 protein
K32-1_02994	secY	preprotein translocase subunit SecY
K32-1_03079	degU	two-component system, NarL family, response regulator DegU
K32-1_03272	spo0F	two-component system, response regulator, stage 0 sporulation protein F
K32-1_03293	livK	branched-chain amino acid transport system substrate-binding protein
K32-1_03294	livH	branched-chain amino acid transport system permease protein
K32-1_03295	livM	branched-chain amino acid transport system permease protein
K32-1_03296	livG	branched-chain amino acid transport system ATP-binding protein
K32-1_03297	livF	branched-chain amino acid transport system ATP-binding protein
Biofilm formation - Pseudomonas aeruginosa		
K32-1_01185	trpE	anthranilate synthase component I
K32-1_01186	trpE	anthranilate synthase component I
K32-1_01202	barA, gacS, varS	two-component system, NarL family, sensor histidine kinase BarA
K32-1_01221	crp	CRP/FNR family transcriptional regulator, cyclic AMP receptor protein
K32-1_01397	fliA, whiG	RNA polymerase sigma factor FliA
K32-1_01440	csrA	carbon storage regulator
K32-1_01445	flgM	negative regulator of flagellin synthesis FlgM
K32-1_01719	barA, gacS, varS	two-component system, NarL family, sensor histidine kinase BarA
K32-1_02679	crp	CRP/FNR family transcriptional regulator, cyclic AMP receptor protein
Biofilm formation - Escherichia coli		
K32-1_01202	barA, gacS, varS	two-component system, NarL family, sensor histidine kinase BarA
K32-1_01221	crp	CRP/FNR family transcriptional regulator, cyclic AMP receptor protein
K32-1_01397	fliA, whiG	RNA polymerase sigma factor FliA
K32-1_01440	csrA	carbon storage regulator
K32-1_01445	flgM	negative regulator of flagellin synthesis FlgM
K32-1_01719	barA, gacS, varS	two-component system, NarL family, sensor histidine kinase BarA
K32-1_02679	crp	CRP/FNR family transcriptional regulator, cyclic AMP receptor protein
K32-1_00702	gspG	general secretion pathway protein G
K32-1_00995	hfq	host factor-I protein
K32-1_01202	barA, gacS, varS	two-component system, NarL family, sensor histidine kinase BarA
K32-1_01221	crp	CRP/FNR family transcriptional regulator, cyclic AMP receptor protein
K32-1_01397	fliA, whiG	RNA polymerase sigma factor FliA
K32-1_01440	csrA	carbon storage regulator
K32-1_01684	paaK	phenylacetate-CoA ligase
K32-1_01719	barA, gacS, varS	two-component system, NarL family, sensor histidine kinase BarA
K32-1_02136	rpoN	RNA polymerase sigma-54 factor
K32-1_02291	tagA, tarA	N-acetylglucosaminyldiphosphoundecaprenol N-acetyl-beta-D-mannosaminyltransferase
K32-1_02319	wecB	UDP-N-acetylglucosamine 2-epimerase (non-hydrolysing)
K32-1_02679	crp	CRP/FNR family transcriptional regulator, cyclic AMP receptor protein
K32-1_02951	cysE	serine O-acetyltransferase
K32-1_03053	paaK	phenylacetate-CoA ligase

Supplementary Table 2 Gene expression levels of methanogenesis-related genes of *M. shengliensis* ZC-1

Pathway	Locus_tag	Description	Monoculture on Methanol_ZC-1 (ZM)			Coculture on formate (ZKF)			Coculture on methanol(ZKM)			ZKF:ZM		ZKM:ZM	
			Avg	Std	Rank	Avg	Std	Rank	Avg	Std	Rank	Log2-FD	p-value	Log2-FD	p-value
methanol => methane	ZC1_00056	Methanol--corrinoid protein co-methyltransferase	35.4	3.0	2	177.5	6	1	16.1	1.3	2	2.3	0.0000	-1.1	0.0005
	ZC1_00057	Methylcobamide:CoM methyltransferase MtaA	2.5	0.0	46	8.6	1	36	2.6	0.4	37	1.8	0.0040	0.0	0.8871
	ZC1_00058	Methanol--corrinoid protein	14.8	1.1	4	106.1	6	3	4.8	0.8	20	2.8	0.0000	-1.6	0.0002
	ZC1_00785	Methanol--corrinoid protein co-methyltransferase	0.0	0.0	1420	0.1	0	1315	0.0	0.0	1414	2.2	0.0000	-1.0	0.0015
	ZC1_01463	Methanol--corrinoid protein co-methyltransferase	0.0	0.0	1594	0.0	0	1577	0.0	0.0	1605	2.0	0.0006	-1.1	0.0116
	ZC1_01612	Methanol--corrinoid protein co-methyltransferase	0.0	0.0	1615	0.0	0	1592	0.0	0.0	1610	2.1	0.0012	-0.8	0.0215
methylamines => methane	ZC1_00651	Dimethylamine corrinoid protein	0.0	0.0	1338	0.1	0	1341	0.0	0.0	1454	1.4	0.0002	-2.1	0.0001
	ZC1_01133	Methylated-thiol--coenzyme M methyltransferase	0.6	0.0	360	3.0	0	85	0.1	0.0	724	2.3	0.0013	-2.0	0.0000
	ZC1_01134	Trimethylamine corrinoid protein	0.7	0.0	328	4.2	0	62	0.3	0.0	398	2.7	0.0025	-0.9	0.0049
	ZC1_01511	Monomethylamine methyltransferase MtmB1	2.3	0.2	60	9.5	1	31	0.8	0.0	169	2.1	0.0002	-1.5	0.0001
	ZC1_01512	Monomethylamine methyltransferase MtmB1	2.4	0.1	53	7.3	1	43	1.7	0.1	71	1.6	0.0180	-0.6	0.0006
	ZC1_01513	Trimethylamine corrinoid protein	4.8	0.3	21	11.9	2	25	6.5	0.2	14	1.3	0.0268	0.4	0.0013
	ZC1_01520	Dimethylamine methyltransferase MtbB2	3.8	0.4	24	15.6	1	17	0.9	0.0	154	2.0	0.0001	-2.1	0.0049
	ZC1_01521	Dimethylamine methyltransferase MtbB2	5.3	0.5	17	21.4	4	12	2.1	0.1	52	2.0	0.0140	-1.3	0.0071
	ZC1_01522	Dimethylamine corrinoid protein	9.8	0.6	8	28.7	6	6	9.1	0.5	8	1.6	0.0329	-0.1	0.1673
	ZC1_01526	Monomethylamine methyltransferase MtmB1	0.0	0.0	1277	0.8	0	415	0.0	0.0	1296	4.1	0.0039	-1.2	0.0000
	ZC1_01530	Trimethylamine corrinoid protein	2.5	0.2	43	12.8	1	23	2.5	0.2	40	2.3	0.0047	0.0	0.7086

	ZC1_01531	Trimethylamine methyltransferase MttB	3.1	0.2	31	13.5	2	22	2.9	0.3	30	2.1	0.0134	-0.1	0.4515
	ZC1_01532	Trimethylamine methyltransferase MttB	5.6	0.4	16	22.7	3	10	6.6	0.4	13	2.0	0.0003	0.2	0.0440
CO2 => methane	ZC1_00148	Ferredoxin/F(420)H(2)-dependent CoB-CoM heterodisulfide reductase subunit A	0.2	0.0	744	0.5	0	650	0.2	0.0	582	1.0	0.0020	-0.3	0.0372
	ZC1_00425	Formylmethanofuran--tetrahydromethanopterin formyltransferase	0.5	0.0	425	0.7	0	516	0.5	0.0	317	0.4	0.0249	-0.1	0.2000
	ZC1_00467	Molybdenum-containing formylmethanofuran dehydrogenase 1 subunit C	0.7	0.0	305	1.0	0	334	0.2	0.0	659	0.5	0.0005	-2.0	0.0000
	ZC1_00468	Molybdenum-containing formylmethanofuran dehydrogenase 1 subunit C	0.6	0.0	385	0.9	0	362	0.1	0.0	731	0.7	0.0002	-2.0	0.0000
	ZC1_00691	Methenyltetrahydromethanopterin cyclohydrolase	0.8	0.0	259	1.6	0	187	1.4	0.1	86	1.1	0.0001	0.8	0.0007
	ZC1_00708	H(2):CoB-CoM heterodisulfide,ferredoxin reductase subunit C	0.7	0.1	325	1.3	0	252	0.4	0.0	370	1.0	0.0003	-0.8	0.0014
	ZC1_00787	Ferredoxin	1.8	0.2	89	1.7	0	174	1.4	0.3	85	0.0	0.8707	-0.3	0.1483
	ZC1_00963	F420-dependent methylenetetrahydromethanopterin dehydrogenase	1.8	0.0	84	4.0	0	64	2.4	0.1	44	1.1	0.0000	0.4	0.0004
	ZC1_01079	H(2):CoB-CoM heterodisulfide,ferredoxin reductase subunit B	1.2	0.1	146	1.4	0	230	0.4	0.0	371	0.2	0.0236	-1.7	0.0000
	ZC1_01081	F420-non-reducing hydrogenase iron-sulfur subunit D	1.0	0.1	189	1.2	0	257	0.1	0.0	733	0.3	0.0241	-2.8	0.0000
acetate => methane	ZC1_01114	Acetyl-CoA decarbonylase/synthase complex subunit delta 1	1.2	0.1	144	1.0	0	358	0.2	0.0	675	-0.4	0.0269	-2.9	0.0035
	ZC1_01115	Acetyl-CoA decarbonylase/synthase complex subunit gamma 1	0.8	0.1	246	0.8	0	448	0.1	0.0	993	-0.1	0.4792	-3.6	0.0016
	ZC1_01334	Acetyl-CoA decarbonylase/synthase complex subunit beta 2	0.4	0.0	475	0.9	0	404	0.1	0.0	829	1.0	0.0001	-2.0	0.0001
	ZC1_01335	Acetyl-CoA decarbonylase/synthase complex subunit epsilon 2	0.2	0.0	895	0.3	0	870	0.0	0.0	1380	0.8	0.0002	-3.7	0.0017
	ZC1_01336	Acetyl-CoA decarbonylase/synthase complex subunit alpha 1	0.5	0.1	441	0.5	0	610	0.0	0.0	1215	0.1	0.3608	-4.0	0.0048
methane	ZC1_00647	Tetrahydromethanopterin S-methyltransferase subunit H	0.0	0.0	1437	0.1	0	1383	0.0	0.0	1453	2.1	0.0001	-1.2	0.0017
	ZC1_00705	F420-non-reducing hydrogenase iron-sulfur subunit D	0.6	0.0	379	1.7	0	180	0.1	0.0	821	1.6	0.0000	-2.3	0.0000
	ZC1_00706	H(2)/formate:CoB-CoM heterodisulfide,ferredoxin reductase subunit A	0.8	0.1	232	2.4	0	123	0.2	0.0	522	1.5	0.0000	-1.9	0.0002

	ZC1_00707	H(2):CoB-CoM heterodisulfide,ferredoxin reductase subunit B	0.7	0.1	313	1.6	0	196	0.3	0.0	462	1.2	0.0002	-1.2	0.0008
	ZC1_00896	Tetrahydromethanopterin S-methyltransferase subunit H	0.3	0.0	645	1.4	0	218	0.3	0.0	420	2.3	0.0001	0.1	0.3088
	ZC1_01082	Formate dehydrogenase subunit beta	1.1	0.1	169	1.4	0	236	0.2	0.0	689	0.3	0.0592	-2.8	0.0001
	ZC1_01125	5,10-methylenetetrahydromethanopterin reductase	1.2	0.0	152	2.9	0	91	1.2	0.0	104	1.3	0.0001	0.1	0.3251
	ZC1_01188	Methyl-coenzyme M reductase subunit beta	3.6	0.2	25	9.5	0	30	1.4	0.2	84	1.4	0.0000	-1.3	0.0001
	ZC1_01189	Methyl-coenzyme M reductase I operon protein D	1.9	0.1	78	5.8	0	52	0.5	0.1	308	1.6	0.0000	-2.0	0.0000
	ZC1_01190	Methyl-coenzyme M reductase I operon protein C	1.6	0.1	102	6.1	0	50	0.5	0.1	306	1.9	0.0000	-1.8	0.0001
	ZC1_01191	Methyl-coenzyme M reductase subunit gamma	1.9	0.0	75	8.2	0	40	0.5	0.1	299	2.1	0.0005	-2.0	0.0000
	ZC1_01192	Methyl-coenzyme M reductase subunit alpha	3.2	0.1	29	15.5	1	18	0.8	0.2	170	2.3	0.0027	-2.0	0.0000
	ZC1_01592	Tetrahydromethanopterin S-methyltransferase subunit H	0.4	0.0	559	2.8	0	95	0.2	0.0	511	2.9	0.0000	-0.6	0.0154
	ZC1_01593	Tetrahydromethanopterin S-methyltransferase subunit G	0.1	0.0	1266	0.4	0	797	0.0	0.0	1207	2.8	0.0000	-0.7	0.0118
	ZC1_01594	Tetrahydromethanopterin S-methyltransferase subunit F	0.1	0.0	1111	0.6	0	557	0.1	0.0	1046	2.7	0.0000	-0.8	0.0147
	ZC1_01595	Tetrahydromethanopterin S-methyltransferase subunit A 1	0.3	0.0	584	2.1	0	135	0.2	0.1	579	2.6	0.0000	-0.8	0.0190
	ZC1_01596	Tetrahydromethanopterin S-methyltransferase subunit B	0.3	0.0	642	1.1	0	303	0.1	0.0	778	1.8	0.0000	-1.3	0.0028
	ZC1_01597	Tetrahydromethanopterin S-methyltransferase subunit C	0.6	0.1	386	1.6	0	201	0.2	0.0	544	1.5	0.0002	-1.3	0.0016
	ZC1_01598	Tetrahydromethanopterin S-methyltransferase subunit D	1.1	0.1	171	2.1	0	139	0.5	0.1	277	0.9	0.0001	-1.1	0.0014
	ZC1_01599	Tetrahydromethanopterin S-methyltransferase subunit E	2.9	0.2	34	3.9	0	67	1.8	0.2	63	0.4	0.0040	-0.6	0.0020
Electron transfer	ZC1_01290	F(420)H(2) dehydrogenase subunit A	0.6	0.0	398	0.4	0	704	0.2	0.0	508	-0.3	0.1698	-1.2	0.0007
	ZC1_01291	F(420)H(2) dehydrogenase subunit B	0.6	0.0	376	0.7	0	490	0.2	0.0	589	0.3	0.1619	-1.5	0.0001
	ZC1_01293	F(420)H(2) dehydrogenase subunit D	0.4	0.0	579	0.6	0	529	0.2	0.1	563	0.8	0.0296	-0.7	0.0289
	ZC1_01294	F(420)H(2) dehydrogenase subunit H	0.2	0.0	875	0.4	0	785	0.1	0.0	805	1.0	0.0349	-0.7	0.0529
	ZC1_01296	F(420)H(2) dehydrogenase subunit J	0.0	0.0	1363	0.1	0	1203	0.0	0.0	1176	2.3	0.0474	0.3	0.4444
	ZC1_01298	F(420)H(2) dehydrogenase subunit K	0.0	0.0	1331	0.2	0	1102	0.0	0.0	1101	2.4	0.0270	0.5	0.0667
	ZC1_01299	F(420)H(2) dehydrogenase subunit L	0.1	0.0	1224	0.3	0	889	0.1	0.0	969	2.3	0.0050	0.3	0.4015

ZC1_01300	F(420)H(2) dehydrogenase subunit M	0.1	0.0	1182	0.4	0	808	0.1	0.0	899	2.3	0.0029	0.3	0.3085
ZC1_01301	F(420)H(2) dehydrogenase subunit N	0.1	0.0	1235	0.3	0	847	0.1	0.0	970	2.5	0.0022	0.3	0.4200
ZC1_01302	F(420)H(2) dehydrogenase subunit O	0.1	0.0	1170	0.5	0	664	0.1	0.0	944	2.6	0.0006	0.0	0.8875

Notes: Gene expression profiles were evaluated in terms of reads per kilobase transcript per million mapped reads (RPKM) normalized to the average of ribosomal protein. Ave, the average of three replicates; Std, the standard deviation of three replicates; Rank, the rank of gene expression profiles based on normalized RPKM values; Log2-FD, Log2 Fold change.

Supplementary Table 3 Gene expression levels for formate degradation, electron transduction, and energy conservation of *Z. formicivorans*

Reaction		Locus_Tag	Description	Monoculture on yeast extract_K32 (KY)			Coculture on formate (ZKF)			Coculture on methanol (ZKM)			ZKF:KY		ZKM:KY	
				Avg	Std	Rank	Avg	Std	Rank	Avg	Std	Rank	Log2-FD	p-value	Log2-FD	p-value
Formate -> Formaldehyde	●	K32-1_02759	4Fe-4S dicluster domain-containing protein	0.00	0.00	2695	3.58	1.63	85	0.37	0.61	835	9.61	0.0628	6.33	0.4102
	●	K32-1_02760	Aldehyde ferredoxin oxidoreductase	0.01	0.00	2380	9.63	4.26	14	1.21	0.93	252	9.72	0.0596	6.73	0.1543
	●	K32-1_02761	YdhW family putative oxidoreductase system protein	0.01	0.00	2433	5.17	1.87	48	2.21	0.90	109	9.00	0.0411	7.78	0.0519
	●	K32-1_02762	Formate dehydrogenase accessory sulfurtransferase FdhD	0.01	0.00	2291	7.76	1.63	21	1.61	1.59	179	9.09	0.0145	6.82	0.2246
Formaldehyde -> Methanol	●	K32-1_00231	Iron-containing alcohol dehydrogenase	9.77	0.05	4	4.56	1.45	58	8.20	0.84	13	-1.10	0.0247	-0.25	0.0821
Formate -> Formyl-THF	●	K32-1_02922	Formate-tetrahydrofolate ligase	1.04	0.06	109	5.05	2.51	50	2.28	0.41	101	2.28	0.1098	1.13	0.0315
Formyl-THF -> Methenyl-TFH -> Methylene-THF	●	K32-1_00737	Bifunctional 5,10-methylene-tetrahydrofolate dehydrogenase/5,10-methylene-tetrahydrofolate cyclohydrolase	0.75	0.02	171	1.97	1.48	192	2.08	0.69	118	1.39	0.2908	1.47	0.0795
Methylene-THF -> Glycine	●	K32-1_01311	Glycine cleavage system protein GcvH	0.33	0.02	465	0.97	0.31	450	1.54	1.14	189	1.58	0.0685	2.24	0.2062
Glycine -> Serine	●	K32-1_00082	Serine hydroxymethyltransferase	0.85	0.02	148	2.02	0.19	186	2.45	1.01	92	1.25	0.0080	1.53	0.1117
Serine -> Pyruvate		K32-1_00076	L-serine ammonia-lyase, iron-sulfur-dependent, subunit beta	0.19	0.01	771	0.22	0.05	1461	0.12	0.19	1500	0.22	0.3630	-0.61	0.6123
		K32-1_00077	L-serine ammonia-lyase, iron-sulfur-dependent, subunit alpha	0.15	0.01	943	0.62	0.36	712	0.43	0.07	737	2.03	0.1557	1.51	0.0023
	●	K32-1_02021	Serine dehydratase subunit alpha family protein	0.25	0.01	604	1.08	0.58	401	1.71	0.51	161	2.12	0.1300	2.79	0.0386

Pyruvate -> Actyl-CoA	●	K32-1_02733	Ferredoxin oxidoreductase	1.49	0.02	70	6.51	2.25	36	1.94	0.64	136	2.12	0.0612	0.38	0.3457
CO -> CO2	●	K32-1_00865	Carbon monoxide dehydrogenase accessory protein	0.11	0.06	1213	0.37	0.19	1067	0.39	0.49	801	1.79	0.0804	1.87	0.4185
CO -> CO2	●	K32-1_00868	Anaerobic carbon-monoxide dehydrogenase catalytic subunit	0.21	0.12	689	1.93	0.92	197	0.65	0.50	502	3.18	0.0811	1.62	0.2112
	●	K32-1_00869	CO dehydrogenase/CO-methylating acetyl-CoA synthase complex subunit beta	0.26	0.17	576	2.80	0.93	122	0.94	0.34	341	3.40	0.0095	1.82	0.0376
Actyl-CoA -> CO + Methylated corrionid iron protein	●	K32-1_00870	Acetyl-CoA decarbonylase/synthase complex subunit gamma	0.31	0.19	490	4.01	0.96	70	1.45	1.05	206	3.71	0.0028	2.24	0.1371
	●	K32-1_00871	Uncharacterized 2Fe-2S iron-sulfur cluster binding domain	0.29	0.17	521	4.11	1.49	68	2.30	1.39	99	3.80	0.0457	2.96	0.1277
	●	K32-1_00872	Carbon monoxide dehydrogenase accessory protein, AAA domain	0.23	0.13	650	3.17	1.29	105	2.23	0.48	104	3.79	0.0567	3.28	0.0022
	●	K32-1_00873	Acetyl-CoA decarbonylase/synthase complex subunit delta	0.24	0.14	619	2.50	1.50	139	1.40	1.40	219	3.38	0.1200	2.54	0.2899
Methylated corrionid iron protein -> Methyl-THF	●	K32-1_00874	Methyltetrahydrofolate cobalamin methyltransferase	0.34	0.19	438	7.32	2.20	27	4.04	1.28	39	4.42	0.0308	3.56	0.0351
Methyl-THF -> Methylene-THF	●	K32-1_00875	Methylenetetrahydrofolate reductase C-terminal domain-containing protein	0.50	0.01	284	3.29	1.73	96	1.36	0.15	227	2.73	0.1068	1.46	0.0101
		K32-1_02858	Methylenetetrahydrofolate reductase	0.00	0.00	2719	0.09	0.15	2037	0.01	0.00	1692	4.40	0.4308	1.76	0.0382
Formate -> CO2		K32-1_00963	Cytochrome b subunit of formate dehydrogenase	0.01	0.00	2552	0.03	0.05	2428	0.01	0.00	1692	2.17	0.4899	0.95	0.0346
		K32-1_00968	Cytochrome c3	0.24	0.03	631	0.13	0.09	1843	0.01	0.00	1692	-0.92	0.1025	-4.06	0.0060
		K32-1_00971	Cytochrome b subunit of formate dehydrogenase	0.39	0.03	379	0.05	0.08	2299	0.01	0.00	1692	-2.96	0.0024	-4.78	0.0013
		K32-1_01726	4Fe-4S dicluster domain-containing protein	0.04	0.03	1811	0.07	0.11	2190	0.01	0.00	1692	0.60	0.7500	-1.62	0.2119
		K32-1_01729	4Fe-4S dicluster domain-containing protein	0.11	0.01	1167	0.12	0.20	1877	0.01	0.00	1692	0.06	0.9686	-2.99	0.0004
		K32-1_02856	Formate dehydrogenase subunit alpha,bidirectional hydrogenase complex protein HoxU	0.00	0.00	2671	0.00	0.00	2506	0.01	0.00	1692	-1.12	0.0007	1.52	0.0436
		K32-1_02857	Formate dehydrogenase subunit alpha	0.01	0.00	2557	0.00	0.00	2506	0.01	0.00	1692	-1.67	0.0001	0.96	0.0742

	•	K32-1_03286	NADH-quinone oxidoreductase subunit NuoF	0.07	0.00	1558	0.62	0.26	704	0.23	0.21	1162	3.24	0.0660	1.80	0.3021
	•	K32-1_03287	Molybdopterin oxidoreductase Fe4S4 domain	0.07	0.00	1512	0.35	0.19	1099	0.13	0.19	1477	2.32	0.1237	0.87	0.6571
	•	K32-1_03288	Formate dehydrogenase subunit alpha,Molybdopterin oxidoreductase	0.10	0.00	1295	0.88	0.65	503	0.11	0.17	1538	3.20	0.1717	0.25	0.8677
	•	K32-1_03289	Formate dehydrogenase subunit alpha	0.12	0.00	1142	0.67	0.26	659	0.32	0.13	929	2.53	0.0659	1.48	0.1127
Formate transporter		K32-1_02853	Formate/nitrite transporter family protein	0.00	0.00	2978	0.00	0.00	2506	0.01	0.00	1692	0.25	0.1861	2.88	0.0258
		K32-1_00576	4Fe-4S dicluster domain-containing protein	0.04	0.00	1906	0.69	0.26	643	0.61	0.75	536	4.26	0.0482	4.08	0.3162
		K32-1_01218	4Fe-4S dicluster domain-containing protein	0.01	0.00	2541	0.00	0.00	2506	0.01	0.00	1692	-1.74	0.0002	0.89	0.0330
		K32-1_01219	Anaerobic carbon-monoxide dehydrogenase catalytic subunit	0.02	0.00	2113	0.02	0.04	2479	0.01	0.00	1692	0.09	0.9530	-0.64	0.0238
CO -> CO2		K32-1_01489	Anaerobic carbon-monoxide dehydrogenase catalytic subunit	0.01	0.00	2495	0.07	0.07	2181	0.01	0.00	1692	2.96	0.2684	0.72	0.0581
		K32-1_01971	Anaerobic carbon-monoxide dehydrogenase catalytic subunit	0.00	0.00	3156	0.00	0.00	2506	0.01	0.00	1692	1.18	0.0040	3.81	0.0226
	•	K32-1_02449	Anaerobic carbon-monoxide dehydrogenase catalytic subunit	0.09	0.03	1363	2.52	0.63	137	0.43	0.04	739	4.84	0.0212	2.29	0.0003
	•	K32-1_02450	4Fe-4S dicluster domain-containing protein	0.13	0.04	1082	3.23	1.37	99	1.02	0.46	313	4.68	0.0591	3.02	0.0751
CO2 -> HCO3-		K32-1_00383	Carbonic anhydrase	0.01	0.00	2540	0.04	0.07	2351	0.01	0.00	1692	2.51	0.4747	0.89	0.0806
		K32-1_03252	Carbonic anhydrase	0.25	0.01	606	0.46	0.33	908	0.01	0.00	1692	0.89	0.3851	-4.12	0.0000
		K32-1_00271	Nitroreductase family protein	0.11	0.01	1200	0.25	0.29	1355	0.99	0.44	321	1.22	0.4791	3.20	0.0740
		K32-1_00333	Nitroreductase	0.52	0.02	270	1.05	0.58	410	2.12	0.53	111	1.02	0.2504	2.03	0.0348
Nfn	•	K32-1_00735	Sulfide/dihydroorotate dehydrogenase-like FAD/NAD-binding protein	0.33	0.01	452	1.13	0.20	389	0.45	0.76	705	1.75	0.0193	0.44	0.8121
	•	K32-1_00736	NADPH-dependent glutamate synthase	0.43	0.03	341	1.41	0.11	310	1.07	0.44	300	1.71	0.0001	1.31	0.1296
Hdr:Flox complex	•	K32-1_01374	Anaerobic sulfite reductase contains an FAD and NADPH binding module	0.77	0.03	168	1.85	1.20	210	2.55	0.84	86	1.27	0.2584	1.73	0.0661

	• K32-1_01375	4Fe-4S dicluster domain-containing protein	0.75	0.03	173	2.31	0.98	154	2.25	0.39	103	1.62	0.1112	1.58	0.0216
	• K32-1_01376	4Fe-4S dicluster domain-containing protein	0.68	0.04	206	1.88	0.72	203	2.33	0.43	96	1.47	0.1003	1.78	0.0216
	• K32-1_01377	Methyl-viologen-reducing hydrogenase, delta subunit	0.14	0.01	988	0.47	0.17	890	0.25	0.41	1100	1.72	0.0836	0.82	0.6893
	• K32-1_01378	Heterodisulfide reductase, subunit A (polyferredoxin)	0.68	0.04	205	1.83	1.56	214	1.57	0.28	185	1.43	0.3296	1.21	0.0288
	• K32-1_01379	Heterodisulfide reductase iron-sulfur subunit A	0.58	0.04	239	1.18	1.30	367	1.02	0.95	314	1.03	0.5056	0.82	0.5067
	• K32-1_01380	Heterodisulfide reductase iron-sulfur subunit B	0.55	0.04	255	1.27	1.10	335	1.23	0.70	246	1.20	0.3740	1.15	0.2367
	• K32-1_01381	Heterodisulfide reductase iron-sulfur subunit C	0.77	0.03	166	1.81	1.05	216	1.28	0.56	237	1.23	0.2295	0.74	0.2537
	• K32-1_01382	Membrane protein	0.02	0.00	2262	0.00	0.00	2506	0.01	0.00	1692	-2.76	0.0000	-0.13	0.5556
	• K32-1_01383	Formate dehydrogenase accessory sulfurtransferase FdhD	0.35	0.01	423	0.27	0.19	1294	0.40	0.09	779	-0.38	0.5368	0.19	0.4535
	• K32-1_02309	F0FATP synthase subunit epsilon	1.06	0.07	106	1.83	0.93	215	0.59	0.59	556	0.78	0.2915	-0.84	0.3036
	• K32-1_02310	F0FATP synthase subunit beta	1.46	0.02	75	2.45	0.39	144	2.04	0.96	124	0.75	0.0467	0.49	0.4021
	• K32-1_02311	F0FATP synthase subunit gamma	0.72	0.01	183	1.39	0.29	314	1.18	0.37	260	0.94	0.0559	0.70	0.1645
	• K32-1_02312	F0FATP synthase subunit alpha	0.84	0.02	150	1.04	0.10	414	1.26	0.67	241	0.31	0.0247	0.59	0.3900
	• K32-1_02313	F0FATP synthase subunit delta	0.58	0.08	237	0.82	0.89	545	0.78	1.09	421	0.49	0.6936	0.43	0.7796
ATPase	• K32-1_02314	F0FATP synthase subunit B	0.55	0.01	260	0.66	0.48	668	0.59	0.74	558	0.26	0.7349	0.11	0.9289
	• K32-1_02315	ATP synthase F0 subunit C	1.90	0.04	40	2.78	1.33	126	0.91	0.99	357	0.54	0.3728	-1.07	0.2252
	• K32-1_02316	F0FATP synthase subunit A	0.86	0.08	144	2.20	0.48	165	1.96	0.61	133	1.35	0.0089	1.19	0.0862
	• K32-1_02317	Hypothetical protein	0.37	0.03	405	0.60	0.33	736	0.49	0.82	668	0.70	0.3525	0.40	0.8272
	• K32-1_02318	AtpZ/AtpI family protein	0.24	0.02	612	0.36	0.27	1095	0.01	0.00	1692	0.56	0.5320	-4.09	0.0000
	K32-1_02732	ATP synthase	0.42	0.02	350	1.77	0.78	219	0.15	0.23	1406	2.08	0.0962	-1.47	0.1863
	K32-1_02827	FMN-binding glutamate synthase family protein	0.03	0.00	2008	0.14	0.08	1792	0.15	0.15	1400	2.19	0.1614	2.37	0.3013
Glycine cleavage system	K32-1_02828	Glycine cleavage system aminomethyltransferase GcvT	0.30	0.02	501	0.17	0.05	1638	0.01	0.00	1692	-0.83	0.0121	-4.41	0.0000
	K32-1_02829	Glycine cleavage system protein GcvH	0.24	0.02	637	0.12	0.20	1889	0.29	0.47	1005	-1.02	0.4040	0.30	0.8628
	K32-1_02830	Aminomethyl-transferring glycine dehydrogenase subunit GcvPA	0.29	0.01	530	0.51	0.03	838	0.47	0.39	685	0.83	0.0002	0.70	0.5122

		K32-1_02831	Aminomethyl-transferring glycine dehydrogenase subunit GcvPB	0.30	0.02	510	0.41	0.18	982	0.19	0.15	1279	0.47	0.3940	-0.68	0.3321
Methylamines	●	K32-1_00404	Trimethylamine methyltransferase family protein	0.00	0.00	2687	1.56	1.31	2687	0.01	0.00	1692	8.37	0.1747	1.59	0.0414
	●	K32-1_00409	Dimethylamine:corrinoid methyltransferase	0.00	0.00	3005	2.14	1.75	3005	0.01	0.00	1692	10.22	0.1678	2.98	0.0251
	●	K32-1_00410	Dimethylamine methyltransferase	0.00	0.00	3117	1.16	1.07	3117	0.01	0.00	1692	9.90	0.2013	3.55	0.0232
	●	K32-1_00411	Cobalamin B12-binding domain-containing protein	0.00	0.00	2990	1.92	1.14	2990	0.01	0.00	1692	10.01	0.0999	2.93	0.0237
	●	K32-1_00412	Trimethylamine methyltransferase family protein	0.00	0.00	2861	2.25	1.84	2861	0.01	0.00	1692	9.63	0.1688	2.32	0.0293
	●	K32-1_00413	Trimethylamine methyltransferase family protein	0.00	0.00	2870	2.82	2.40	2870	0.01	0.00	1692	10.01	0.1790	2.37	0.0050
	●	K32-1_01876	Trimethylamine methyltransferase family protein	0.02	0.00	2246	1.54	1.08	2246	0.22	0.23	1198	6.58	0.1352	3.74	0.2653
	●	K32-1_01928	Methyltransferase cognate corrinoid protein	0.83	0.03	155	14.29	9.67	155	1.52	1.31	190	4.11	0.1374	0.88	0.4544
	●	K32-1_01933	Trimethylamine methyltransferase family protein, partial	0.00	0.00	2691	0.96	0.94	2691	0.01	0.00	1692	7.69	0.2201	1.61	0.0394
	●	K32-1_01934	Methyltransferase cognate corrinoid protein	0.00	0.00	3004	0.42	0.39	3004	0.01	0.00	1692	7.87	0.1996	2.97	0.0247
	●	K32-1_01935	Trimethylamine methyltransferase family protein	0.00	0.00	3100	0.75	0.91	3100	0.01	0.00	1692	9.18	0.2890	3.45	0.0235

Notes: Gene expression profiles were evaluated in terms of reads per kilobase transcript per million mapped reads (RPKM) normalized to the average of ribosomal protein. Ave, the average of three replicates; Std, the standard deviation of three replicates; Rank, the rank of gene expression profiles based on normalized RPKM values; Log2-FD, Log2 Fold change. Main enzymes are marked with "●".

Acknowledgments

Words cannot express my gratitude to all the people supporting me during the Doctor Course. Firstly, I would like to express my deepest appreciation to my supervisor Assoc. Prof. Dr. Souichiro Kato of Graduate school of Agriculture, Hokkaido University, and my co-supervisor Dr. Masaru K. Nobu of the National Institute of Advanced Industrial Science and Technology (AIST) to support me to chase a Ph.D. degree in Hokkaido University. I am also deeply grateful to Dr. Kensuke Igarashi of AIST, who generously provided knowledge and expertise. Additionally, I am deeply indebted to Prof. Dr. Lei Cheng of Biogas Institute of Ministry of Agriculture and Rural Affairs (BIOMA) for his generous support to initiate and conduct this research. Their excellent expertise, invaluable patience, and inspiring guidance made it possible for me to carry out this challenging research. I indeed enjoyed the time working with you.

Many thanks also go to Assoc. Prof. Dr. Wataru Kitagawa, Assoc. Prof. Dr. Yoshitomo Kikuchi, Prof. Dr. Teruo, and Dr. Takashi Narihiro for the valuable suggestion, critical comments, and worthy guidance during my daily research work. I am also thankful to the researchers and technicians in AIST, Dr. Mitani, Dr. Shusei Kanie, Dr. Maiko Furubayashi, Ms. Motoko Takashino, Ms. Mika Yamamoto, Ms. Ai Miura, and the all who provided me help. Without their support, I could not conduct the experiments smoothly. Special thanks also extend to the Anaerobic Microbiology Group of BIOMA in China to give me the chance and provide intangible support to work in Japan.

I would like to extend my sincere thanks to my mates in Bioproduction Research Institute of AIST and laboratory of Applied Molecular Microbiology, Dr. Ruoyun Xie, Dr. Zhihao Tu, Dr. Putcha Jyothi Priya, Dr. Motoyuki Watanabe, Dr. Ishigami Kota, Dr. Helena de Fátima Silva Lopes, Dr. Ling Leng, Dr. Ran Mei, Tomoya Numadate and Shota Fukukawa. Thanks for their kind help in and out of the laboratory.

Last but not the least, I'd like to appreciate my family and all my sincere friends for their emotional support, and also acknowledge the DX fellowship of Hokkaido University to support this research.